27718

NATIONAL LIBRARY
OTTAWA

CANADA

BIBLIOTHÈQUE NATIONALE
OTTAWA

NAME OF AUTHOR....OLALEKAN JACOB OLAOSEBIKAN

TITLE OF THESIS....ON THE VIBRATION OF
....ELASTIC SPHERICAL SHELLS
....

UNIVERSITY.....UNIVERSITY OF ALBERTA

DEGREE FOR WHICH THESIS WAS PRESENTED..MASTER OF SCIENCE

YEAR THIS DEGREE GRANTED..........1976..................

Permission is hereby granted to THE NATIONAL LIBRARY OF CANADA to microfilm this thesis and to lend or sell copies of the film.

The author reserves other publication rights, and neither the thesis nor extensive extracts from it may be printed or otherwise reproduced without the author's written permission.

(Signed)..............................

PERMANENT ADDRESS:

....P. O. BOX 1834
....IBADAN NIGERIA.
....

DATED...8...MARCH.....1976

NL-91 (10-68)

INFORMATION TO USERS

THIS DISSERTATION HAS BEEN
MICROFILMED EXACTLY AS RECEIVED

This copy was produced from a microfiche copy of the original document. The quality of the copy is heavily dependent upon the quality of the original thesis submitted for microfilming. Every effort has been made to ensure the highest quality of reproduction possible.

PLEASE NOTE: Some pages may have indistinct print. Filmed as received.

Canadian Theses Division
Cataloguing Branch
National Library of Canada
Ottawa, Canada K1A 0N4

AVIS AUX USAGERS

LA THESE A ETE MICROFILMEE
TELLE QUE NOUS L'AVONS RECUE

Cette copie a été faite à partir d'une microfiche du document original. La qualité de la copie dépend grandement de la qualité de la thèse soumise pour le microfimage. Nous avons tout fait pour assurer une qualité supérieure de reproduction.

NOTA BENE: La qualité d'impression de certaines pages peut laisser à désirer. Microfilmée telle que nous l'avons reçue.

Division des thèses canadiennes
Direction du catalogage
Bibliothèque nationale du Canada
Ottawa, Canada K1A 0N4

THE UNIVERSITY OF ALBERTA

ON THE VIBRATION OF ELASTIC SPHERICAL SHELLS

by

©

OLALEKAN JACOB OLAOSEBIKAN

A THESIS
SUBMITTED TO THE FACULTY OF GRADUATE STUDIES AND RESEARCH
IN PARTIAL FULFILMENT OF THE REQUIREMENTS FOR THE DEGREE
OF MASTER OF SCIENCE

DEPARTMENT OF MECHANICAL ENGINEERING
EDMONTON, ALBERTA
SPRING, 1976

THE UNIVERSITY OF ALBERTA

FACULTY OF GRADUATE STUDIES AND RESEARCH

The undersigned certify that they have read, and recommend to the Faculty of Graduate Studies and Research, for acceptance, a thesis entitled "On the Vibration of Elastic Spherical Shells" submitted by Olalekan Jacob Olaosebikan in partial fulfilment of the requirements for the degree of Master of Science.

J.B. Haddow
Supervisor

J Kennedy

Gary Faulkner

R.J. Tait

Date March 5, 1976

ABSTRACT

The transient response, to time dependent pressure and velocity inputs, of elastic spherical shells made of an isotropic and homogeneous material is investigated. Standard numerical methods are used to solve the governing equations for the incompressible thin and thick shell and for the compressible thin shell problems of non-linear elasticity while a numerical procedure is developed for the method of characteristics to solve the compressible thick shell problem of linear elasticity. The results obtained for the free and forced vibrations of the thin and thick shells considered agree well with existing analytical and numerical solutions.

ACKNOWLEDGEMENTS

The author is profoundly grateful to Dr. J. B. Haddow who supervised this study.

The author also wishes to thank the University of Alberta for the financial support given him during the course of this study.

TABLE OF CONTENTS

PAGE

LIST OF TABLES ix

LIST OF FIGURES x

LIST OF PROGRAMS FOR THE HP9830 CALCULATOR xv

LIST OF SYMBOLS xvii

CHAPTER 1. INTRODUCTION 1

CHAPTER 2. THE HYPERELASTIC MATERIAL 6

2.1 The Use of Strain Energy Functions 6

2.2 Particular Strain Energy Functions 7

CHAPTER 3. THIN SHELL PROBLEMS 9

3.1 Approximate Theory for Thin-walled Shells 9

3.2 The Incompressible Case 12

3.3 The Compressible Case 15

3.4 Specific Examples 18

3.5 Free Oscillations 20

CHAPTER 4. THICK SHELL PROBLEMS 22

4.1 General Discussion 22

4.2 Incompressible Shell Problem in Linear Elasticity: Free Radial Oscillation by Rayleigh's Method 23

4.3 Compressible Shell Problem in Linear Elasticity: The Method of Characteristics 27

TABLE OF CONTENTS (continued)

PAGE

4.4 Finite Oscillation of the Incompressible Shell in non-Linear Elasticity 33

4.5 Special Cases 36

CHAPTER 5. OTHER METHODS OF SOLUTION 38

CHAPTER 6. DISCUSSION OF RESULTS 42

6.1 Precautions in Numerical Computations 42

6.2 Specific Results 43

6.3 Comparison of Results 48

CHAPTER 7. CONCLUDING REMARKS 52

FIGURES 56

PROGRAMS FOR THE HP9830 CALCULATOR 100

REFERENCES 124

APPENDIX A. NUMERICAL METHODS AND ERROR ANALYSES 126

A.1 Numerical Scheme for the Discrete Variable Method 126

A.2 Error Analysis of the Discrete Variable Method 128

A.3 The Fourth Order Runge-Kutta Process 129

A.4 Error Analysis of the Method of Characteristics 131

A.5 Algorithm for Integrating the Governing Equations for the Thin Compressible Shell 132

TABLE OF CONTENTS (continued)

PAGE

APPENDIX B. CONDITIONS FOR A PERIODIC MOTION 135

B.1 Periodicity of Motion 135

B.2 The Critical Value of Constant, c, for Mooney-Rivlin Material 138

B.3 The Maximum Step Input Pressure, Q_{max}, for a Periodic Motion 140

APPENDIX C. NOTES ON THE METHOD OF CHARACTERISTICS 142

C.1 Integration of the Characteristic Equations 142

C.2 Boundary Conditions and the Constants K and K' 146

APPENDIX D. PROOFS OF THEOREMS 150

D.1 Proof of the Hydrostatic Stress Theorem 150

D.2 The Characteristic Curves: Derivation of the Equations 151

LIST OF TABLES

TABLE	Description	PAGE
1.	Comparison of results obtained by different methods for the period of free oscillation of a thin-walled neo-Hookean shell	49

LIST OF FIGURES

FIGURE PAGE

1. Static pressure - stretch relation for Mooney-Rivlin material, material with logarithmic strain energy function and Blatz-Ko material 56

2. Phase plane diagrams for different step input pressures 57

3. Diagram illustrating the free radial oscillation of a thick-walled incompressible shell 58

4. Characteristic field for a thick-walled compressible shell under a step function application of pressure 59

5. Flow diagram for numerical solution of the governing equation for the incompressible thin shell by the method of discrete variables 60

6. Flow diagram for numerical solution of the governing equations for the compressible thin shell by the method of discrete variables 61

7. Diagram illustrating the critical value, c_{crit}, of constant c, for the Mooney-Rivlin material 62

8. Types of meshes in the characteristic field of Fig. 4 63

9a. Static pressure - stretch relation for the thin incompressible shell of Mooney-Rivlin material 64

9b. Static pressure - stretch relation for the the thin incompressible shell of material with logarithmic strain energy function 65

9c. Static pressure - stretch relation for the thin compressible shell of Blatz-Ko material 66

LIST OF FIGURES (continued)

FIGURE		PAGE
10a.	Phase plane diagrams for a neo-Hookean thin-walled shell under various step function applications of pressure	67
10b.	Phase plane diagram illustrating the limiting case of periodic motion for a neo-Hookean thin-walled shell	68
10c.	Phase plane diagram for a neo-Hookean thin-walled shell as the step input pressure, Q approaches zero	69
10d.	Phase plane diagram for free oscillation of a neo-Hookean thin-walled shell, with small amplitude.	70
10e.	Phase plane diagram for free oscillation of a neo-Hookean thin-walled shell, with small amplitude	71
10f.	Phase plane diagram for free oscillation of a neo-Hookean thin-walled shell, with small amplitude	72
11a.	Phase plane diagram for a thin incompressible shell of Mooney-Rivlin material, illustrating limiting case of periodic motion	73
11b.	Phase plane diagrams for a thin incompressible shell of Mooney-Rivlin material, under various step input pressures	74
11c.	Phase plane diagram for a thin incompressible shell of Mooney-Rivlin material, illustrating periodic motion for large stretches	75
12.	Phase plane diagrams for a thin incompressible shell of material with logarithmic strain energy function	76

LIST OF FIGURES (continued)

FIGURE		PAGE
13a.	Phase plane diagrams for a thin-walled neo-Hookean shell, obtained as a limiting case of the Blatz-Ko material as ν approaches 0.5	77
13b.	Phase plane diagrams for the thin compressible shell of Blatz-Ko material under various step input pressures	78
13c.	Phase plane diagram for the thin compressible shell of Blatz-Ko material, illustrating a case of periodic motion	79
14a.	Dynamic response curves for a thin-walled neo-Hookean shell under various step function applications of pressure, Q	80
14b.	Dynamic response curve for a thin-walled neo-Hookean shell as applied pressure, Q approaches zero	81
14c.	Dynamic response curve for a thin-walled neo-Hookean shell for a particular step input pressure, Q	82
15.	Dynamic response curve for a thin incompressible shell of Mooney-Rivlin material under a step function application of pressure	83
16.	Dynamic response curve for a thin incompressible shell of material with logarithmic strain energy function under a step function application of pressure	84
17a.	Dynamic response curves for thin compressible shells of Blatz-Ko material under a step function application of pressure	85

LIST OF FIGURES (continued)

FIGURE PAGE

17b. Dynamic response curve for a thin compressible shell of Blatz-Ko material: a particular case 86

18. Dynamic response curve for free oscillation of a neo-Hookean thin-walled shell, with small amplitude 87

19a. Dynamic response curve of the inner and outer surfaces of a thick compressible shell, with B/A = 2, under a step function application of pressure, Q 88

19b. Dynamic response curve of the inner surface of a thick compressible shell with B/A = 11, under a step function application of pressure, Q 89

19c. Dynamic response curve of a thin compressible shell obtained as a limiting case of Fig. 19a as B/A approaches 1 90

19d. Dynamic response curve of a thin compressible shell obtained as a limiting case of Fig. 19a: case of Q approaching zero 91

19e. Comparison of a response curve of Fig. 19a with that obtained by other investigators 92

19f. Comparison of response curve of Fig. 19b with that obtained by other investigators 93

20. Variation of tangential stress with time at the inner surface of a thick compressible shell under a step function application of pressure 94

LIST OF FIGURES (continued)

FIGURE		PAGE
21.	Variation of particle velocity with time at the inner surface of a thick compressible shell under a step function application of pressure	95
22.	Variation of shear stress with time at the inner surface of a thick compressible shell under a step input pressure	96
23a.	Dynamic response curve of the inner surface of thick-walled incompressible neo-Hookean shells under a given step input pressure	97
23b.	Dynamic response curve of the inner surface of a thick neo-Hookean shell under various step input pressures	98
23c.	Dynamic response curve of a thin-walled neo-Hookean shell obtained as a limiting case of Fig. 23a, as B/A approaches 1	99

LIST OF PROGRAMS FOR HP9830

PROGRAM	Description	PAGE
1.	Program for solving the equilibrium equation for the thin compressible shell of Blatz-Ko material	100
2a.	Program for evaluating the maximum step input pressure, Q_{max}, for periodic motion of an incompressible shell of Mooney-Rivlin material	102
2b.	Program for evaluating the maximum step input pressure, Q_{max}, for periodic motion of an incompressible shell of material with logarithmic strain energy function	104
2c.	Program for evaluating the maximum step input pressure, Q_{max}, for periodic motion of a compressible shell of Blatz-Ko material	105
3a.	Discrete variable method for solving the governing equation for a thin incompressible shell of Mooney-Rivlin material	107
3b.	Discrete variable method for solving the governing equation for a thin compressible shell of Blatz-Ko material	109
4a.	Fourth order Runge-Kutta process for solving the governing equation for a thin incompressible shell of Mooney-Rivlin material	111
4b.	Fourth order Runge-Kutta process for solving the governing equations for a thin compressible shell of Blatz-Ko material	112

PROGRAM	Description	PAGE
5a.	Program for finding the period of oscillation of a thin incompressible shell of Mooney-Rivlin material	114
5b.	Program for finding the period of oscillation of a thin incompressible shell of material with logarithmic strain energy function	115
5c.	Program for finding the period of oscillation of a thin compressible shell of Blatz-Ko material	117
6.	Method of characteristics for solving the governing equations for the thick compressible shell	118
7.	Program for solving the governing equation for the thick-walled incompressible neo-Hookean shell	123

LIST OF SYMBOLS

1. Nomenclature for the Thin Shell Problem of non-Linear Elasticity

(A,a) = inner radius in the (undeformed, deformed) state

(B,b) = outer radius in the (undeformed, deformed) state

(R,r) = radial coordinate of particle in the (undeformed, deformed) state

(T,t) = shell wall thickness in the (undeformed, deformed) state

$(\bar{R},\bar{r})$ = mean radius in the (undeformed, deformed) state

R,Θ,Φ = spherical coordinates in the undeformed state

r,θ,ϕ = spherical coordinates in the deformed state

(q_i,q_o) = (internal, external) applied pressure

τ = time

$\bar{\tau} = \frac{\tau}{\bar{R}}\sqrt{\frac{\mu}{\rho}}$ = non-dimensionalized time

μ = shear modulus for infinitesimal strain from the undeformed state

ρ = mean density of the shell

ν = Poisson's ratio for infinitesimal strain from the undeformed state

$\bar{\sigma}$ = mean stress

W = strain energy function

$\bar{W} = \frac{W}{\mu}$ = non-dimensionalized strain energy function

LIST OF SYMBOLS (continued)

2. Nomenclature for the Thick Shell Problem:

Incompressible Case of non-Linear Elasticity

(A,a) = inner radius in the (undeformed, deformed) state

(B,b) = outer radius in the (undeformed, deformed) state

(R,r) = radial coordinate of particle in the (undeformed, deformed) state

u = radial displacement at reference radius, r

t = time

τ = $\frac{t}{A}\sqrt{\frac{\mu}{\rho}}$ = non dimensionalized time

ρ = density

μ = shear modulus for infinitesimal strain from the undeformed state

W = strain energy function

$\overline{W} = \frac{W}{\mu}$ = non-dimensionalized strain energy function

LIST OF SYMBOLS (continued)

3. Nomenclature for the Thick Shell Problem: Compressible Case in Linear Elasticity

c = wave speed

ρ = density

λ, μ = Lame's constants

ν = time

r = radial distance

u = radial displacement

$v = \frac{\partial u}{\partial t}$ = particle velocity

(A,B) = (inner, outer) radius

σ_r = radial stress

σ_θ = tangential stress

$\bar{\sigma} = \frac{\sigma}{\mu} =$ = non-dimensionalized stress

$\bar{r} = \frac{r}{A}$ = non-dimensionalized radial distance

$T = (B-A)$ = shell thickness

$\bar{v} = \frac{v}{c}$ = non-dimensionalized particle velocity

$\bar{u} = \frac{u}{A}$ = non-dimensionalized radial displacement

$\tau = \frac{ct}{A}$ = non-dimensionalized time

$E = 2(1+\nu)\mu$ = Young's modulus

LIST OF SYMBOLS (continued)

$\frac{\rho c^2}{\mu} = 2\,\frac{(1-\nu)}{(1-2\nu)}$ = a dimensionless parameter

$[\sigma] = \sigma_+ - \sigma_-$ = discontinuity in stress, σ

$[v] = v_+ - v_-$ = discontinuity in velocity, v

σ_+ = value of stress, σ, ahead of the wavefront

σ_- = value of stress, σ, behind the wavefront

v_+ = value of velocity, v, ahead of the wavefront

v_- = value of velocity, v, behind the wavefront

CHAPTER 1

INTRODUCTION

In the analysis of the vibration of elastic spherical shells of isotropic and homogeneous materials, different cases of the dynamical problem arise according to (i) whether the linear or the non-linear theory of elasticity is considered; (ii) whether the material of the shell is compressible or incompressible and (iii) whether the shell considered is thin or thick. Free and forced vibrations are usually treated as two aspects of the same problem resulting from different initial and boundary conditions.

The methods which have so far been used to solve these problems are outlined for the different cases as follows.

1. Free oscillations of linear elasticity theory

The linear elasticity problem of the free radial oscillation of the incompressible and compressible thick shells, with the thin shells considered as limiting cases, have been solved by means of spherical harmonics. This method of solution is discussed fully by LOVE [1].

2. Forced vibration of a compressible shell in linear elasticity theory

The forced vibration problem of linear elasticity for a compressible thick shell, again with the thin shell considered as a limiting case, has been solved by a number of analytical and numerical methods. The analytical methods of solution include

(i) a direct infinite series solution using the Midlin-Goodman technique (BAKER and ALLEN [2]),
(ii) a Laplace transform method (TRANTER [3]), and
(iii) a finite Hankel transform method (CINELLI [4]).

Numerical methods of solution include

(i) the discontinuous step method (MEHTA and DAVIDS [5]),
(ii) a finite difference method (SMITH [6]),
(iii) a combined characteristic-difference method (CHOU and GREIF [7]), and
(iv) the method of characteristics (CHOU and KOENIG [8]; LEONARD and BUDIANSKY [9]; CHOU and GREIF [7]).

3. Forced vibration of the incompressible thin and thick shells of non-linear elasticity theory

These non-linear elasticity problems of the thin and thick incompressible shells have been solved for admissible strain energy functions (ERINGEN [10], ZHONG-HENG and SOLECKI [11]). A well-known admissible strain energy function for an incompressible material is the Mooney-Rivlin type [given by equation (2.6) of Section (2.2)] from which the neo-Hookean form is obtainable as a special case.

4. Forced vibration of the thin compressible shell of non-linear elasticity

This problem has also been solved for admissible strain energy functions. The strain energy function considered here is the Blatz-Ko type [given by equation (2.8) of Section (2.2)] proposed for a class of rubbery materials. It gives the neo-Hookean form as a limiting case when the value of Poisson's, ratio, ν, approaches 0.5. A number of other strain energy functions, which are admissible for a compressible material, have been discussed by HADDOW and FAULKNER [12].

In this investigation, the following free and forced vibration problems are considered.

(i) The incompressible thin shell problem of nonlinear elasticity theory for the Mooney-Rivlin and a logarithmic strain energy functions.

(ii) The compressible thin shell problem of nonlinear elasticity for the Blatz-Ko strain energy function.

(iii) The incompressible thick shell problem of nonlinear elasticity theory for the neo-Hookean solid.

(iv) The compressible thick shell problem of linear elasticity solved by the method of characteristics.

For forced vibrations, a step input application of pressure is considered but only a little modification of the governing equations is required for other types of pressure and velocity inputs.

For all the problems considered the governing differential equations of motion, expressed in nondimensional form for generalization, are integrated by suitable numerical methods which are discussed in the appropriate sections of this thesis.

In order to verify the results of these analyses, various comparisons are made between the results. For example, the results for the period of free radial oscillation of the neo-Hookean thin shell, obtained separately from the incompressible thin shell theory, the compressible thin shell theory and as a limiting case of the Hookean thick shell theory, are compared. The computed results are also compared with the solutions obtained by other investigators for a number of different boundary and initial conditions of the forced oscillation of the thin and thick shells.

In all these comparisons, the results, shown in graphical and tabular forms, are found to be consistent.

Finally, for completeness of the investigation, the variation with time of the tangential and shear stresses at the inner surface of the compressible thick-walled shell are plotted as shown in Figures 20 and 22.

CHAPTER 2

THE HYPERELASTIC MATERIAL

2.1 Strain Energy Functions and Constitutive Relations

The strain energy function, W per unit undeformed volume, of an isotropic hyperelastic solid is a function

$$W = W(I_1, I_2, I_3) \tag{2.1}$$

of the basic invariants

$$I_1 = \text{tr}\, \underset{\sim}{B},\ I_2 = \tfrac{1}{2}[(\text{tr}\, \underset{\sim}{B})^2 - \text{tr}\, \underset{\sim}{B}^2] \text{ and}$$

$$I_3 = \det \underset{\sim}{B} \tag{2.2}$$

of the left Cauchy-Green strain tensor $\underset{\sim}{B} = \underset{\sim}{F}\underset{\sim}{F}^T$ where $\underset{\sim}{F}$ is the deformation gradient tensor.

The constitutive equation is

$$\underset{\sim}{\sigma} = p\, \underset{\sim}{I} + (\phi + I_1\psi)\underset{\sim}{B} - \psi\underset{\sim}{B}^2 \tag{2.3}$$

where $\underset{\sim}{\sigma}$ is the Cauchy stress tensor and

$$p = 2\, I_3^{\frac{1}{2}} \frac{\partial W}{\partial I_3},\ \phi = 2\, I_3^{-\frac{1}{2}} \frac{\partial W}{\partial I_1},\ \psi = 2\, I_3^{-\frac{1}{2}} \frac{\partial W}{\partial I_2} \tag{2.4}$$

The constitutive equation (2.3) reduces to the classical stress-strain relation

$$\underset{\sim}{\sigma} = 2\,\mu\,\underset{\sim}{e} + (\lambda \operatorname{tr} \underset{\sim}{e})\,\underset{\sim}{I} \tag{2.5}$$

when terms $O(\underset{\sim}{e}^2)$ are neglected.

When the material is incompressible, $I_3 = 1$ and p becomes a Lagrangian multiplier, which is no longer determined by the deformation but must be obtained from equilibrium conditions.

2.2 Particular Strain Energy Functions

We consider the following strain energy functions

$$W = \frac{\mu}{2}\,[c(I_1-3) + (1-c)(I_2-3)] \quad \text{where } 0<c\leq 1 \tag{2.6}$$

$$W = \frac{\mu}{2}\,[c(I_1-3) + 3(1-c)\ell n \frac{I_2}{3}] \quad \text{where } c>0 \tag{2.7}$$

and

$$W = \frac{\mu}{2}\,[(I_1-3) - \frac{1}{s}(I_3^{\,s} - 1)] \tag{2.8}$$

where μ is the shear modulus for infinitesimal strain from the undeformed state and

$$s = \frac{-\nu}{1-2\nu} \tag{2.9}$$

where ν is Poisson's ratio for infinitesimal deformation from the undeformed state.

The strain energy function given by equation (2.6) was proposed for an incompressible material independently by Mooney and Rivlin*. Equation (2.7) is also for an incompressible material and was proposed jointly by Gent and Thomas*, while the function given by equation (2.8) was proposed for a class of compressible rubbery materials jointly by Blatz and Ko+. This latter strain energy function has been examined in detail by HADDOW AND FAULKNER [12] for the static problem of finite expansion.

A special case of each of these strain energy functions is the neo-Hookean form

$$W = \frac{\mu}{2} (I_1 - 3) \qquad (2.10)$$

which is obtained from equations (2.6) and (2.7) when $c = 1$ and as a limiting case of equation (2.8) as ν approaches 0.5.

The restrictions on W, which must be satisfied to ensure a periodic motion of the spherical shell, are discussed in section (B.1) of Appendix B.

---

* See ADKINS [15].

+ See BLATZ and KO [16].

CHAPTER 3

THIN SHELL PROBLEMS

3.1 Approximate Theory for Thin-walled Shells

Using the notations for the thin shell problem, let

$$\varepsilon = \frac{T}{R} \tag{3.1}$$

and assume that ε is small enough to justify the neglect of terms $O(\varepsilon^2)$, and this is done without comment in what follows. The mean radial and circumferential stretches are then given by

$$\bar{\delta} = \frac{t}{T} \quad \text{and} \quad \bar{\lambda} = \frac{\bar{r}}{\bar{R}} \tag{3.2}$$

respectively, and

$$\frac{t}{\bar{r}} = \frac{\varepsilon\bar{\delta}}{\bar{\lambda}} . \tag{3.3}$$

The following relations, then, hold

$$B = \bar{R}\ (1 + \frac{\varepsilon}{2}), \quad A = \bar{R}\ (1 - \frac{\varepsilon}{2}) \tag{3.4}$$

and

$$b = \bar{r}\ (1 + \frac{\varepsilon\bar{\delta}}{2\bar{\lambda}}), \quad a = \bar{r}\ (1 - \frac{\varepsilon\bar{\delta}}{2\bar{\lambda}}) \tag{3.5}$$

Mean radial and circumferential stresses are defined by the equation

$$[\bar{\sigma}_r, \bar{\sigma}_\theta] = 3(b^3-a^3)^{-1}\int_a^b [\sigma_r,\sigma_\theta]\eta^2 d\eta \tag{3.6}$$

This equation, along with equations (3.5), gives the relation

$$\bar{\sigma}_r = -\frac{1}{2}(q_i + q_o) \ . \tag{3.7}$$

The equation of motion of the thin shell can now be derived from the theorem that relates surface tractions to the mean hydrostatic stress as follows.

This theorem, the proof of which is given in Section D.1 of Appendix D, leads to the equation

$$\int_S \underset{\sim}{T} \cdot \underset{\sim}{r}\, dS - \int_V \rho\ddot{\underset{\sim}{r}} \cdot \underset{\sim}{r}\, dV = 3V\sigma \tag{3.8}$$

where V is the volume, S the surface, $\underset{\sim}{T}$ the surface traction, $\underset{\sim}{r}$ the position or radius vector and σ is the average hydrostatic stress.

It follows from this last equation, along with equations (3.5) and (3.6), that

$$\bar{\sigma}_\theta = \frac{1}{2}\left[\frac{\bar{\lambda}}{\varepsilon\bar{\delta}}(q_i-q_o-\rho\ddot{\bar{r}}t) - (q_i+q_o)\right] \tag{3.9}$$

and on substituting equation (3.7) we get

$$\overline{\sigma}_\theta - \overline{\sigma}_r = \frac{\overline{\lambda}}{2\varepsilon\overline{\delta}} (q_i - q_o - \rho\ddot{\overline{r}}t) \ . \qquad (3.10)$$

This is the equation of motion for the thin-walled shell of either compressible or incompressible material, the final form of which is obtained after substituting for $\overline{\sigma}_\theta$ and $\overline{\sigma}_r$ from equation (2.3) for a given strain energy function, W.

For convenience, we drop the bars on the mean quantities so that equations (3.7) and (3.10) become respectively

$$\sigma_r = -\frac{1}{2} (q_i + q_o) \qquad (3.11)$$

and

$$\sigma_\theta - \sigma_r = \frac{\lambda}{2\varepsilon\delta} (q_i - q_o - \rho\ddot{r}t) \qquad (3.12)$$

where $\rho = \rho_0/(\delta\lambda^2)$ is the mean density of the shell, ρ_0 is the density in the undeformed state, and $\ddot{r}$ is the second derivative of r with respect to dimensioned time τ.

For a thin-walled spherical shell, the mean physical components of the tensor $\underset{\sim}{B}$ are given by

$$\begin{bmatrix} \delta^2 & 0 & 0 \\ 0 & \lambda^2 & 0 \\ 0 & 0 & \lambda^2 \end{bmatrix} \qquad (3.13)$$

3.2 The Incompressible Case

Incompressibility condition gives

$$\delta = \lambda^{-2} \tag{3.14}$$

Substituting equations (3.13) and (3.14) in equation (2.3) and putting the resulting expressions for σ_r and σ_θ in equation (3.12) we obtain the equation of motion

$$q_i - q_o - \rho\ddot{r}t = 2\varepsilon[(\frac{1}{\lambda} - \frac{1}{\lambda^7})\phi + (\lambda - \frac{1}{\lambda^5})\psi]. \tag{3.15}$$

To non-dimensionalize this equation, we divide it through by μ to obtain

$$\frac{q_i - q_o}{\mu} - \frac{\rho\ddot{r}t}{\mu} = 2\varepsilon[(\frac{1}{\lambda} - \frac{1}{\lambda^7})\frac{\phi}{\mu} + (\lambda - \frac{1}{\lambda^5})\frac{\psi}{\mu}]. \tag{3.16}$$

Putting $\frac{q_i - q_o}{\mu} = Q$ as the non-dimensional input pressure at the inner surface,

$$\Phi = \frac{\phi}{\mu} \text{ and } \Psi = \frac{\psi}{\mu} \tag{3.17}$$

and noting that

$$\frac{\rho\ddot{r}t}{\mu} = \frac{\rho_o\ddot{r}t}{\mu\lambda^2\delta} = \frac{r''t}{\lambda^2\delta R^2} = \frac{\lambda''\varepsilon}{\lambda^2} \tag{3.18}$$

where r'' is the second derivative of r with respect to the non-dimensional time, $\overline{\tau}$, then equation (3.16) becomes

$$\frac{Q\lambda^2}{\varepsilon} = \lambda'' + 2\left[\left(\lambda - \frac{1}{\lambda^5}\right)\Phi + \left(\lambda^3 - \frac{1}{\lambda^3}\right)\Psi\right] . \tag{3.19}$$

On substituting values for Φ and Ψ for a given strain energy function W, subject to the incompressibility condition (3.14), equation (3.19) gives the final non-dimensional form of the equation of motion of the thin incompressible shell. It is a second order non-linear ordinary differential equation which can be solved numerically by using for example, the fourth order Runge-Kutta process or a modified version of the method of discrete variables as described in Appendix A and shown in Programs 3a and 4a.

We note further that after substituting for Φ, Ψ and Q, equation (3.19) can be integrated directly to obtain the energy equation. Thus, for the Mooney-Rivlin material, the equation of motion is

$$\lambda'' = \frac{Q\lambda^2}{\varepsilon} - 2\,c\left(\lambda - \frac{1}{\lambda^5}\right) - 2(1-c)\left(\lambda^3 - \frac{1}{\lambda^3}\right) \tag{3.20}$$

for constant Q.

This equation gives

$$\frac{\lambda' d\lambda'}{d\lambda} = \frac{Q\lambda^2}{\varepsilon} - 2c(\lambda - \frac{1}{\lambda^5}) - 2(1-c)(\lambda^3 - \frac{1}{\lambda^3}) . \tag{3.21}$$

Integrating this last equation and using the initial conditions

$$\lambda'(0) = 0 \quad \text{and} \quad \lambda(0) = 1 \tag{3.22}$$

we get the energy equation

$$\frac{\lambda'^2}{2} = \frac{Q}{3\varepsilon}(\lambda^3 - 1) - 2c(\frac{\lambda^2}{2} + \frac{1}{4\lambda^4})$$

$$- 2(1-c)(\frac{\lambda^4}{4} + \frac{1}{2\lambda^2}) + \frac{3}{2} . \tag{3.23}$$

The conditions for the motion of the shell to be periodic follow at once as discussed in Section B.1 of Appendix B.

In the special case of the neo-Hookean solid, for which c = 1 in the foregoing equations, equations (3.20) and (3.23) reduce respectively to

$$\lambda'' = \frac{Q\lambda^2}{\varepsilon} - 2(\lambda - \frac{1}{\lambda^5}) \tag{3.24}$$

and

$$\frac{\lambda'^2}{2} = \frac{Q}{3\varepsilon}(\lambda^3 - 1) - 2(\frac{\lambda^2}{2} + \frac{1}{4\lambda^4} - \frac{3}{4}) . \tag{3.25}$$

To find the maximum value, Q_{max}, of the applied step input pressure Q, for which a periodic motion is possible, we consider the critical case depicted by curve (b) of Fig. 2, for which λ_d is a common root of equations (3.24) and (3.25). Following the procedure of Section B.3 of Appendix B, we solve these equations simultaneously, when $\lambda'' = 0$ and $\lambda' = 0$ respectively, to obtain for $\varepsilon = 0.05$, $Q_{max} = 0.0556$ at $\lambda_d = 1.7317$. This critical condition is shown in Fig. 10b. Furthermore, for a value of $Q < Q_{max}$, say $Q = 0.02$, the finite period of oscillation is 2.0864. The response curve for this case is shown in Fig. 14a. Also, as Q approaches zero, say $Q = 10^{-6}$, the period of oscillation is approximately 1.8141. This is the same as the result of linear elasticity theory as further discussed in Section 6.3. The response curve for this limiting case is shown in Fig. 14b, and the phase diagram in Fig. 10c. This latter curve is elliptic, which indicates a harmonic oscillation, as further discussed in Section 6.3.

3.3 The Compressible Case

Let $q_i = q$ and $q_o = 0$, then equations (3.11) and (3.12) become respectively

$$\sigma_r = -\frac{1}{2} q \tag{3.26}$$

and

$$\sigma_\theta - \sigma_r = \frac{1}{2}\left[\frac{\lambda}{\varepsilon\delta}\left(q - \frac{\lambda''\varepsilon}{\lambda^2}\right)\right] . \qquad (3.27)$$

For the Blatz-Ko material, the strain energy function W, given in equation (2.8), is

$$W = \frac{\mu}{2}\left[(I_1 - 3) - \frac{1}{s}(I_3{}^s - 1)\right]$$

where

$$s = \frac{-\nu}{1-2\nu}$$

and ν is Poisson's ratio for infinitesimal deformation from the undeformed state. From this expression and equation (2.3), we have

$$\sigma_r = \frac{\delta}{\lambda^2} - (\lambda^2\delta)^{2s-1} \qquad (3.28)$$

and

$$\sigma_\theta = \frac{1}{\delta} - (\lambda^2\delta)^{2s-1} \qquad (3.29)$$

Substituting equation (3.28) in (3.26), we get

$$q = -2\left[\frac{\delta}{\lambda^2} - (\lambda^2\delta)^{2s-1}\right] \qquad (3.30)$$

and substituting equations (3.28) and (3.29) in (3.27), we have

$$\lambda'' = \frac{q\lambda^2}{\varepsilon} - 2\left(\lambda - \frac{\delta^2}{\lambda}\right) \qquad (3.31)$$

Equations (3.30) and (3.31) are a pair of non-linear ordinary differential equations, in λ and δ, governing the motion of a thin-walled shell of compressible Blatz-Ko material. This pair of equations is integrated numerically by combining the Newton-Raphson root-finding method with the method of discrete variables as described in the algorithm of Section A.5 of Appendix A.

The static curves of Fig. 1c are obtained by solving equations (3.30) and (3.31) simultaneously for $\lambda'' = 0$. These curves are the same form as the static curve (i) of Fig. 1a for the neo-Hookean material. Hence the conditions for a periodic motion of the thin shell of compressible Blatz-Ko material, are the same as given for the neo-Hookean thin shell in Section B.1 of Appendix B.

The neo-Hookean solid is a limiting case of the Blatz-Ko material as Poisson's ratio, ν, approaches 0.5. For $\nu = 0.49$ and $\varepsilon = 0.05$, results computed from equations (3.30) and (3.31) agree well with those of Section 3.2. Thus, $Q_{max} = 0.0556$ and $\lambda_d = 1.7320$. Also, for $Q = 0.02$, the finite period of oscillation is 2.0893 and as $Q \to 0$, the period is approximately 1.8157.

3.4 Specific Examples

Based on the foregoing analyses, the following specific examples have been evaluated.

(i) The neo-Hookean solid,

(ii) the Mooney-Rivlin material for which $c = 0.9$ and

(iii) the Blatz-Ko material for which $\nu = 0.3$.

3.4.1 The neo-Hookean solid

The neo-Hookean solid is a special case of the Mooney-Rivlin material and a limiting case of the Blatz-Ko material. Results of numerical calculations, based on the strain energy functions for each of these latter materials, agree well. Thus, as shown previously in Sections 3.2 and 3.3, $Q_{max} = 0.0556$, $\lambda_d = 1.732$, the period of oscillation for $Q = 0.02$ is approximately 2.088 and as $Q \to 0$, the period is approximately 1.815.

3.4.2 The Mooney-Rivlin material

Consider the case $c = 0.9$ in equations (3.20) and (3.23) when $\varepsilon = 0.05$. Computation, described in Program 2a, gives $Q_{max} = 0.0633$. This is shown in the phase plane diagram of Fig. 11a. For $Q < Q_{max}$, say $Q = 0.06$, the phase plane trajectory, of Fig. 11b, closes, so that the motion is periodic with a finite period of oscillation computed from Program 5a to be 4.2455.

3.4.3 The Blatz-Ko material

Consider the case $\nu = 0.3$ in equations (3.30) and (3.31) when $\varepsilon = 0.05$. Computation, described in Program 2c, gives $Q_{max} = 0.047545$. This is shown in the phase plane diagram of Fig. 13b. For $Q < Q_{max}$, say $Q = 0.02$, the phase plane trajectory of Fig. 13c, closes, and so the motion is periodic with a finite period of oscillation, 2.6925. Also shown in the phase plane diagram of Fig. 13b is the case $Q = 0.06 > Q_{max}$, for which the phase plane trajectory does not close and so the motion is non-periodic.

3.5 Free Oscillations

For free oscillation, $q_o = q_i = 0$, and the initial conditions are, in general,

$$\lambda(0) = \lambda_0 \quad \text{and} \quad \lambda'(0) = \lambda_0' . \qquad (3.32)$$

If the initial perturbation is a purely radial displacement or velocity, then we have the simpler boundary conditions

$$\lambda(0) = \lambda_0 \quad \text{and} \quad \lambda'(0) = 0 \qquad (3.33)$$

and

$$\lambda(0) = 1 \quad \text{and} \quad \lambda'(0) = \lambda_0' \qquad (3.34)$$

respectively.

When the amplitude of oscillation approaches zero, the response approaches that predicted by linear elasticity theory.

For the Mooney-Rivlin material, the equation of motion, for free oscillation, obtained from equation (3.20), is

$$\lambda'' = -2c(\lambda - \frac{1}{\lambda^5}) - 2(1 - c)(\lambda^3 - \frac{1}{\lambda^3}) . \qquad (3.35)$$

This is a second order non-linear ordinary differential equations which can be integrated numerically as before, subject now to any of the initial conditions (3.32) - (3.34).

In particular, for c = 1, and with the initial conditions: $\lambda_0' = 0$ and $\lambda_0 \approx 1$, say 1.005, equation (3.35) describes a free radial oscillation of the neo-Hookean thin shell. Computations yield the phase plane diagrams of Fig. 10d. This phase trajectory is an ellipse, which indicates that the motion is harmonic. The period of oscillation is 1.8140, which is the same as the result obtained from the linear theory*.

---

* See Rayleigh's method of Section 4.2.

CHAPTER 4

THICK SHELL PROBLEMS

4.1 General Discussion

The ratio ε, of wall thickness T, to the mean radius $\overline{R}$, of a shell is given, in the notation for thick shells, by the equation

$$\varepsilon = \frac{T}{\overline{R}} = \frac{2(\frac{B}{A} - 1)}{(1 + \frac{B}{A})} \tag{4.1}$$

where A and B are respectively the inner and outer radii of the shell in the undeformed state. When ε is sufficiently large that terms $O(\varepsilon^2)$ are no longer negligible, the spherical shell is considered thick-walled. This condition usually holds for shells for which $\frac{B}{A} > 1.1$ or $\frac{T}{A} > 0.1$.

For such thick-walled shells, the following problems are considered.

(i) Free radial oscillation of the thick incompressible shell of linear elasticity using Rayleigh's method.

(ii) Forced oscillation, under a step function application of pressure, of the thick compressible shell of linear elasticity using the method of characteristics.

(iii) Finite oscillation of the thick incompressible shell of non-linear elasticity using a strain energy function and an acceleration potential.

The following special cases are then examined in Section 4.5.

(i) The thick shell results approaching those of the thin shell theory when $\frac{T}{A} \leq 0.1$.

(ii) The results of non-linear elasticity approaching those of linear elasticity as deformation approaches zero.

4.2 Incompressible Shell in Linear Elasticity: Free Radial Oscillation by Rayleigh's Method

Consider a shell of incompressible material with inner and outer radii, A and B respectively, as shown in Fig. 3. For radial oscillation, this body is a single degree of freedom system and since there is no dissipation of energy, the single or fundamental frequency of vibration can be determined, using Rayleigh's method, from the energy equation

$$T_{max} = V_{max} \tag{4.2}$$

where T_{max} is the maximum kinetic energy and V_{max} is the maximum potential energy of the system.

To find T_{max}, let a be the amplitude of oscillation at the inner radius A, and u the amplitude at the reference radius R, then, since the motion is harmonic, the maximum velocity at R is $(u\omega)$, where ω is the fundamental frequency of free oscillation in radians per second. If dm is the mass of the elemental shell of radius R, thickness dR, and volume $d\overline{V}$, then

$$T_{max} = \int_A^B \frac{1}{2} (u\omega)^2 \, dm, \tag{4.3}$$

and

$$dm = \rho d\overline{V} = 4\pi\rho R^2 dR \tag{4.4}$$

where ρ is the density. It follows then from equations (4.3) and (4.4) that

$$T_{max} = \int_A^B 4\frac{\pi}{2}\rho\omega^2 u^2 R^2 dR \, . \tag{4.5}$$

For an incompressible material, a and u are related by the equation

$$\frac{4}{3}\pi(R^3 - A^3) = \frac{4}{3}\pi[(R + u)^3 - (A + a)^3] \tag{4.6}$$

Neglecting terms $O(a^2)$, this equation gives

$$u \approx \frac{A^2}{R^2} a \quad . \tag{4.7}$$

Substituting for u from equation (4.7) in (4.5), we get

$$T_{max} = 2\pi\rho\omega^2 A^4 a^2 \int_A^B \frac{dR}{R^2}$$

Thus

$$T_{max} = 2\pi\rho\omega^2 A^4 a^2 \left(-\frac{1}{B} + \frac{1}{A}\right) . \qquad (4.8)$$

To find V_{max}, we consider the strain energy V, per unit volume given by

$$V = \frac{1}{2}\,\sigma_{ij}\,e_{ij} \qquad (4.9)$$

where the physical components of the strain tensor, e_{ij}, are given by

$$\begin{bmatrix} \frac{du}{dR} & 0 & 0 \\ 0 & \frac{u}{R} & 0 \\ 0 & 0 & \frac{u}{R} \end{bmatrix} . \qquad (4.10)$$

For an incompressible material, the linear stress-strain relation (2.5) reduces to the 'deviatoric' relation

$$\sigma'_{ij} = 2\mu\, e'_{ij} \qquad (4.11)$$

where μ is the shear modulus for infinitesimal strain from the undeformed state.

Substituting for σ_{ij} from equation (4.11) in (4.9) we get

$$V = \mu\, e_{ij}\, e_{ij}$$

and from equation (4.10), this becomes

$$V = \mu\left[\left(\frac{du}{dR}\right)^2 + 2\left(\frac{u}{R}\right)^2\right] . \qquad (4.12)$$

Since $e_{kk} = 0$ for an incompressible material, equation (4.10) gives the relation

$$\frac{du}{dR} = -2\left(\frac{u}{R}\right) . \qquad (4.13)$$

From equations (4.13) and (4.12) we have

$$V = 6\mu\left(\frac{u}{R}\right)^2 . \qquad (4.14)$$

Using equation (4.7) and the expression

$$d\overline{V} = 4\pi R^2 dR ,$$

we find

$$V_{max} = \int_A^B 24\pi\mu A^4 a^2 \frac{dR}{R^4}$$

which, on integrating, gives

$$V_{max} = 8\mu\pi A a^2 \frac{(B^3-A^3)}{B^3}$$

Now, by equation (4.2), equations (4.8) and (4.15) give for the frequency, ω, of the single mode of vibration the expression

$$\omega = [4\mu(B^2 + AB + A^2)/\rho A^2 B^2]^{\frac{1}{2}} \qquad (4.16)$$

Putting $\frac{B}{A} = N$, equation (4.16) can be written as

$$\omega = \frac{2}{B} \left[\frac{\mu}{\rho} (N^2 + N + 1) \right]^{\frac{1}{2}} \qquad (4.17)$$

and the period of oscillation, T, is

$$T = \frac{2\pi}{\omega} = \pi B \{\rho / [\mu (N^2 + N + 1)]\}^{\frac{1}{2}}$$

If we non-dimensionalize the period by using the expression

$$\bar{T} = \frac{T}{A}\sqrt{\frac{\mu}{\rho}},$$

we find that the non-dimensional period, $\bar{T}$, is

$$\bar{T} = \pi N (N^2 + N + 1)^{-\frac{1}{2}} \quad .$$

For $N = \frac{B}{A} = 2$, the period is 2.3758.

In the case of a thin shell, $N \approx 1$, and so the period of free radial oscillation is 1.8146 which agrees with the result obtained in Section 3.5 for the thin-walled neo-Hookean shell.

4.3 Compressible Shell Problem in Linear Elasticity: The Method of Characteristics

4.3.1 Governing equations

The equations describing spherically symmetric motion are

$$\frac{\partial \sigma_r}{\partial t} - \bar{E}(1-\nu) \frac{\partial v}{\partial r} = 2 \bar{E}\nu \frac{v}{r} \qquad (4.18)$$

$$\frac{\partial \sigma_\theta}{\partial t} - \bar{E}\nu \frac{\partial v}{\partial r} = \bar{E}\,\frac{v}{r} \qquad (4.19)$$

$$-\rho\frac{\partial v}{\partial t} + \frac{\partial \sigma_r}{\partial r} = -2\,\frac{(\sigma_r - \sigma_\theta)}{r} \qquad (4.20)$$

where

$$\bar{E} = E/[(1+\nu)(1-2\nu)] \quad . \qquad (4.21)$$

Equations (4.18) - (4.20) form a system of three linear first order partial differential equations with σ_r, σ_θ and v as the dependent variables and r and t as the independent variables. These equations are fully hyperbolic and they permit the propagation of jumps in the derivatives of σ_r, σ_θ and v in the characteristic directions. The equations of these characteristic curves can be derived as follows.

4.3.2 Equations of the characteristic curves

The curves in the (r,t) plane along which σ_r, σ_θ and v are continuous but their derivatives are not necessarily so are called characteristic curves and the equations governing the variations of σ_r, σ_θ and v along the characteristic curves are called the characteristic equations.

The characteristic curves for the set of equations (4.18) - (4.20), derived in Section D.2

of Appendix D, Are

$$I^{\pm} : \frac{dr}{dt} = \pm c \ , \qquad (4.22)$$

$$II \ : dr = 0 \ . \qquad (4.23)$$

The I^+ characteristic, labelled in Fig. 4, represents the line along which discontinuities in the partial derivatives of σ_r, σ_θ and v propagate to the right with velocity c, while the I^- is the path of propagation of these discontinuities to the left. The II characteristic is the degenerate case of the dynamic wave at a given radial location, r = constant. For homogeneous materials, the quantities E, ν and ρ are constant and so the velocity of wave propagation is also constant. Consequently, the characteristics form three families of parallel straight lines.

Substituting the expressions for dr/dt of equation (4.22) in equations (4.18) and (4.20) and putting that for dr of equation (4.23) in (4.18) and (4.19), we obtain, after using the relation (4.21), the following characteristic equations respectively. Along $I^{\pm}$, we have

$$d\sigma_r \mp \rho c dv = [-2(\sigma_r - \sigma_\theta) \pm 2\rho c \frac{\nu}{1-\nu} v] \frac{dr}{r} \ , \qquad (4.24)$$

and along II, the characteristic equation is

$$\nu d\sigma_r = (1-\nu)d\sigma_\theta - E\frac{v}{r}dt , \qquad (4.25)$$

where E is Young's modulus for infinitesimal strain from the undeformed state.

4.3.3 Strong discontinuities in σ_r, σ_θ and v across the wavefront

For a shell of finite thickness, say with $\frac{T}{A} = 1$, the characteristic field obtained from equations (4.22) and (4.23) is shown schematically in Fig. 4. The arrows indicate the path of the wavefront. Reflections of the wave occur on the inner and outer boundaries at points C, D, E etc. AC is the initial propagation line and so the region ABC has zero stresses and velocity and is called the undisturbed region.

Jumps occur in the values of σ_r, σ_θ and v as the wave propagates back and forth in the medium under a step function application of internal pressure. These jumps are the difference in values of the quantities σ_r, σ_θ and v ahead of and behind the wavefront. At the instant of reflection a double jump occurs, once across the I^+ and the other across the I^- characteristic.

The equations governing the propagation of these strong discontinuities have been derived from the governing equations by CHOU and KOENIG [8] and these lead to the general discontinuity relations

$$[\sigma_r] = \frac{K}{r} \tag{4.26}$$

$$[\sigma_\theta] = \frac{\nu}{1-\nu}\frac{K}{r} \tag{4.27}$$

$$[v] = \mp \frac{1}{\rho c}\frac{K}{r} \tag{4.28}$$

where K is a constant which is determined from given boundary conditions as indicated in Section C.2 of Appendix C. The upper and lower signs of equation (4.28) are for the I^+ and I^- wavefronts respectively.

In using the boundary condition at the inner surface to find K, we note that if the input function is not suddenly applied, K = 0, and there is no discontinuity in the values of σ_r, σ_θ and v across the wavefronts.

4.3.4 Integration of the characteristic equations

The procedure for integrating the characteristic equations (4.24) and (4.25), which incorporates the discontinuity relations (4.26) - (4.28) is discussed in Section C.1 of Appendix C. The method has been developed from the procedure used by LEONARD and BUDIANSKY [9] to solve some beam vibration problems.

The response curves of the inner and outer surfaces of the shell with $\frac{B}{A} = 2$, for a step input pressure $Q = 1.0$, are shown in Fig. 19a. The curves indicate that this forced motion of the compressible thick-walled shell is non-periodic.

The limiting case of a thin shell is examined by considering a suitable value of ε, the ratio of wall thickness to mean radius, which is given in terms of $\frac{B}{A}$, in equation (4.1), as

$$\varepsilon = 2 \frac{(\frac{B}{A} - 1)}{(1 + \frac{B}{A})} .$$

For example, when $\varepsilon = 0.05$ and $Q = 0.001$, we obtain the response curve of Fig. 19c, which shows the motion to be periodic. Furthermore, as $Q \to 0$, the oscillation approaches a harmonic oscillation, depicted by the diagram of Fig. 19d .

4.4 Finite Oscillation of the Incompressible Shell in non-Linear Elasticity

The equation of motion of the inner surface of a thick incompressible spherical shell, as derived by ERINGEN and ŞUHUBI [10], is, in non-dimensional form,

$$2xx'' \left[1 + \left(1 + \frac{\gamma}{x^3}\right)^{-\frac{1}{3}}\right] + x'^2 \left[3 - 3\left(1 + \frac{\gamma}{x^3}\right)^{-\frac{1}{3}} - \left(\frac{\gamma}{x^3}\right)\left(1 + \frac{\gamma}{x^3}\right)^{-\frac{4}{3}}\right] + \overline{g}\,(x,\gamma) = 2\overline{Q} \tag{4.29}$$

where, using the notation for the thick incompressible shell,

$$x(t) = \frac{a(t)}{A} , \tag{4.30}$$

$$\gamma = \left(\frac{B}{A}\right)^3 - 1 > 0 , \tag{4.31}$$

and

$$\overline{g}(x,\gamma) = 2 \int_{\frac{\gamma+x^3}{1+\gamma}}^{x^3} \frac{d\overline{W}}{du} \frac{du}{(u-1)} , \tag{4.32}$$

where $\overline{W} = \frac{W}{\mu}$ and $u(R,t) = \frac{r^3}{R^3}$. The boundary conditions are represented by

$$\overline{Q} = \frac{Q}{\mu} = \frac{q_i(t) - q_o(t)}{\mu} \qquad (4.33)$$

where $q_i(t)$ and $q_o(t)$ are the internal and external applied pressures and μ is the shear modulus for infinitesimal deformation from the undeformed state.

Equation (4.29) is a second order non-linear ordinary differential equation, the final form of which is obtained by substituting a given expression for $\overline{W}$. The equation is thereafter solved numerically using a suitable numerical technique such as a fourth order Runge-Kutta process or the method of discrete variables as was done for thin shell problems in Sections 3.2 and 3.3.

In the case of the neo-Hookean solid,

$$\overline{W} = \frac{1}{2}(I_1 - 3) \qquad (4.34)$$

from which we have

$$\frac{d\overline{W}}{du} = \frac{4}{3}(u)^{-\frac{1}{3}}(1 - u^{-2})\frac{\partial\overline{W}}{\partial I_1} = \frac{2}{3}(u)^{-\frac{1}{3}}(1 - u^{-2}) \qquad (4.35)$$

and

$$\overline{g}(x,\gamma) = \frac{4}{3}\int_{\frac{\gamma+x^3}{1+\gamma}}^{x^3}\left[\frac{(u)^{-\frac{1}{3}}(1-u^{-2})}{u-1}\right]du \qquad (4.36)$$

On integrating, equation (4.36) gives

$$\bar{g}(x,\gamma) = -\left[4x^{-1} + x^{-4} - 4\left(\frac{\gamma+x^3}{1+\gamma}\right)^{-\frac{1}{3}} - \left(\frac{\gamma+x^3}{1+\gamma}\right)^{-\frac{4}{3}}\right] \qquad (4.37)$$

Substituting equation (4.37) in (4.29) we get the equation of motion

$$x'' = -\frac{x'^2}{2x}\left\{3 - \frac{\left(\frac{\gamma}{x^3}\right)\left(1+\frac{\gamma}{x^3}\right)^{-\frac{4}{3}}}{\left[1-\left(1+\frac{\gamma}{x^3}\right)^{-\frac{1}{3}}\right]}\right\} - \left\{\frac{\left[4x^{-1} + x^{-4} - 4\left(\frac{\gamma+x^3}{1+\gamma}\right)^{-\frac{1}{3}} - \left(\frac{\gamma+x^3}{1+\gamma}\right)^{-\frac{4}{3}} + 2\bar{Q}\right]}{2x\left[1 - \left(1+\frac{\gamma}{x^3}\right)^{-\frac{1}{3}}\right]}\right\} \qquad (4.38)$$

This last equation is solved for (i) various values of γ, corresponding to different thicknesses of the shell, and a fixed value of constant internal pressure Q, the results of which are shown in Fig. 23a and (ii) various values of Q for a fixed value of γ, the results of which are shown in Fig. 23b.

The response of the inner surface, or indeed of any given radial location, of the thick incompressible shell is found to be periodic with a period and an amplitude which vary with the values of the internal step input pressure Q and the ratio $\frac{B}{A}$, of the outer to the inner radius.

In particular, for $Q = 0.05$, and $\frac{B}{A} = 2$, the period of oscillation of the inner surface is 2.4509. The response curve is shown in Fig. 23a.

The result, plotted in Fig. 23c, for the limiting case of a thin shell for which $\varepsilon = 0.05$ under a pressure $Q = 0.02$ is identical to the previous result of Section 3.2 plotted in Fig. 14a. Also, as $Q \rightarrow 0$ in the thin shell limiting case, we get for the period of oscillation the value 1.8158 which agrees with the linear elasticity result quoted in Section 3.2.

4.5 Special Cases

4.5.1 Thin shell as limiting case of the thick shell

When $\varepsilon = \frac{T}{\bar{R}}$, where T is the wall thickness and $\bar{R}$ is the mean radius of the shell, is such that terms $O(\varepsilon^2)$ are negligible, we have an approximation to the thin shell behaviour. Results obtained from the thick shell theory then approach those of the thin shell analysis. For example, the period of free radial oscillation for the thin incompressible neo-Hookean solid with $\varepsilon = 0.05$ is 1.8140, and the thick shell theory gives 1.8158. Further comparison of results is given in Section 6.3.

4.5.2 Linear theory as limiting case of the non-linear theory of elasticity

When the applied pressure Q is small enough to produce only vanishingly small strains, the constitutive equation (2.3) reduces to the linear isotropic stress-strain relation (2.5). Results of the non-linear theory are then in close agreement with the results of linear theory of elasticity. In particular, as $Q \rightarrow 0$ the period of radial oscillation for the thin incompressible neo-Hookean shell, is 1.8141, the value obtained from linear theory is 1.8146.

CHAPTER 5

OTHER METHODS OF SOLUTION

1. For the non-linear problem of the thin incompressible shell, the method of solution used by WANG [13] does not assume a strain energy function, W. Instead, the constitutive equation is written in the form

$$\underset{\sim}{\sigma} = -P\underset{\sim}{I} + f\underset{\sim}{B} + g\underset{\sim}{B}^{-1} \tag{5.1}$$

where $\underset{\sim}{\sigma}$ is the stress tensor, P an undetermined hydrostatic pressure, $\underset{\sim}{B} = \underset{\sim}{F}\underset{\sim}{F}^T$ is the left Cauchy-Green strain tensor and f,g are functions of the invariants I_1, I_2 and I_3 of the tensor $\underset{\sim}{B}$ defined in Section 2.2.

Wang derived the equation of motion under an internal step input pressure Q, in the notations used for thin shells, as

$$-\frac{Qr^2}{R^3\varepsilon} = \rho\ddot{r} + \frac{2}{r}\left[\left(\frac{r^2}{R^2} - \frac{R^4}{r^4}\right)f - \left(\frac{r^4}{R^4} - \frac{R^2}{r^2}\right)g\right] \tag{5.2}$$

This equation is here shown to be equivalent to equation (3.15) as follows. From equations (5.1) and (3.13), we have for σ_r and σ_θ

$$\sigma_r = -P + f\delta^2 + g\delta^{-2} \tag{5.3}$$

$$\sigma_\theta = -P + f\lambda^2 + g\lambda^{-2} \tag{5.4}$$

Using the incompressibility condition (3.14) equation (5.3) becomes

$$\sigma_r = -P + f\lambda^{-4} + g\lambda^4 \tag{5.5}$$

Substituting the expression for σ_θ from equation (5.4) and that for σ_r from equation (5.5) into (3.12) we get for the equation of motion, in terms of f and g,

$$\frac{2\varepsilon\delta}{\lambda}\left[(\lambda^2-\lambda^{-4})f - (\lambda^4-\lambda^{-2})g\right] = (q_i-q_o) - \rho\ddot{r}t. \tag{5.6}$$

Putting $\delta = \lambda^{-2}$, $\rho\ddot{r}t = \rho_0\varepsilon\ddot{\lambda}\lambda^{-2}R^2$ and $q_i - q_o = -Q$, we get

$$-Q = \frac{\rho\ddot{\lambda}\varepsilon R^2}{\lambda^2} + \frac{2\varepsilon}{\lambda^3}\left[(\lambda^2 - \frac{1}{\lambda^4})f - (\lambda^4-\lambda^{-2})g\right] \tag{5.7}$$

which, by setting $\lambda = \frac{r}{R}$, becomes

$$-\frac{Qr^2}{R^3\varepsilon} = \rho\ddot{r} + \frac{2}{r}\left[\left(\frac{r^2}{R^2} - \frac{R^4}{r^4}\right)f - \left(\frac{r^4}{R^4} - \frac{R^2}{r^2}\right)g\right]. \tag{5.8}$$

This is equation (5.2) obtained by Wang.

2. For the thick incompressible shell problem of non-linear elasticity, an alternative method, which does not use an acceleration potential, has been given by ZHONG-HENG and SOLECKI [11]. This method leads to the following form, using the same notation as in Section 4.4, of the equation of motion

$$\frac{d}{dx}\left\{\left[1-\left(1+\frac{\gamma}{x^3}\right)^{-\frac{1}{3}}\right]x^3\dot{x}^2\right\}+x^2\,g(x,\gamma) = \frac{2x^2}{\rho A^2}\,Q \qquad (5.9)$$

which, after performing the differentiation on the left-hand side, becomes

$$2x\ddot{x}\left[1-\left(1+\frac{\gamma}{x^3}\right)^{-\frac{1}{3}}\right]+\dot{x}^2\left[3-3\left(1+\frac{\gamma}{x^3}\right)^{-\frac{1}{3}} -\left(\frac{\gamma}{x^3}\right)\left(1+\frac{\gamma}{x^3}\right)^{-\frac{4}{3}}\right]+g(x,\gamma) = \frac{2}{\rho_A{}^2}\,Q\,. \qquad (5.10)$$

This is the dimensional form of equation (4.29).

3. For the thick compressible shell problem of linear elasticity, a direct analytical method of solution is the infinite series method described by BAKER AND ALLEN [2].

This method is based on the Midlin-Goodman technique which uses an auxiliary variable to eliminate time-dependent boundary conditions.

The results obtained using this method are compared with the solutions obtained in Section 4.3 in Figs. 19e and 19f*. The graphs show that the results are consistent.

---

* See ROSE, CHOU and CHOU [17].

CHAPTER 6

DISCUSSION OF RESULTS

6.1 Precautions in Numerical Computations

All the programs listed at the end of this thesis have been written in the BASIC computer language for running on the 9830 Hewlett Packard desk calculator. To ensure convergence and stability of the numerical computations the integration steps must be suitably chosen. The following integration steps have been found most suitable.

(i) For the method of discrete variables and the fourth order Runge-Kutta process, a time interval, $\delta\tau \leqslant 0.01$ is satisfactory.

(ii) For the method of characteristics, an integration step of $\delta\bar{r} \leqslant 0.05$ is suitable. In the case of a very thick shell, one for which $\frac{T}{A} \geqslant 10$ say, a coarser step of $\delta\bar{r} = 0.1$ has also been found satisfactory.

Computations are relatively slow on the HP9830 calculator, but the overall computing times for specific cases are within acceptable limits. For example, for four cycles of the response curve of Fig. 14a, calculated by the fourth order Runge-Kutta method, using $\delta\tau = 0.01$, the computing time is one hour. For each of the curves in Fig. 19a, using the method of characteristics and an integration step of $\delta\bar{r} = 0.05$, the computing time is three hours and for Fig. 19b, using $\delta\bar{r} = 0.1$, the total time is eight hours.

6.2 Specific Results

6.2.1 Incompressible shells

A periodic motion is obtained, for a shell under an internal step input pressure $Q < Q_{max}$, which is the limiting value of Q discussed in Section B.3 of Appendix B. This type of oscillation is illustrated by phase plane diagrams and response curves, relating the radial stretch λ to the time τ, for the following cases.

1. The thin neo-Hookean shell for which $\varepsilon = 0.05$. Phase plane trajectories for $Q = 0.05 < Q_{max}$, and $Q = 0.06 > Q_{max}$, where $Q_{max} = 0.0556$ are shown in Fig. 10a. That for the limiting case, $Q = Q_{max}$, is shown in Fig. 10b. The response curve for $Q = 0.05$ is shown in Fig. 14c. The motion, in this case, is periodic with a

period of 3.3872.

Free oscillation for vanishingly small amplitude, is represented by the phase plane diagram of Fig. 10d. This is for initial conditions: $\lambda_0 = 1.005$ and $\lambda_0' = 0$. The phase trajectory, in this case, is an ellipse which indicates a harmonic oscillation depicted by the response curve of Fig. 18. The period is computed to be 1.8140.

2. The case of the thin incompressible shell of Mooney-Rivlin material, for which constant, $c = 0.9$ in the strain energy function of equation (2.6). Phase plane trajectories are shown in Figs. 11a and 11b for (i) $Q = 0.06 < Q_{max}$ which gives rise to the periodic oscillation depicted by Fig. 15, (ii) $Q \approx 0.0633 = Q_{max}$, the critical case and (iii) $Q = 0.07 > Q_{max}$.

It is important to note that the periodic motions hitherto considered are for practically realisable values of stretch λ. If, for instance, $\lambda > 3$, a thin shell may rupture because it may not be capable of sustaining such large stretches. Now, an interesting case of $Q > Q_{max}$ is shown in Fig. 11c where the phase trajectory is seen to close again for large enough value of λ, say $\lambda > 5$. This feature is also shown for $Q = Q_{max}$ in Fig. 11a. Whereas these closed trajectories would indicate that periodic motions will occur, these extreme cases may not be realisable in practice.

3. For the thin incompressible shell, of material with the logarithmic strain energy function of equation (2.7), we consider the case for which $c = 2$. Fig. 12 shows the phase plane diagrams for (i) $Q = 0.08 < Q_{max}$ which gives rise to a periodic motion depicted by Fig. 16, (ii) $Q = 0.0811 = Q_{max}$, the critical case and (iii) $Q = 0.082 > Q_{max}$ for which the motion is non-periodic no matter how large a stretch λ is considered. This last case is so because the static curve obtained for the logarithmic strain energy function is similar to that for the neo-Hookean form.

4. The case of the thick incompressible neo-Hookean shell. The response curves for forced motions of shells with various thicknesses, under a constant internal pressure Q, are shown in Fig. 23a. Those for a constant thickness of shell under various internal step input pressures are shown in Fig. 23b.

These graphs indicate that the oscillation is always periodic provided $Q < Q_{max} = 0.0556$.

In the limit, as $\frac{B}{A} \rightarrow 1$ we have the periodic response of Fig. 23c.

6.2.2 Compressible shells

1. The motion of the thin compressible shell, of Blatz-Ko material, under an internal step function application of pressure $Q < Q_{max}$ is found to be periodic. This is illustrated by the phase trajectories of Figs. 13a and 13b and the response curves of Figs. 17a and 17b. In particular, for $Q = 0.02$, $\varepsilon = 0.05$ and $\nu = 0.3$, the response curve and the phase plane diagram are shown respectively in Figs. 17b and 13b. The period of oscillation, for this case, is 2.6925.

2. For the thick compressible shell of linear elasticity, the response of the inner and outer surfaces to an internal constant pressure are shown in Figs. 19a and 19b. The motion, in this case, is non-periodic. In particular, for $\frac{B}{A} = 2$ and $Q = 1$, the response curves of Fig. 19a are obtained. For a very thick shell, for example one for which $\frac{B}{A} = 11$, the response curve of the

inner surface under a pressure Q = 1 is shown in Fig. 19b. This shows an interesting asymptotic feature initiated by the shock wave at the start of motion. The amplitude of motion attenuates in such a way that the displacement approaches the equilibrium state asymptotically like a forced damped oscillation. This is because there is long enough time for the imparted motion to die out before the shock front returns to this surface after reflection at the outer boundary. On return to the inner surface the motion starts again and another cycle of oscillation is performed.

This case of a thick shell illustrates what happens in the case of an infinite medium where the wavefront never gets reflected back into the medium. The response is then similar to one cycle of the thick shell case analogous to forced damped vibration.

Another notable feature in the compressible case is the reflection of the shock front at the bounding surfaces of the shell. These reflections appear as cusps in the response curves. For example, cusps occur on the response curve of Fig. 19a for the inner surface of a shell with

$\frac{B}{2} = 2$ at $\tau = 2, 4, 6...$

Furthermore, we note that the curves of Figs. 19a and 19b agree well with the response curves obtained by other investigators. This is shown by comparing the graphical results, with the series solution obtained by BAKER and ALLEN [2], schematically in Figs. 19e and 19f.

6.3 Comparison of Results

Results obtained by different methods are compared for the following cases.

(i) Free radial oscillation of the thin neo-Hookean shell.

(ii) Free and forced vibration of the thin shell obtained as a limiting case of the thick shell.

(iii) Free and forced vibration of the thin shell of linear elasticity theory obtained as a limiting case of the non-linear theory.

(iv) Forced vibrations of the thick compressible shell compared with the solutions of BAKER and ALLEN [2].

1. Results for the period of free radial oscillation of the thin neo-Hookean shell, obtained by different methods are compared in Table 1. The answers are consistent; giving a period of oscillation of approximately 1.815.

		Thin shell theory		Thin as limiting case of thick shell
		c=1 in Mooney-Rivlin	$\nu \to 0.5$ in Blatz-Ko	
Direct free oscillation for $\lambda_0 = 1.005$, $\dot{\lambda}_0 = 0$		1.8140	1.8154	1.8158
Analytical Solutions	LOVE [1]	N/A	N/A	1.8146
	Rayleigh's Method	N/A	N/A	1.8146

TABLE 1. Comparison of results obtained by different methods for the period of free radial oscillation of a thin neo-Hookean shell, for which $\varepsilon = 0.05$.

2. When ε is taken small enough so that terms $O(\varepsilon^2)$ become negligible, the results of the thick shell theory approach those of the thin shell theory. Consider the following examples.

a) Free oscillation of the neo-Hookean thin shell with $\varepsilon = 0.05$, and initial conditions: $\lambda_0 = 1.005$, and $\lambda_0' = 0$. Thin shell theory gives a period of oscillation of 1.8140, the thick shell theory gives, in the limit, a value 1.8158.

b) Forced vibration of the thin neo-Hookean shell, for which $\varepsilon = 0.05$, under a constant internal pressure $Q = 0.02$. Period obtained from the thin shell theory is 2.0864, that from limiting case of thick shell is 2.1011.

c) Compressible thin shell, with $\nu = 0.3$, $\varepsilon = 0.05$. Period of free oscillation given by LOVE [1] is 2.3062, the result obtained from limiting case of thick shell theory is 2.3054.

3. As Q approaches zero the results of non-linear elasticity approach those of the linear theory. Consider, for example, the thin neo-Hookean shell with $\varepsilon = 0.05$. Period obtained from the linear theory is 1.8146, that obtained

from limiting case of the non-linear theory is 1.8141.

4. Results for the thick compressible shell are compared with the series solution obtained by BAKER and ALLEN [2] in Figs. 19e and 19f.*

---

* See ROSE, CHOU and CHOU [17].

CHAPTER 7

CONCLUDING REMARKS

1. Types of motion

The non-linear elasticity problems of the thin and thick incompressible shells have been solved for admissible strain energy functions. Results indicate that we get the following types of response to an internal step input pressure, Q. Denoting by Q_{max}, the maximum value of Q for which the phase trajectory closes, we have

(i) for $Q < Q_{max}$, motion is periodic with a finite period of oscillation,

(ii) as $Q \rightarrow 0$, the response is that of linear elasticity theory. Consequently, the motion is harmonic with a finite period of oscillation. Free oscillation, which involves only vanishingly small amplitudes, is a special case of the linear theory. For this case, motion is also harmonic with a finite period of oscillation.

(iii) For the linear elasticity problem of the thick compressible shell, where only infinitesimal strains are involved, the motion is non-periodic.

When the shell is very thick, say for $\frac{T}{A} > 10$, each cycle of the response curve resembles that of forced, damped vibration. In the limiting case of a thin shell, when $\frac{B}{A} \rightarrow 1$, the motion approaches a periodic motion, with a finite period of oscillation.

(iv) Forced and free oscillations of non-linear elasticity theory for the thin compressible shell are similar to those of the thin incompressible shell.

2. Numerical methods

Excellent agreement is found between the various computed results, some closed form analytical solutions and the numerical results obtained by other investigators. This validates the results of the numerical methods used in this investigation. These numerical schemes include a modified form of the discrete variable method, the fourth order Runge-Kutta process, and the simple trapezoid rule of integration. Thus proven, these methods can be used reliably to solve spherical shell problems when analytical solutions become intractable.

3. The method of characteristics

The method of characteristics has the advantages, over alternative numerical methods such as the finite-difference method, in being direct, simple and versatile in application. It gives good results especially at instants of wave relections where a truncated series, for example, will give only approximate results. Furthermore, it evaluates the stresses directly during the step-by-step computations, whereas in the alternative methods, these stresses have to be computed separately.

4. Other input functions and boundary conditions

Most of the results have been computed for a step function application of pressure but only a slight modification of the governing equations is required for other pressure and velocity inputs, for example, rectangular and exponential pressure inputs.

In the calculations, non-dimensional quantities have been used. This facilitates a direct extrapolation of the results for similar cases.

5. Extensions

The following extensions can be made to the work presented here.

(i) The theories can be generalised to include cylindrical and plane problems by using appropriate constants in the constitutive equations and by defining the tensor $\underset{\sim}{B}$ accordingly.

(ii) Other admissible strain energy functions, especially for compressible materials, can be investigated. Some of these, discussed by HADDOW and FAULKNER [12], for example the strain energy function

$$\overline{W} = \frac{1}{2}\left[(I_1 - 3) - 2(\sqrt{I_3} - 1) + \frac{1}{1-2\nu}(\sqrt{I_3} - 1)^2\right]$$

will adequately describe the response to dynamic loads of a useful class of compressible materials.

(iii) The analysis based on the method of characteristics can be extended to the non-linear elasticity problem of the thick compressible spherical shell. This problem will be found complex because the characteristic curves are no longer straight lines.

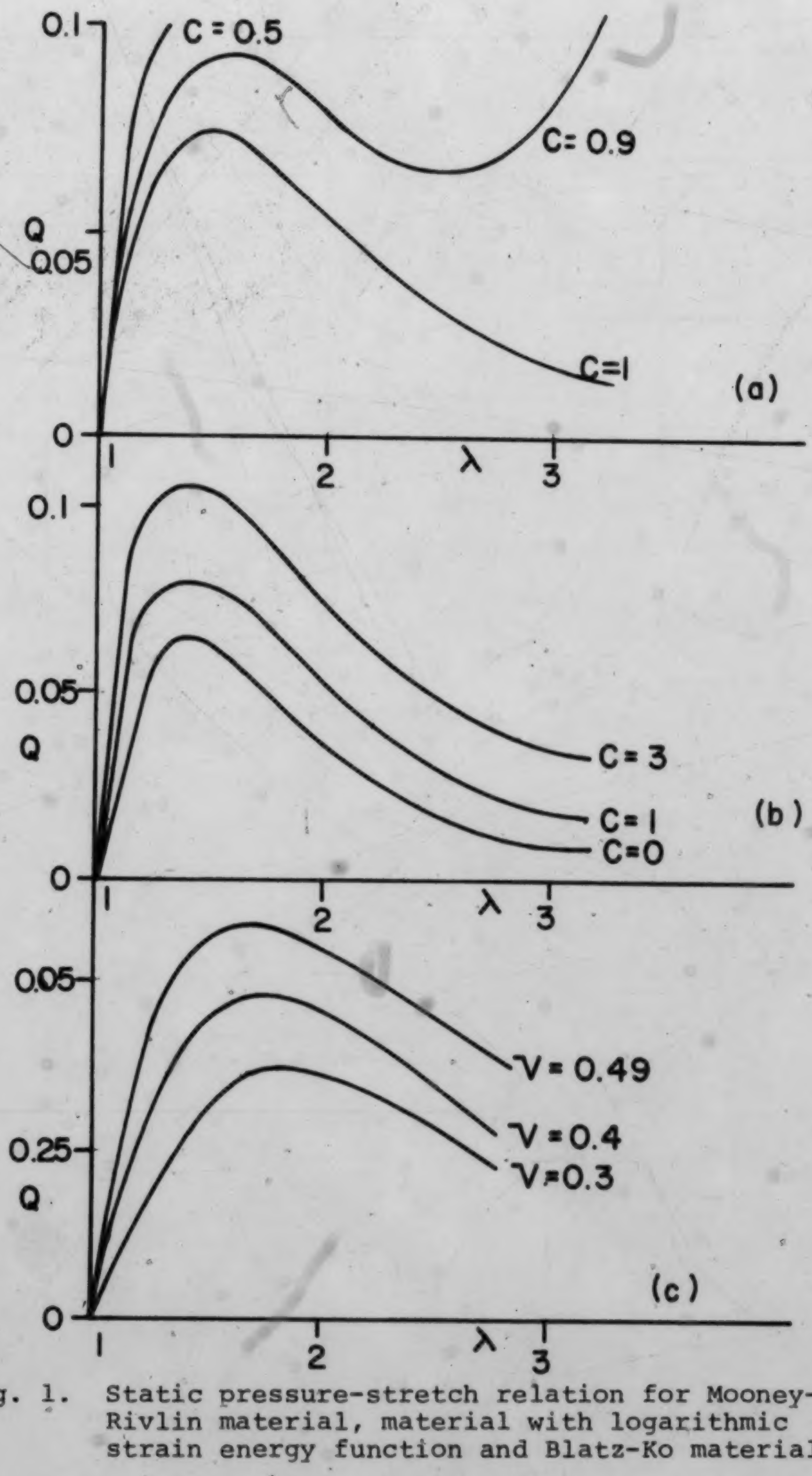

Fig. 1. Static pressure-stretch relation for Mooney-Rivlin material, material with logarithmic strain energy function and Blatz-Ko material.

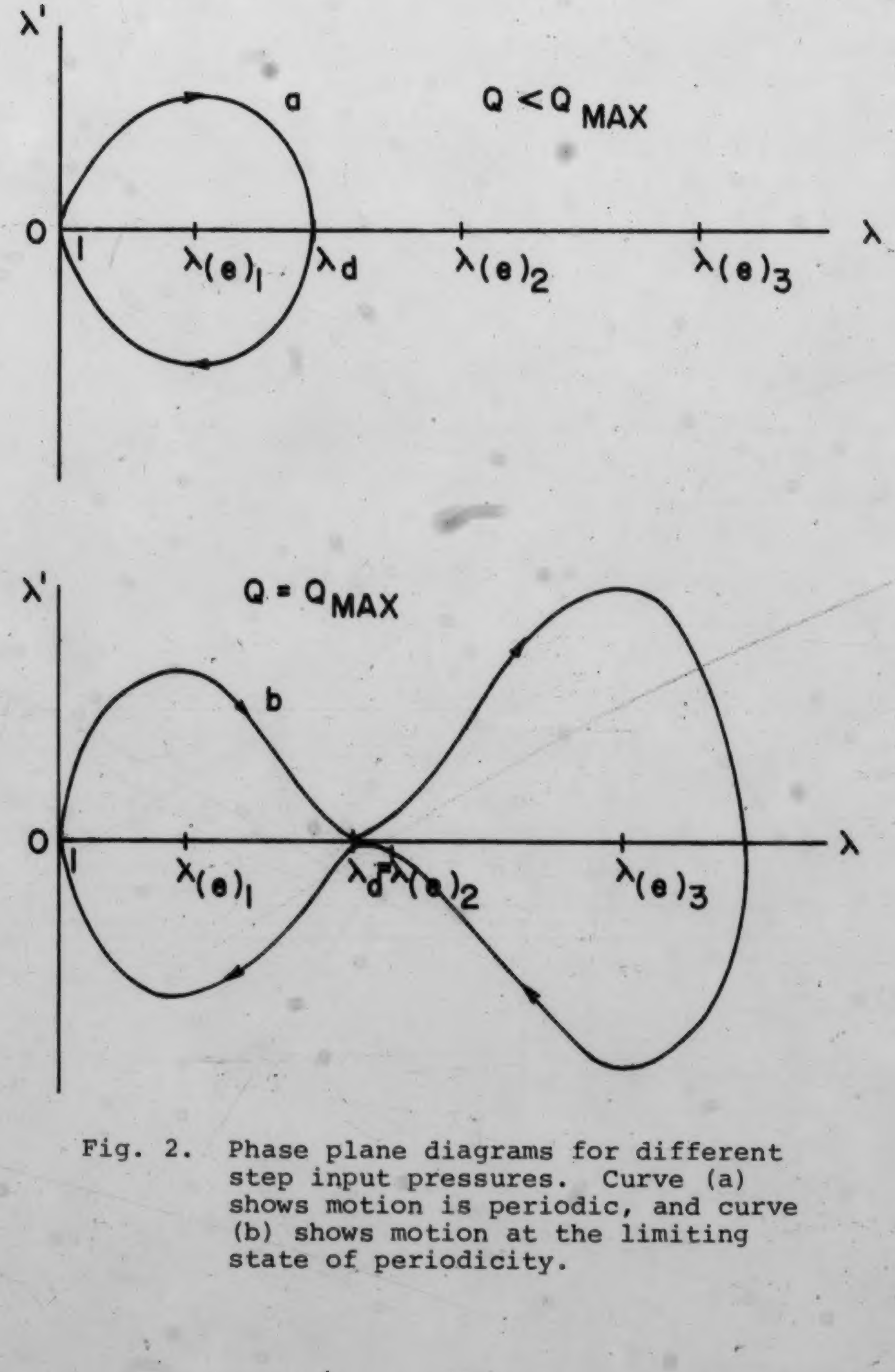

Fig. 2. Phase plane diagrams for different step input pressures. Curve (a) shows motion is periodic, and curve (b) shows motion at the limiting state of periodicity.

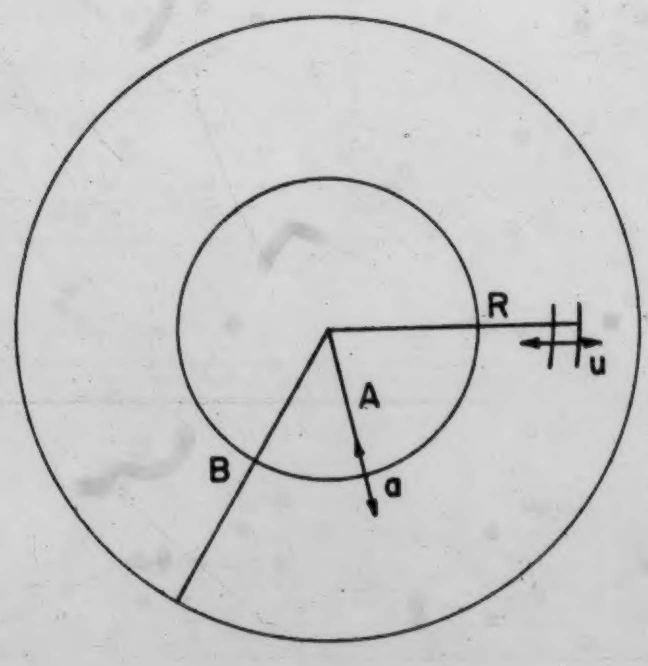

Fig. 3. Diagram illustrating the free radial oscillation of a thick-walled incompressible shell: a is amplitude at inner radius, and u is amplitude at a generic radius, R.

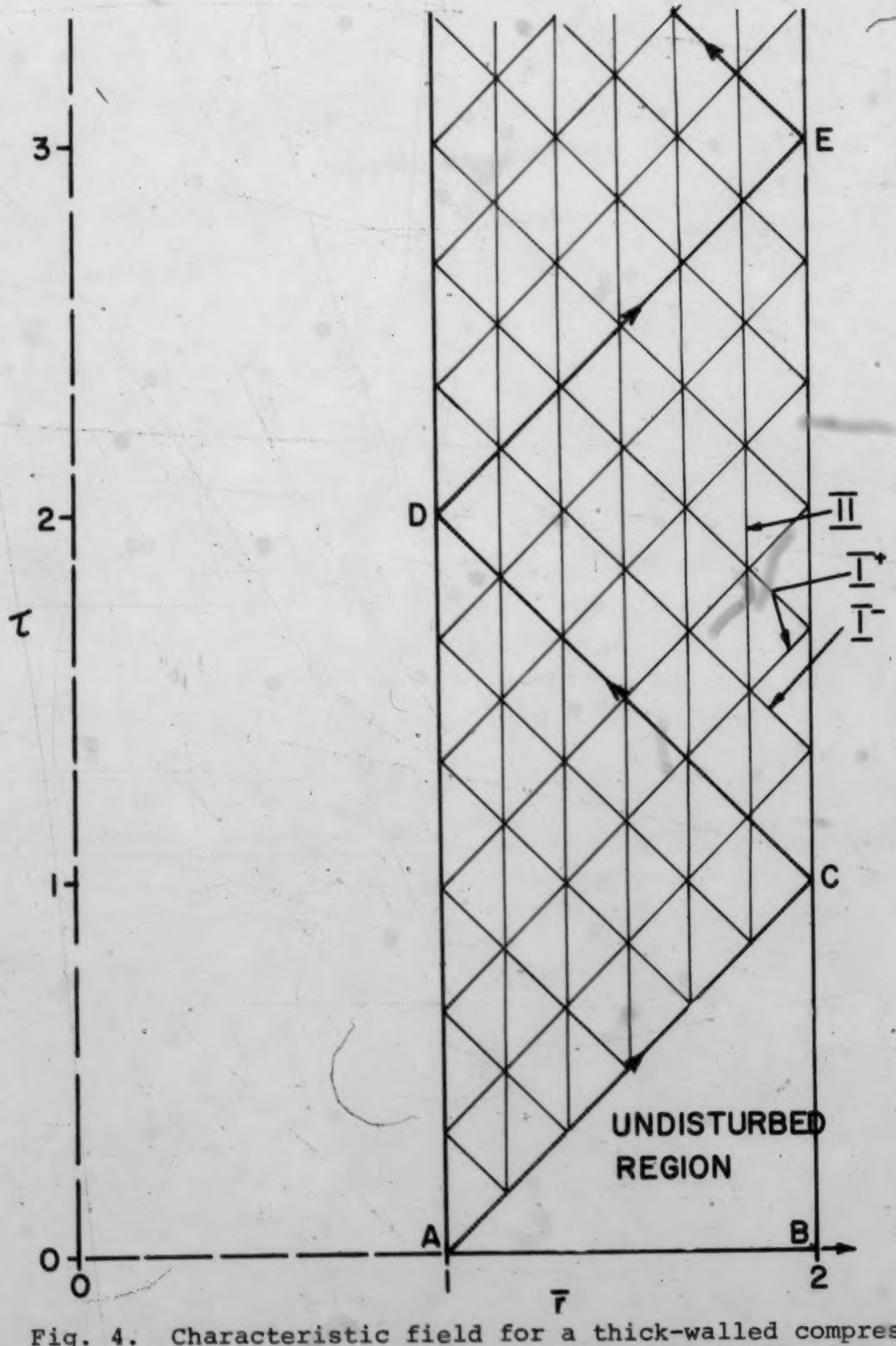

Fig. 4. Characteristic field for a thick-walled compressible shell under a step function application of pressure.

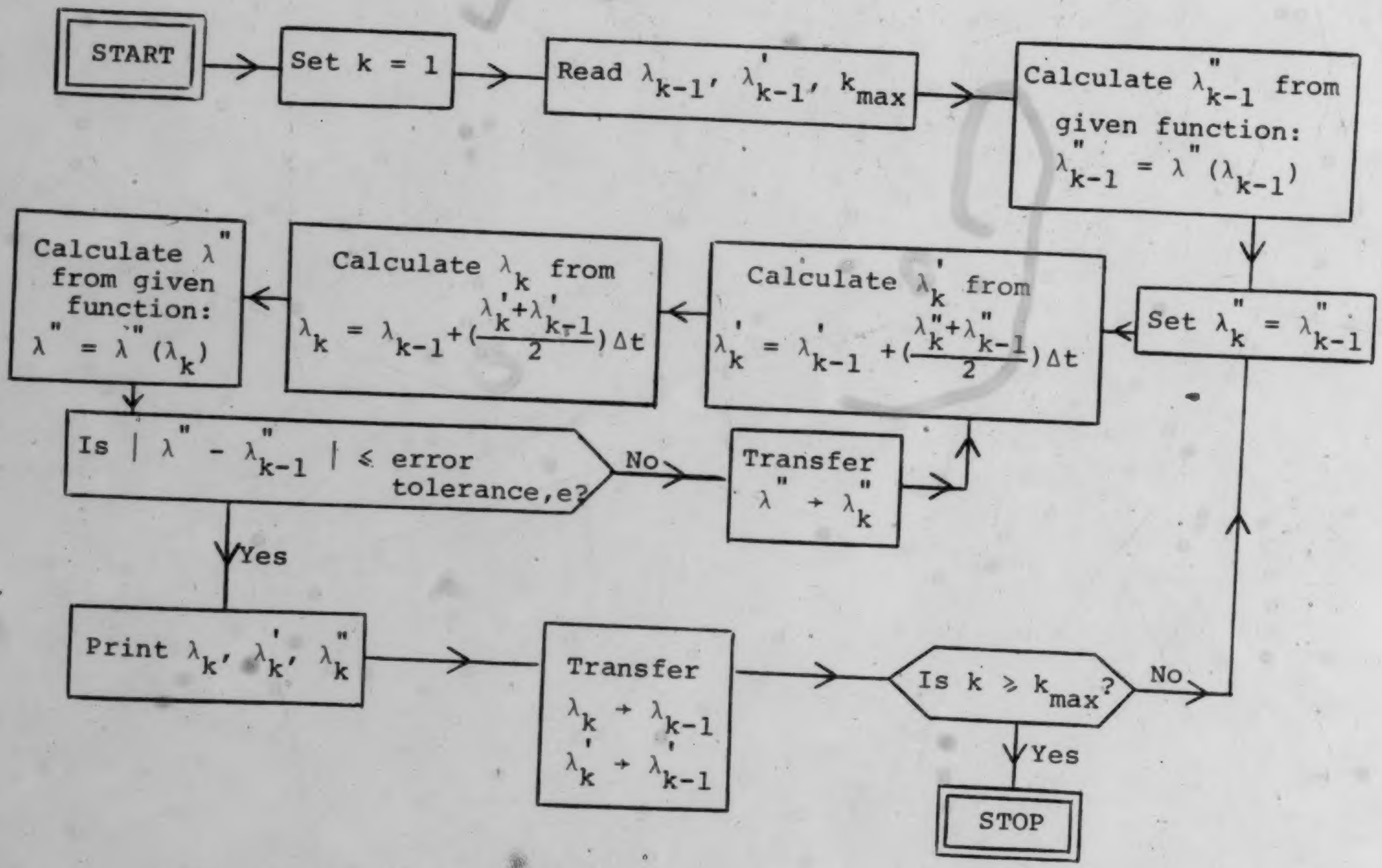
START
Set k = 1
Read λ_{k-1}, λ'_{k-1}, k_{max}
Calculate λ''_{k-1} from given function: $\lambda''_{k-1} = \lambda''(\lambda_{k-1})$
Set $\lambda''_k = \lambda''_{k-1}$
Calculate λ'_k from $\lambda'_k = \lambda'_{k-1} + (\frac{\lambda''_k + \lambda''_{k-1}}{2})\Delta t$
Calculate λ_k from $\lambda_k = \lambda_{k-1} + (\frac{\lambda'_k + \lambda'_{k-1}}{2})\Delta t$
Calculate λ'' from given function: $\lambda'' = \lambda''(\lambda_k)$
Is $|\lambda'' - \lambda''_{k-1}| \leqslant$ error tolerance, e?
No
Transfer $\lambda'' \rightarrow \lambda''_k$
Yes
Print λ_k, λ'_k, λ''_k
Transfer $\lambda_k \rightarrow \lambda_{k-1}$ $\lambda'_k \rightarrow \lambda'_{k-1}$
Is $k \geqslant k_{max}$?
No
Yes
STOP

Fig. 5. Flow diagram for numerical solution of the governing equation for the incompressible thin shell by the method of discrete variables.

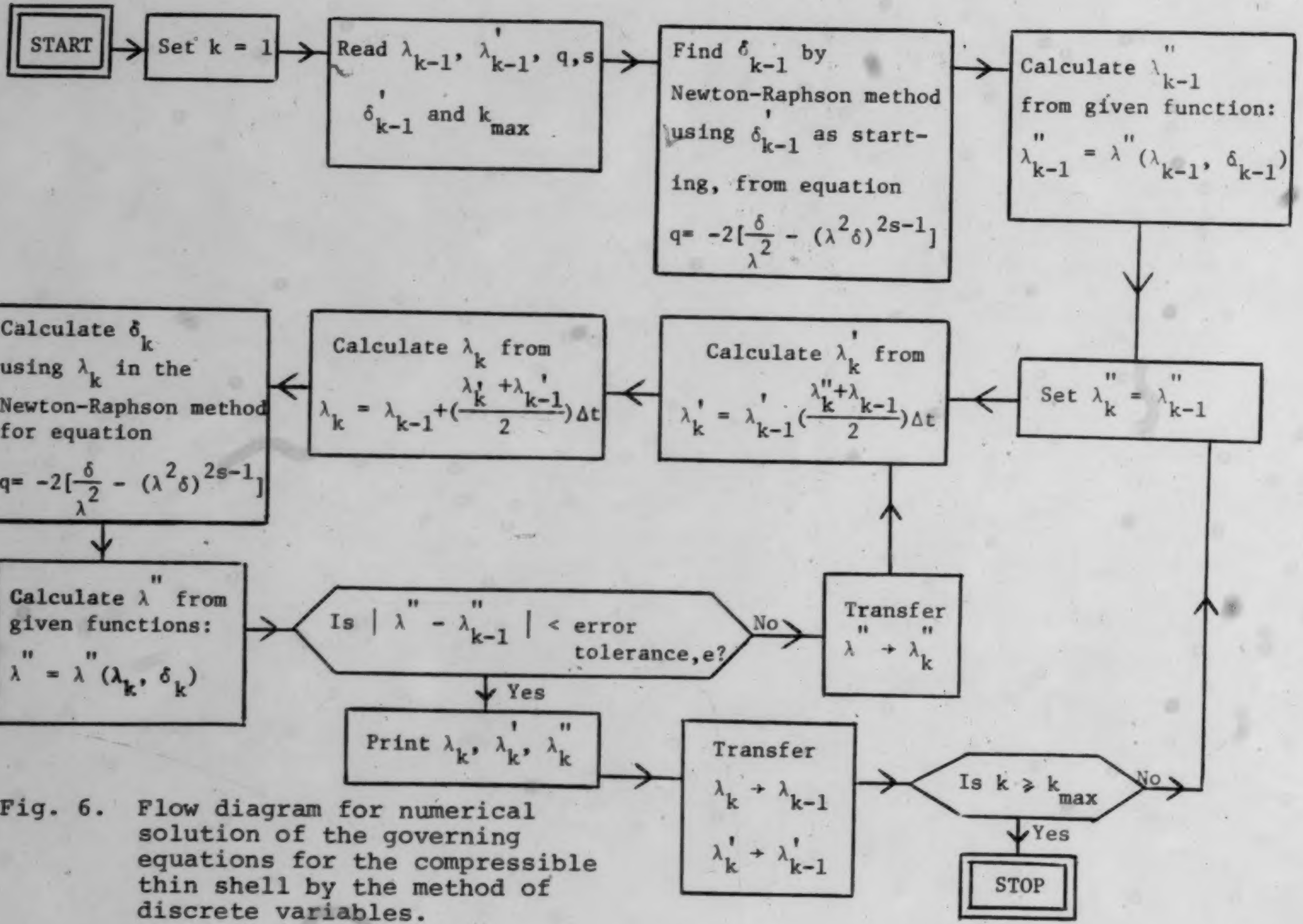
START
Set k = 1
Read λ_{k-1}, λ'_{k-1}, q,s δ'_{k-1} and k_{max}
Find δ_{k-1} by Newton-Raphson method using δ'_{k-1} as starting, from equation $q= -2[\frac{\delta}{\lambda^2} - (\lambda^2\delta)^{2s-1}]$
Calculate λ''_{k-1} from given function: $\lambda''_{k-1} = \lambda''(\lambda_{k-1}, \delta_{k-1})$
Set $\lambda''_k = \lambda''_{k-1}$
Calculate λ'_k from $\lambda'_k = \lambda'_{k-1}(\frac{\lambda''_k+\lambda_{k-1}}{2})\Delta t$
Calculate λ_k from $\lambda_k = \lambda_{k-1}+(\frac{\lambda'_k+\lambda'_{k-1}}{2})\Delta t$
Calculate δ_k using λ_k in the Newton-Raphson method for equation $q= -2[\frac{\delta}{\lambda^2} - (\lambda^2\delta)^{2s-1}]$
Calculate λ'' from given functions: $\lambda'' = \lambda''(\lambda_k, \delta_k)$
Is $|\lambda'' - \lambda''_{k-1}| <$ error tolerance,e?
No
Transfer $\lambda'' \rightarrow \lambda''_k$
Yes
Print λ_k, λ'_k, λ''_k
Transfer $\lambda_k \rightarrow \lambda_{k-1}$ $\lambda'_k \rightarrow \lambda'_{k-1}$
Is $k \geqslant k_{max}$
No
Yes
STOP

Fig. 6. Flow diagram for numerical solution of the governing equations for the compressible thin shell by the method of discrete variables.

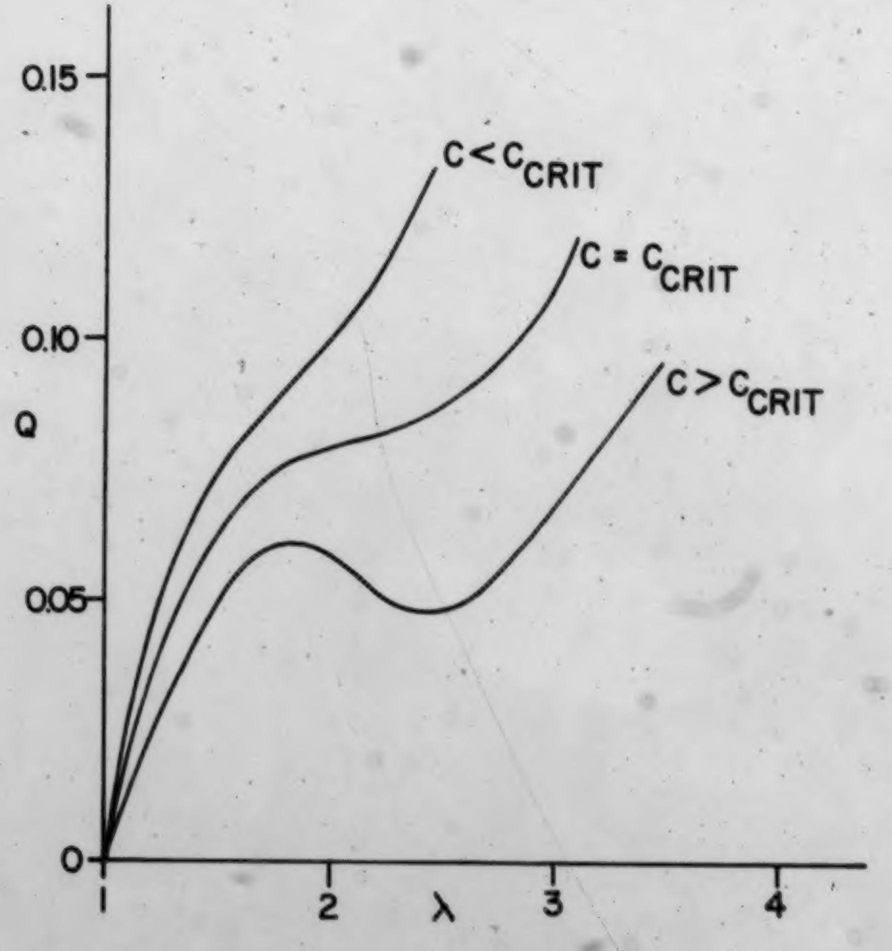

Fig. 7. Diagram illustrating the critical value, c_{crit}, of constant c, for the Mooney-Rivlin material.

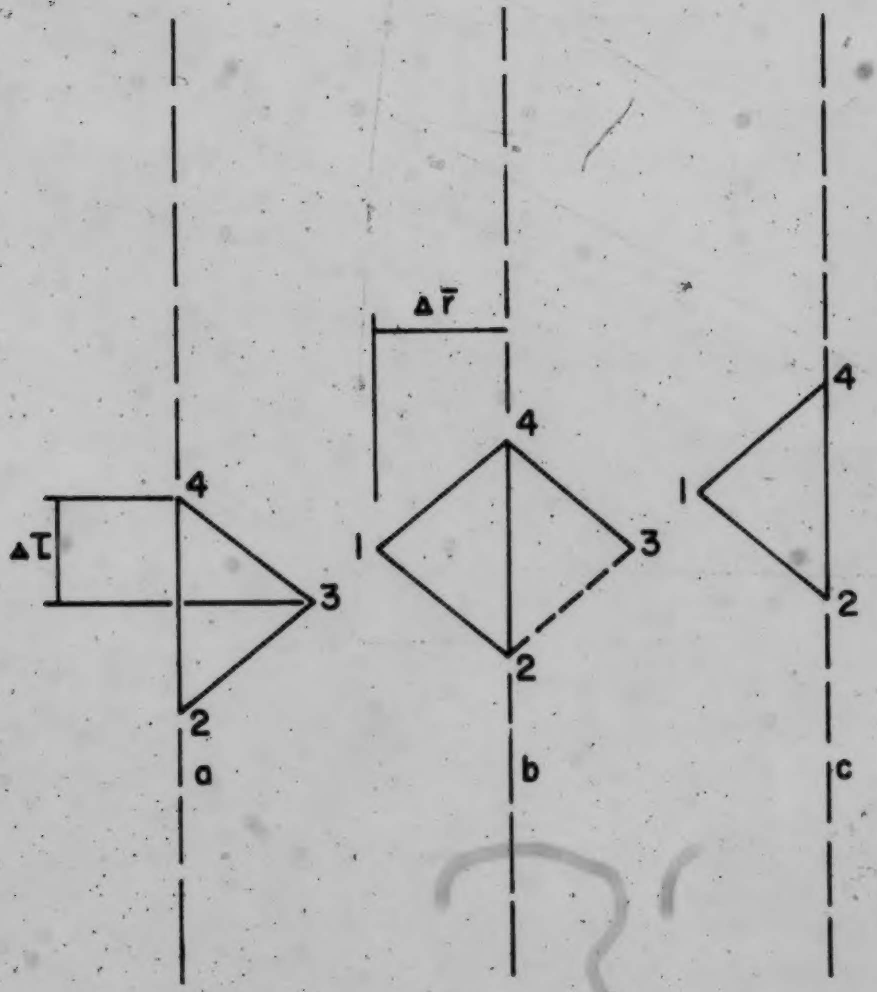

Fig. 8. Types of meshes in the characteristic field of Fig. 4. Mesh (a) is an inner half-mesh, mesh (b) is an interior full mesh, and mesh (c) is an outer half-mesh.

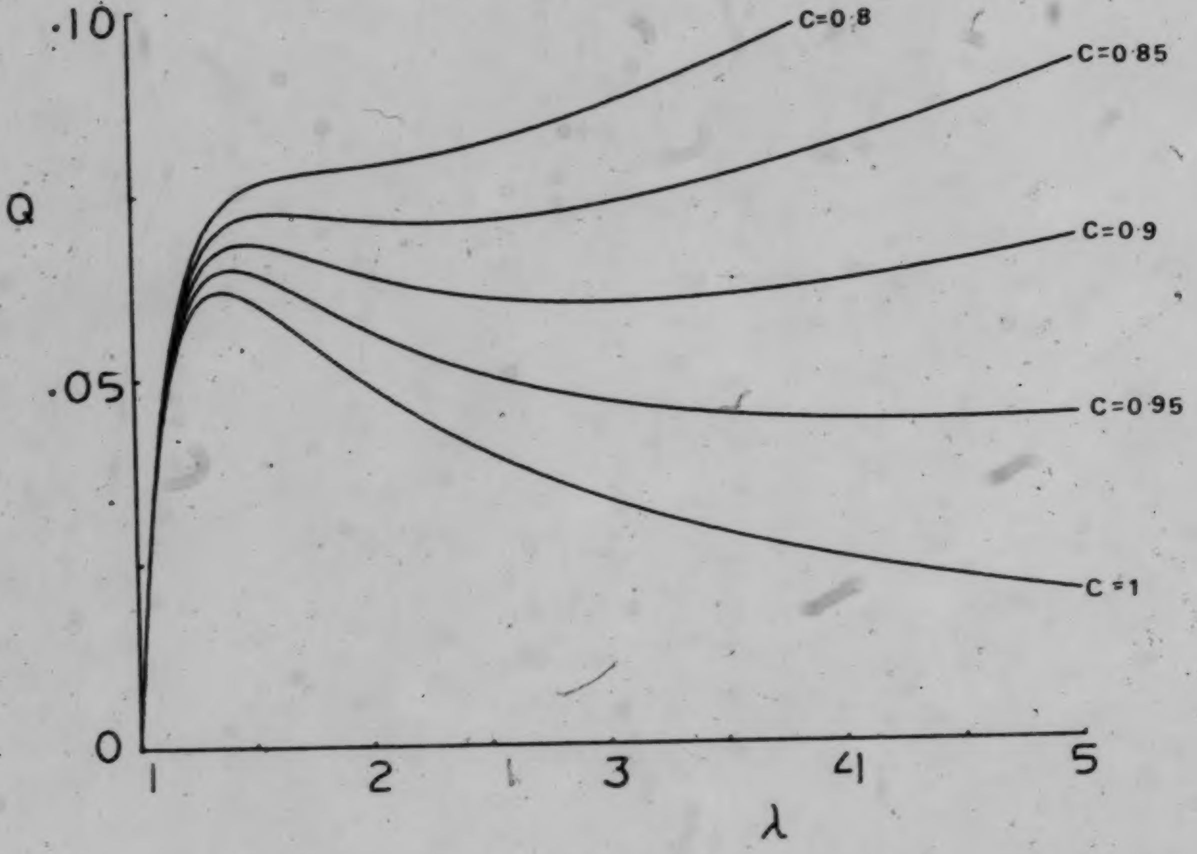

Fig. 9a. Static pressure-stretch relation for the thin incompressible shell of Mooney-Rivlin material.

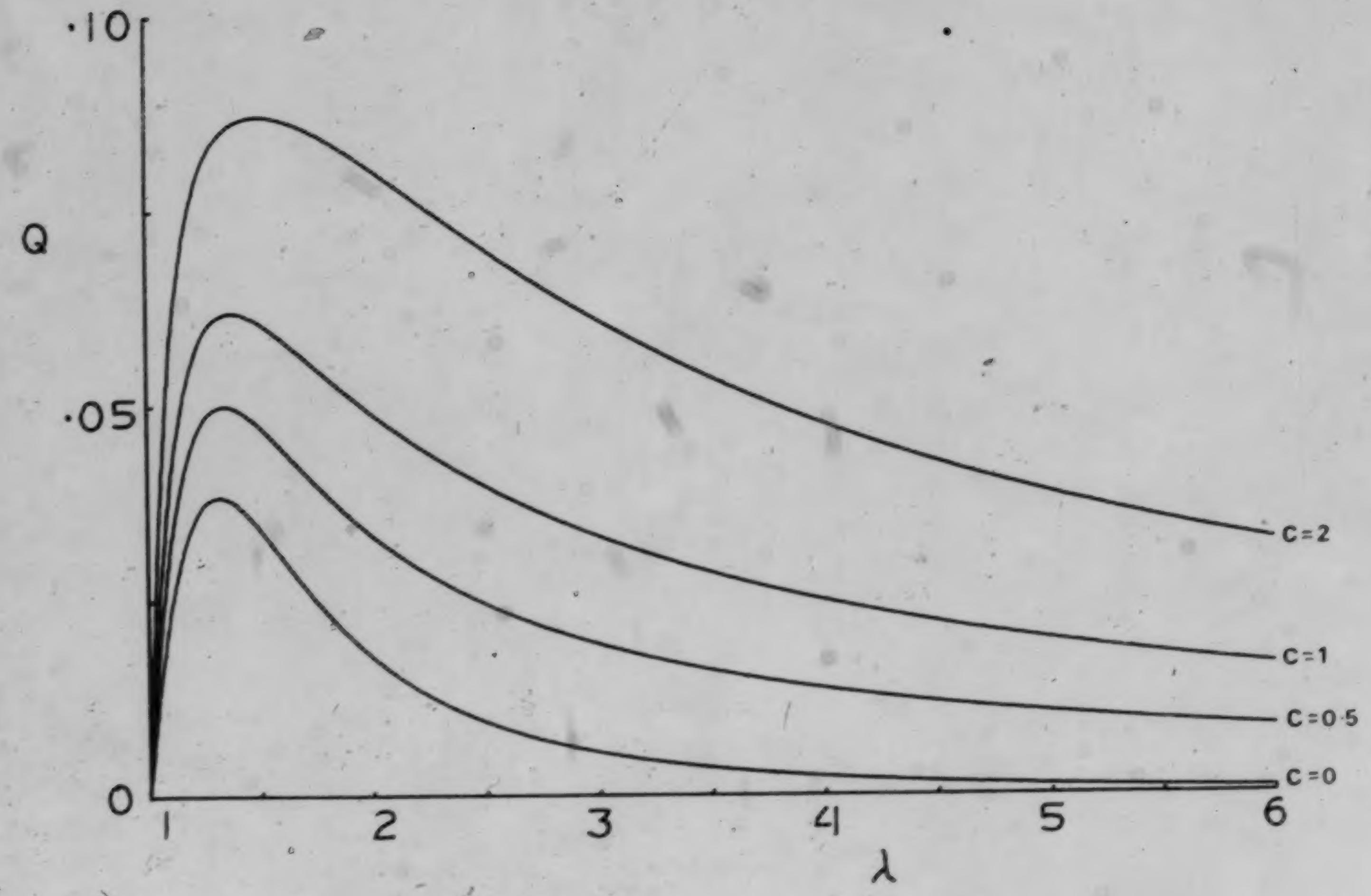

Fig. 9b. Static pressure-stretch relation for the thin incompressible shell of material with logarithmic strain energy function.

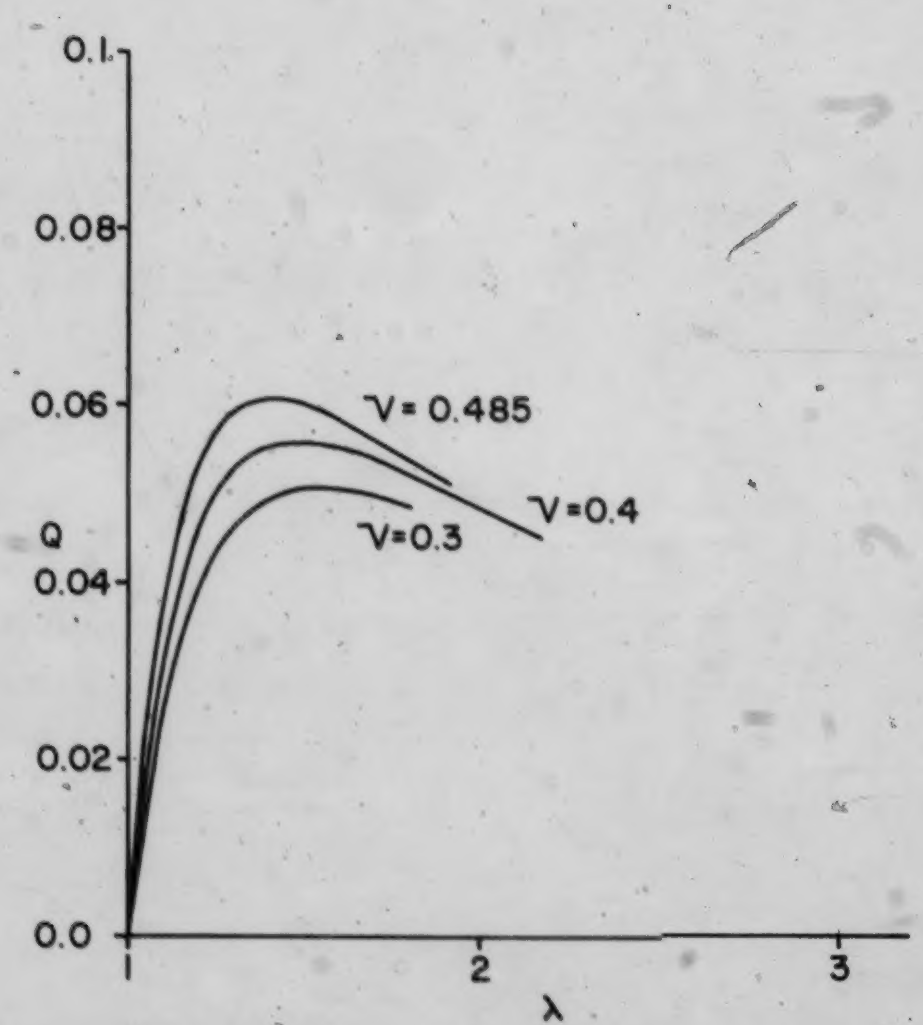

Fig. 9c. Static pressure-stretch relation for the thin compressible shell of Blatz-Ko material.

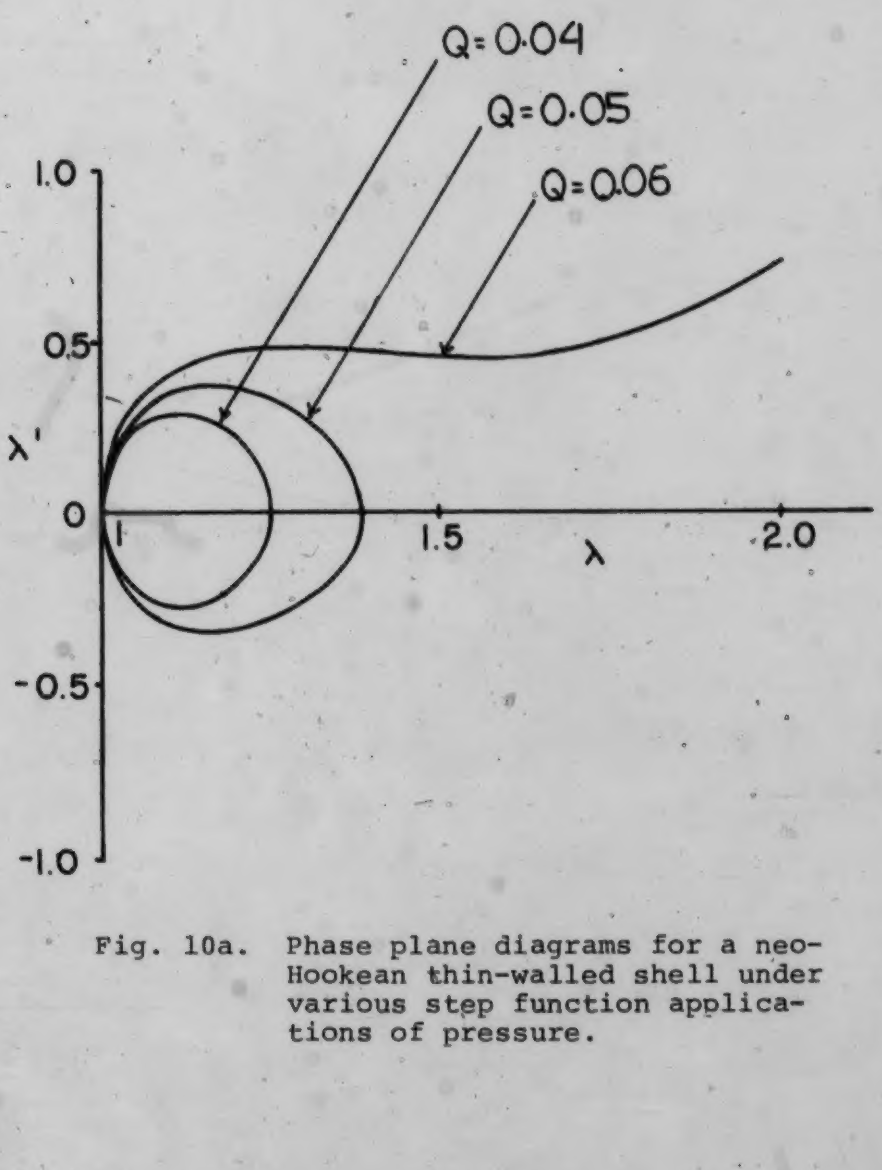

Fig. 10a. Phase plane diagrams for a neo-Hookean thin-walled shell under various step function applications of pressure.

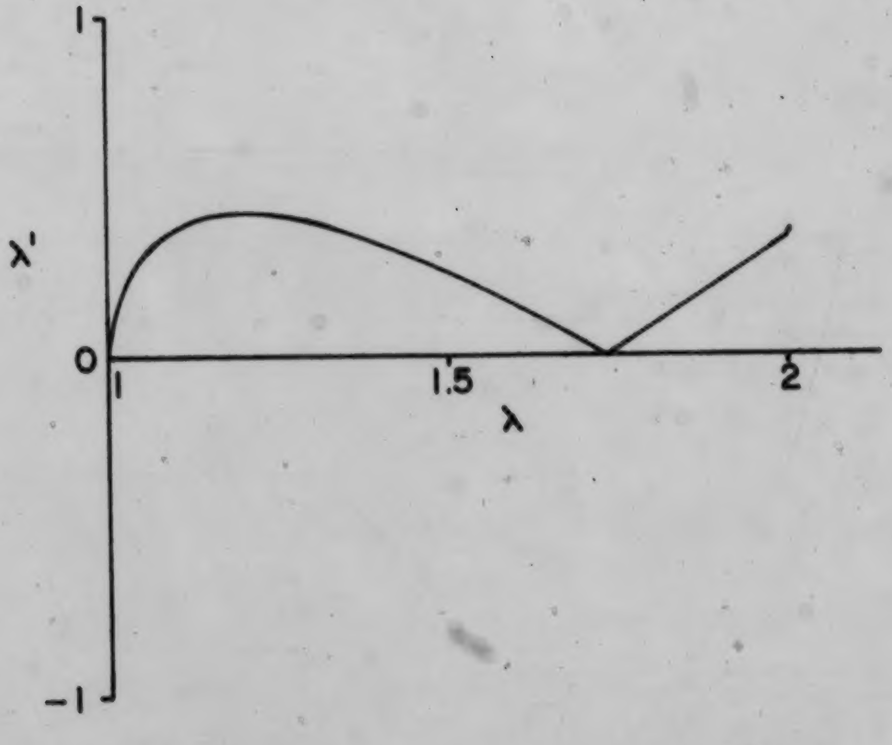

Fig. 10b. Phase plane diagram illustrating the limiting case of periodic motion for a neo-Hookean thin-walled shell: $Q_{max} = 0.0556065$.

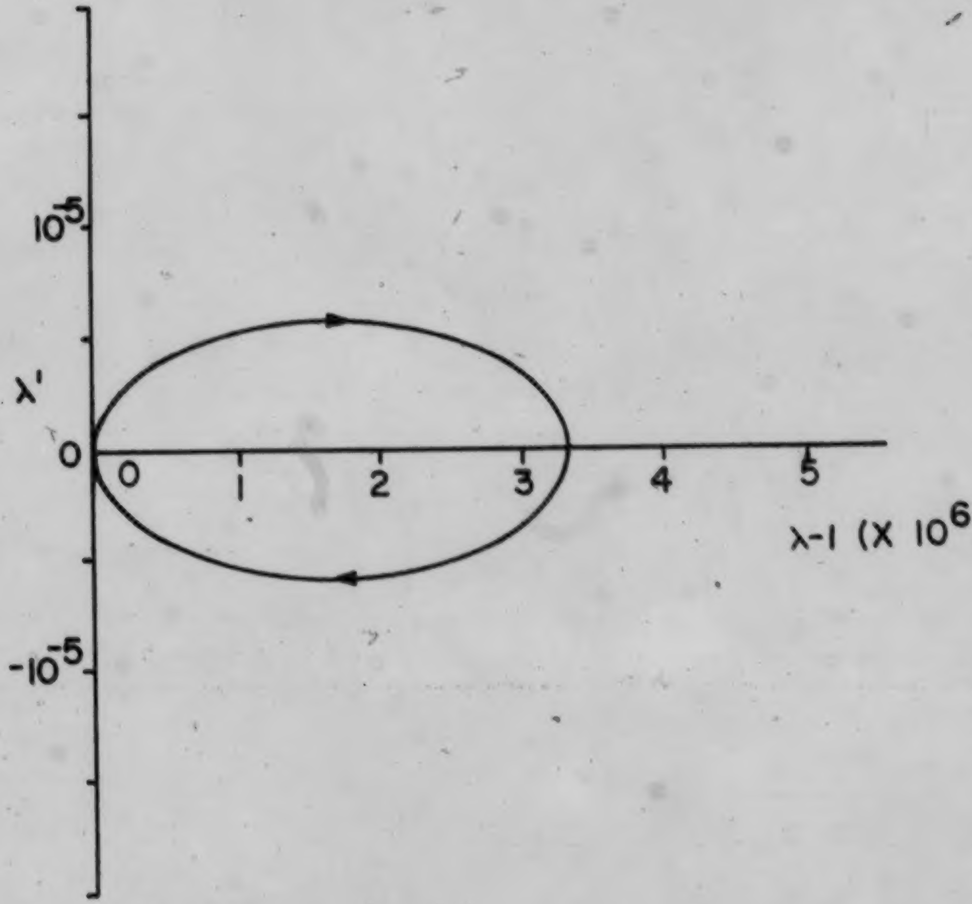

Fig. 10c. Phase plane diagram for a neo-Hookean thin-walled shell as the step input pressure, Q approaches zero.

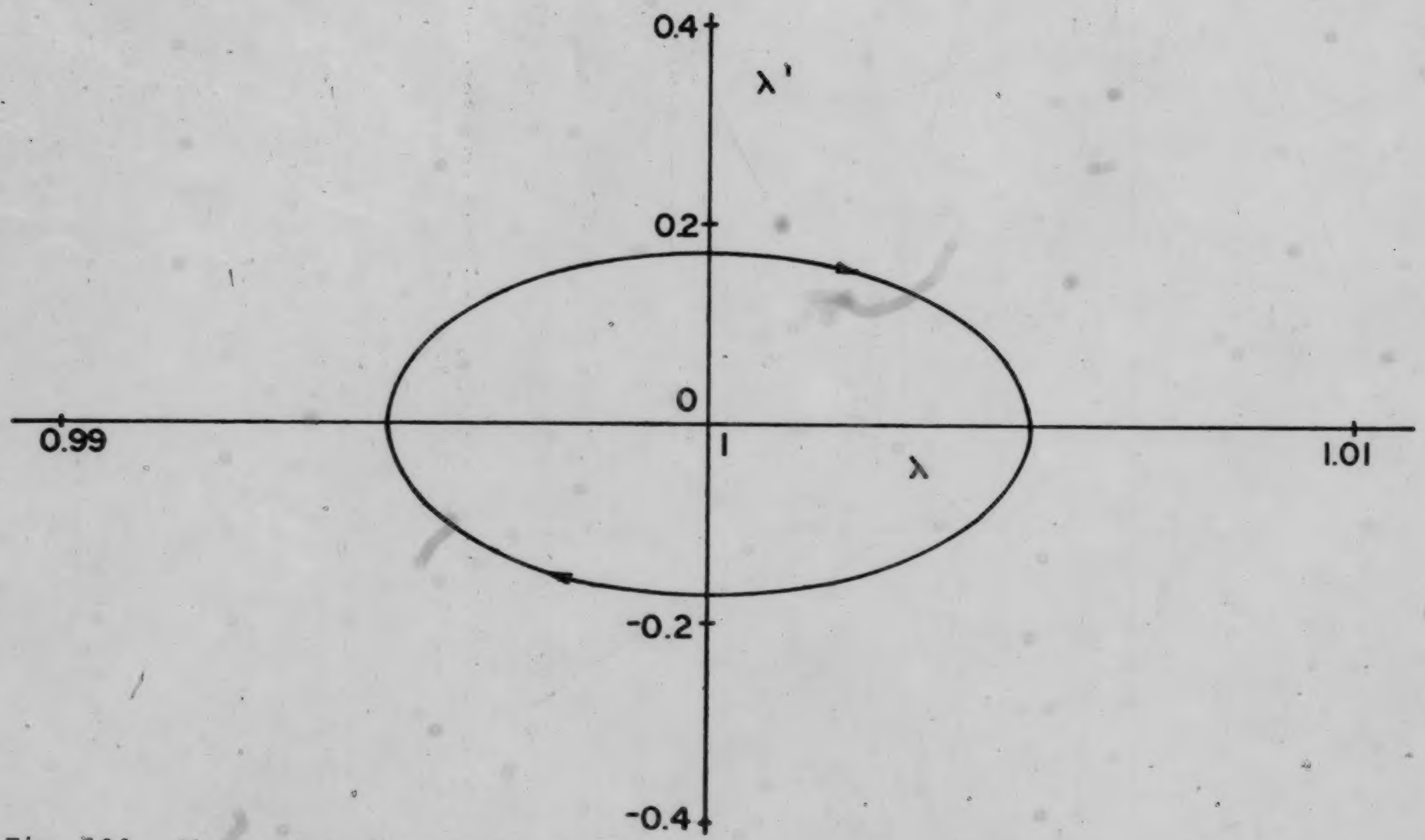

Fig. 10d. Phase plane diagram for free oscillation, of a neo-Hookean thin-walled shell, with small amplitude: $\lambda_0 = 1.005$, $\lambda_0' = 0$. See also Figs. 10e and 10f.

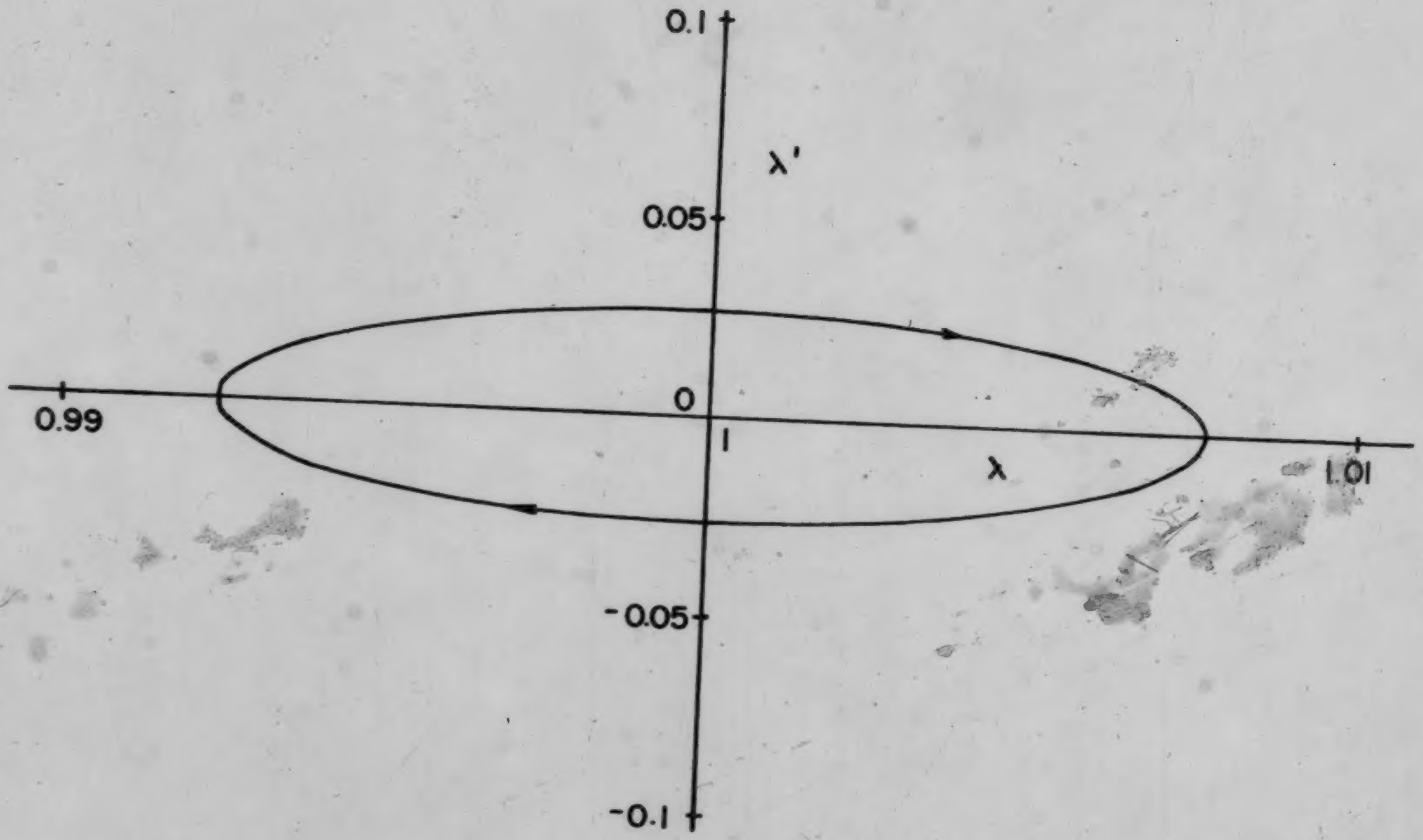

Fig. 10e. Phase plane diagram for free oscillation, of a neo-Hookean thin-walled shell, with small amplitude: $\lambda_0 = 1.0025$, $\lambda_0' = 0.025$.

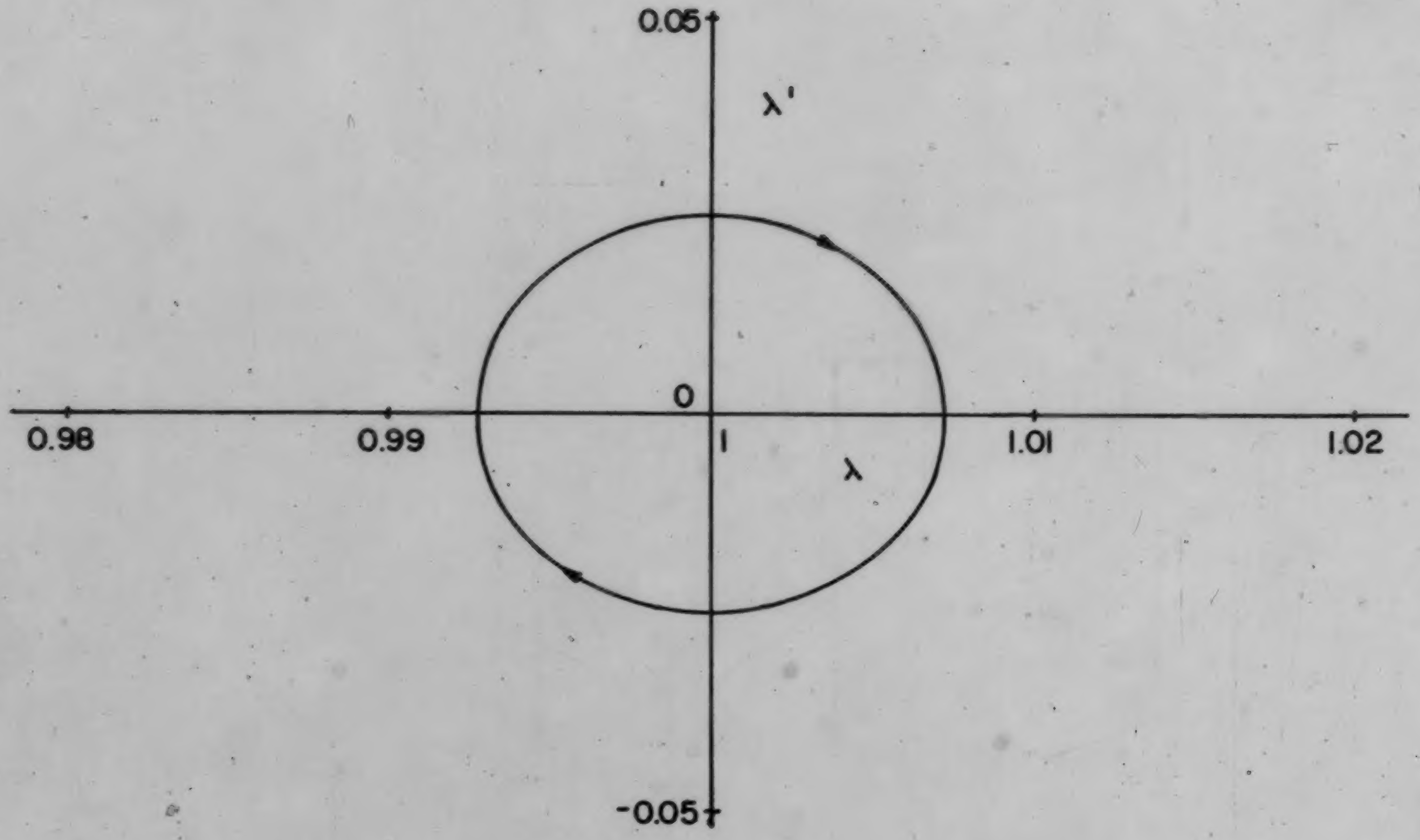

Fig. 10f. Phase plane diagram for free oscillation, of a neo-Hookean thin-walled shell, with small amplitude: $\lambda_0 = 1$, $\lambda_0' = 0.025$.

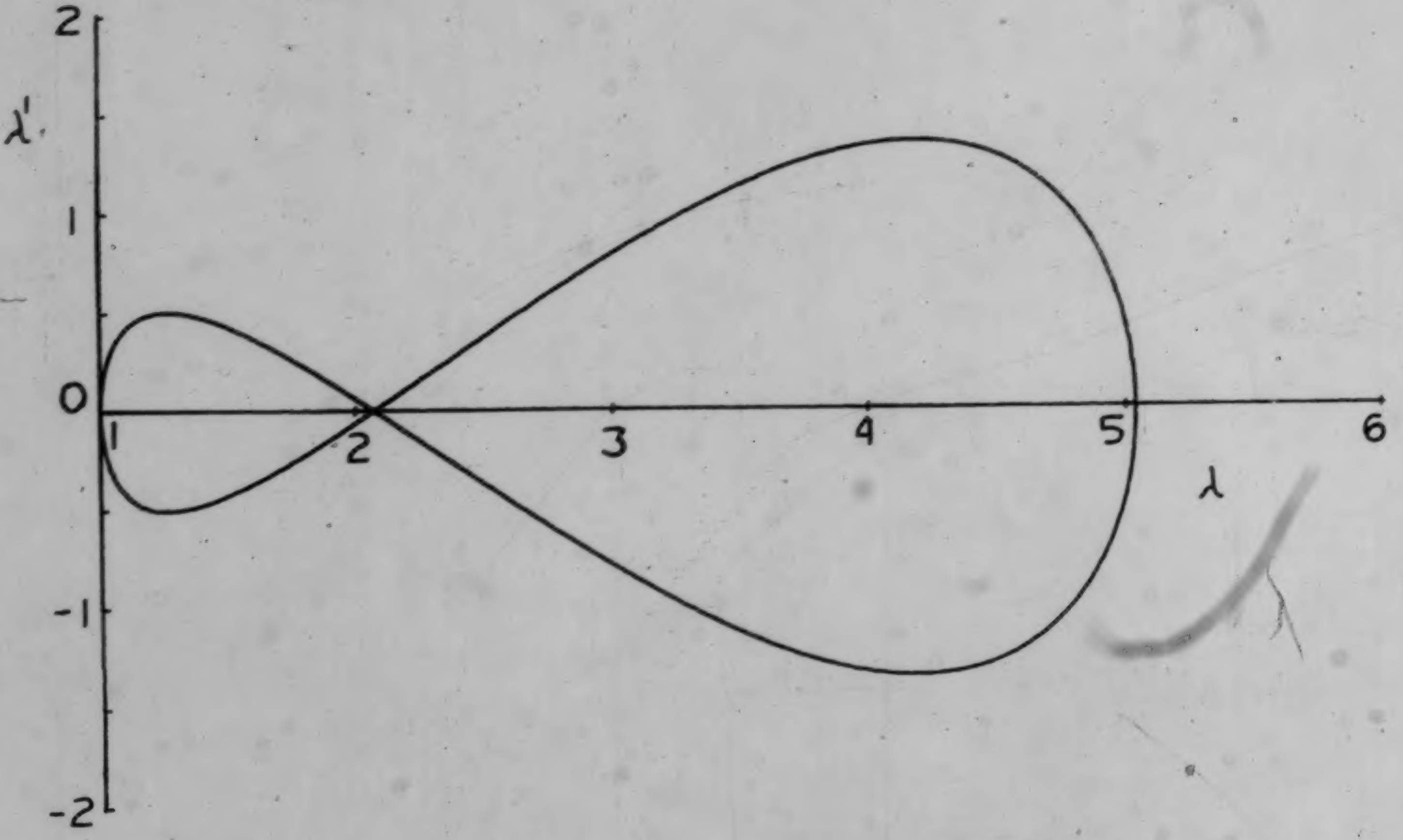

Fig. 11a. Phase plane diagram for a thin incompressible shell of Mooney-Rivlin material, illustrating limiting case of periodic motion: $Q_{max} = 0.063323854$.

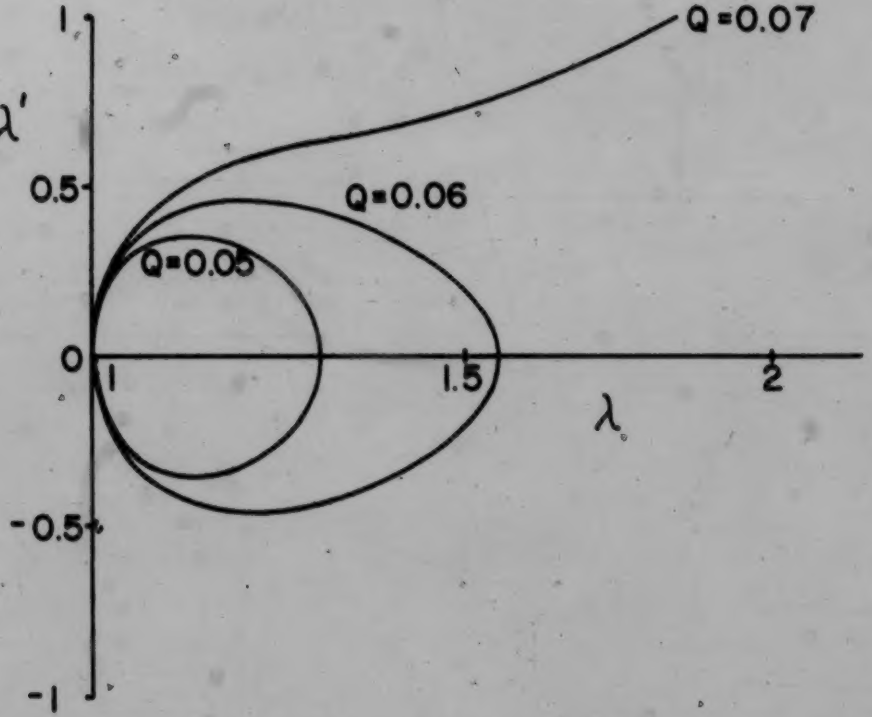

Fig. 11b. Phase plane diagrams for a thin incompressible shell of Mooney-Rivlin material, under various step input pressures.

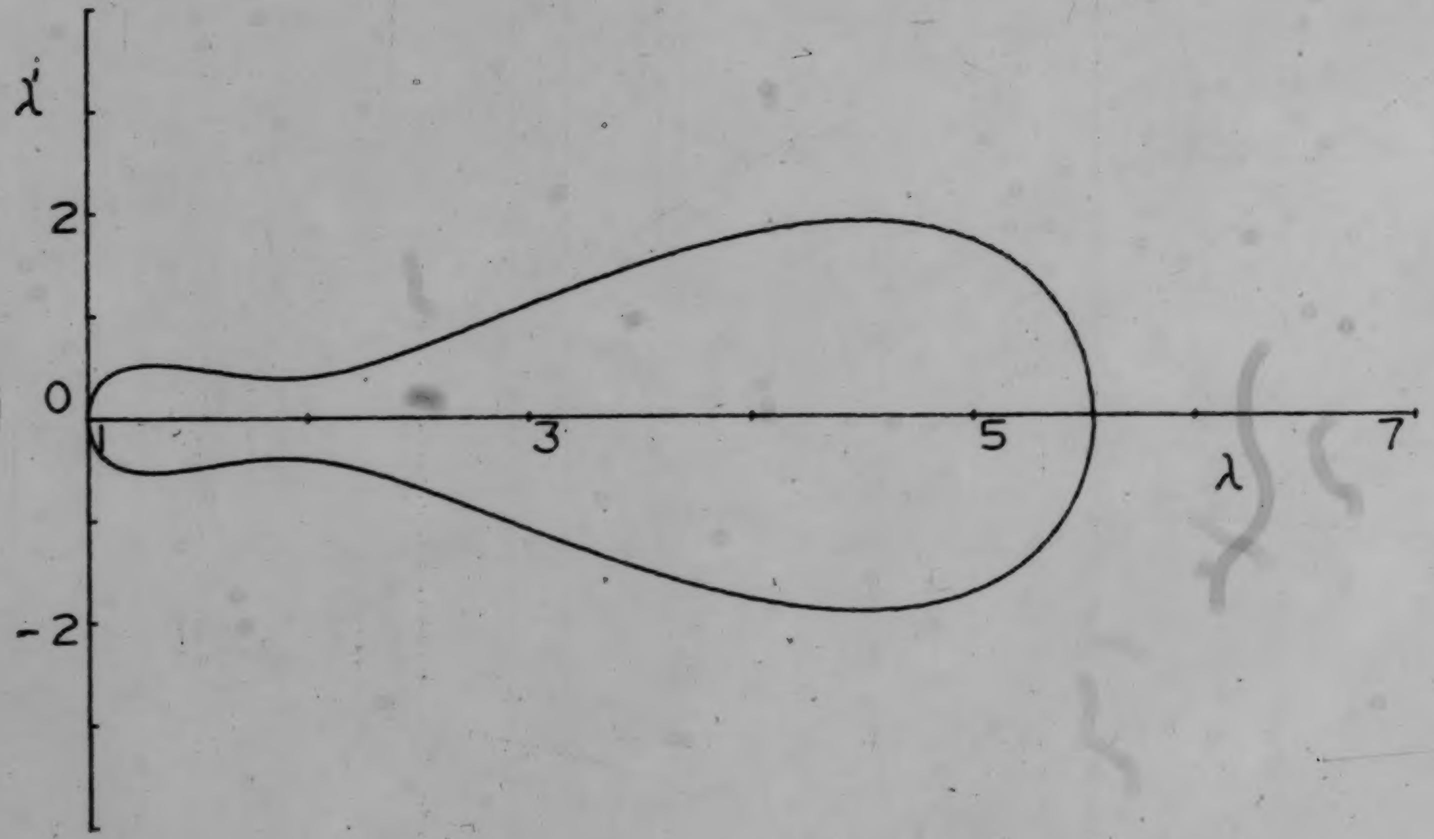

Fig. 11c. Phase plane diagram for a thin incompressible shell of Mooney-Rivlin material, illustrating periodic motion for large stretches.

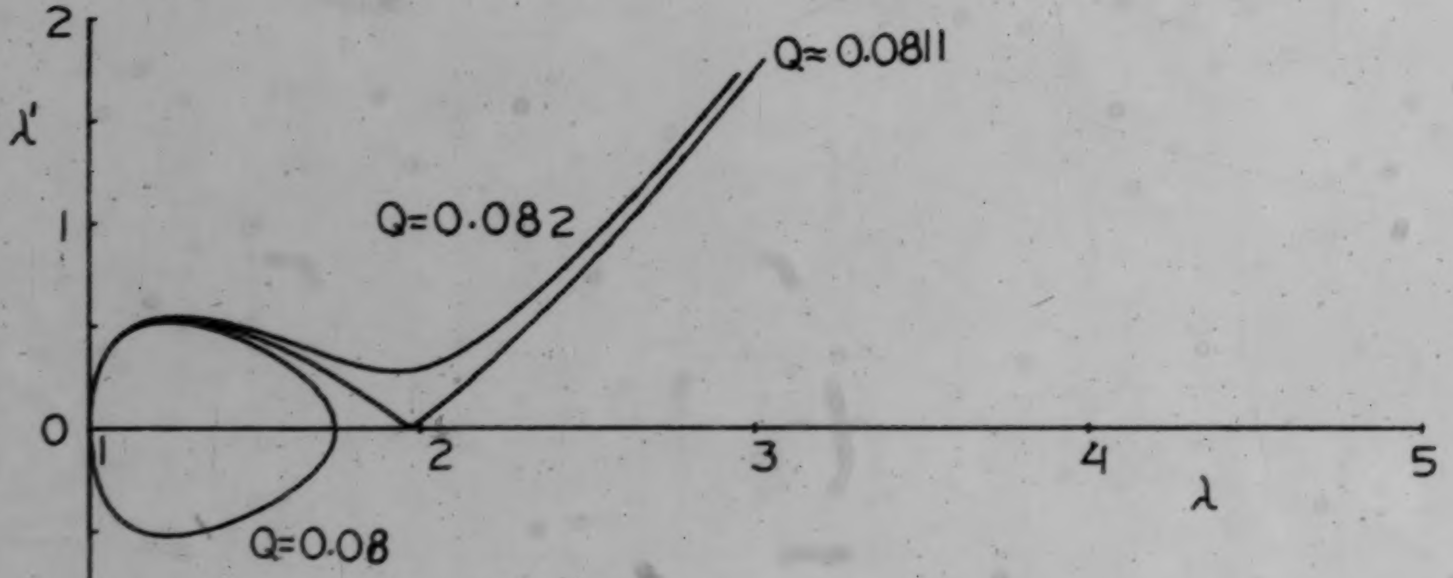

Fig. 12. Phase plane diagrams for a thin incompressible shell of material with logarithmic strain energy function.

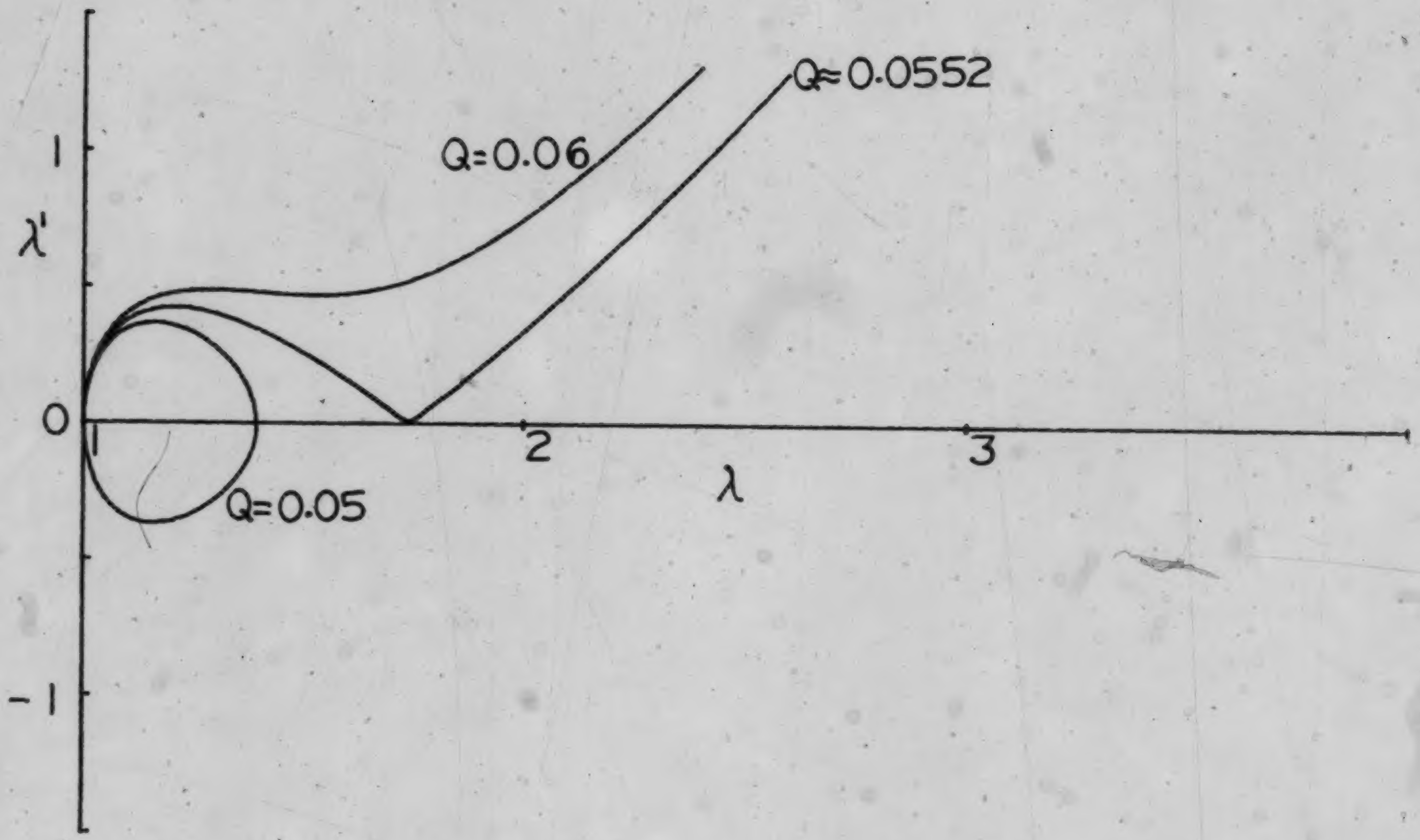

Fig. 13a. Phase plane diagrams for a thin-walled neo-Hookean shell, obtained as a limiting case of the Blatz-Ko material as ν approaches 0.5.

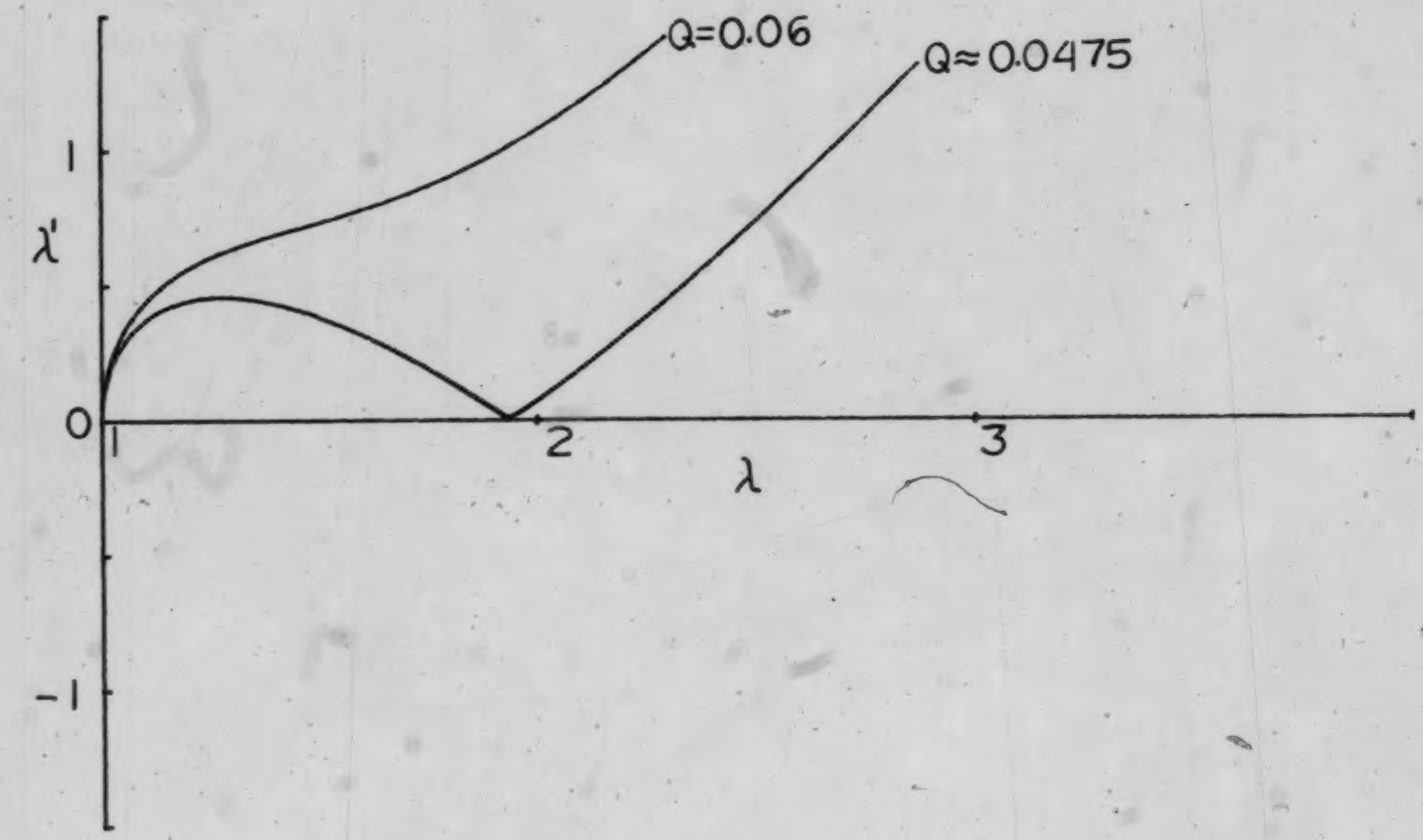

Fig. 13b. Phase plane diagrams for the thin compressible shell of Blatz-Ko material under various step input pressures.

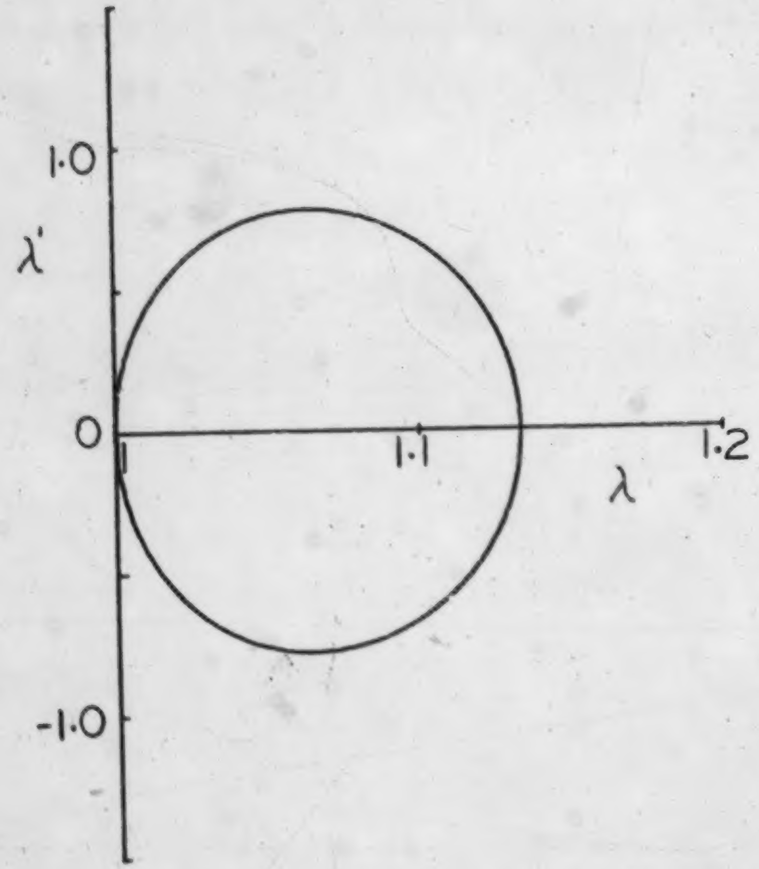

Fig. 13c. Phase plane diagram for the thin compressible shell of Blatz-Ko material, illustrating a case of periodic motion for $Q = 0.02$ and $\nu = 0.3$.

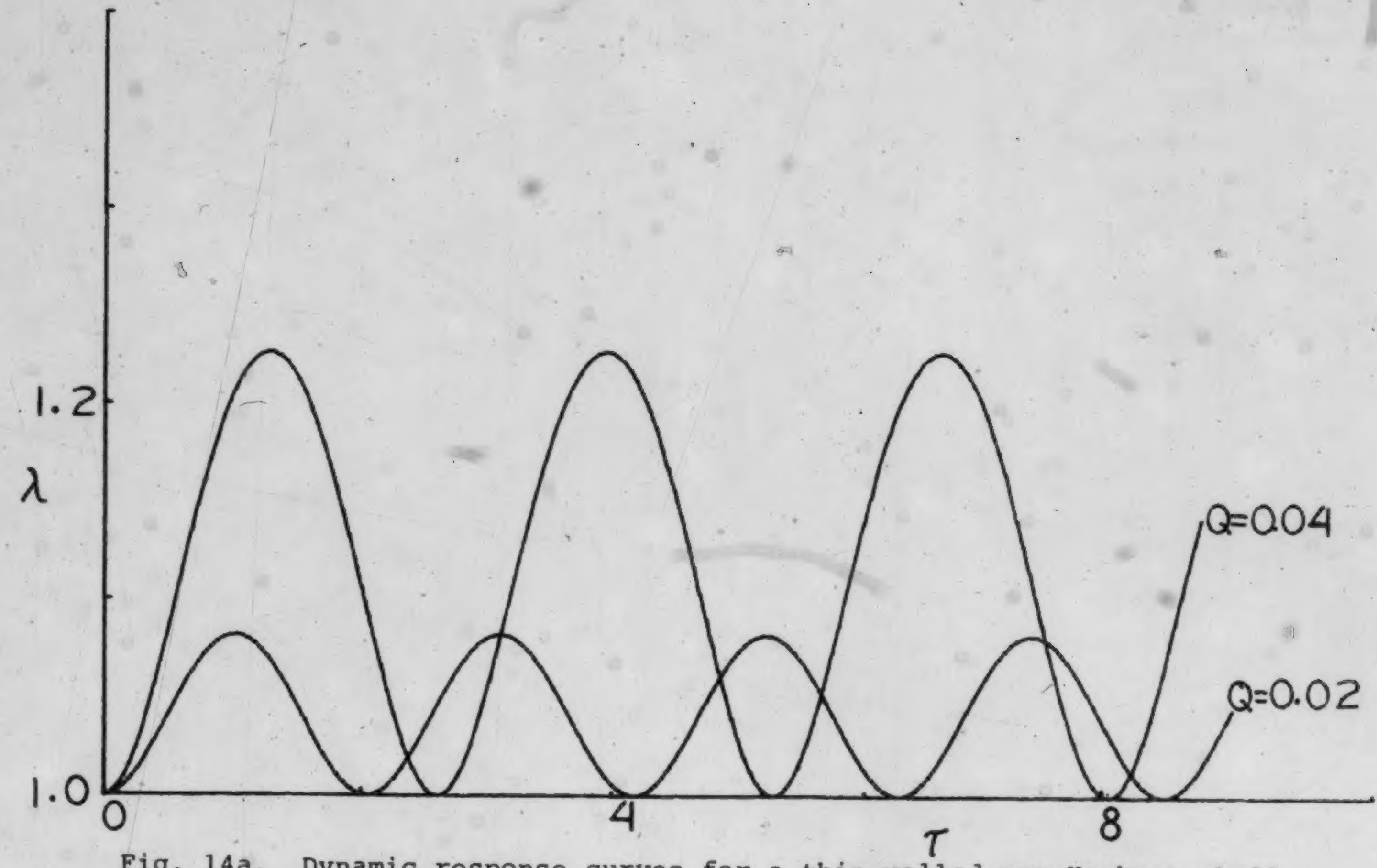

Fig. 14a. Dynamic response curves for a thin-walled neo-Hookean shell under various step function applications of pressure, Q.

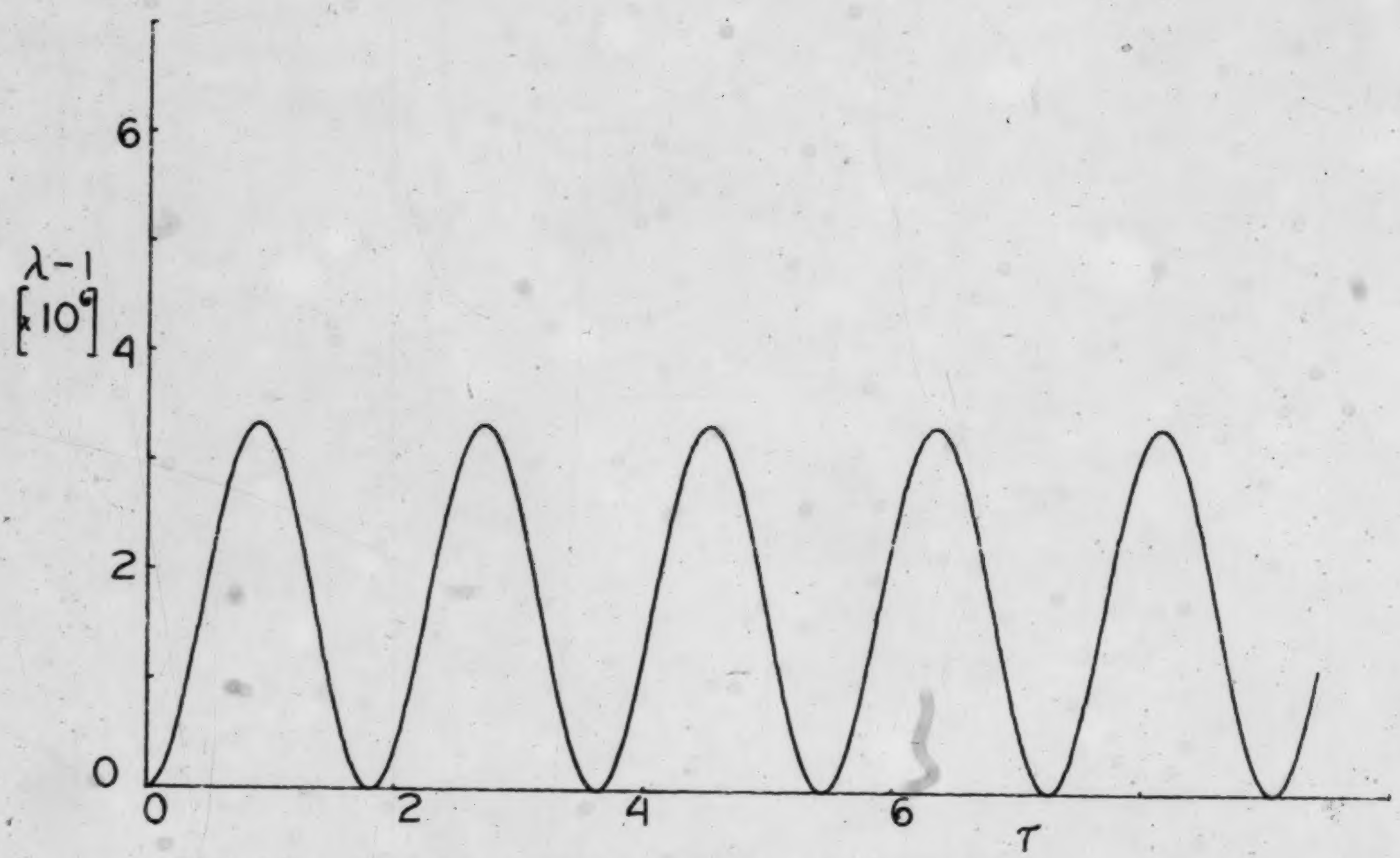

Fig. 14b. Dynamic response curve for a thin-walled neo-Hookean shell as applied pressure, Q approaches zero.

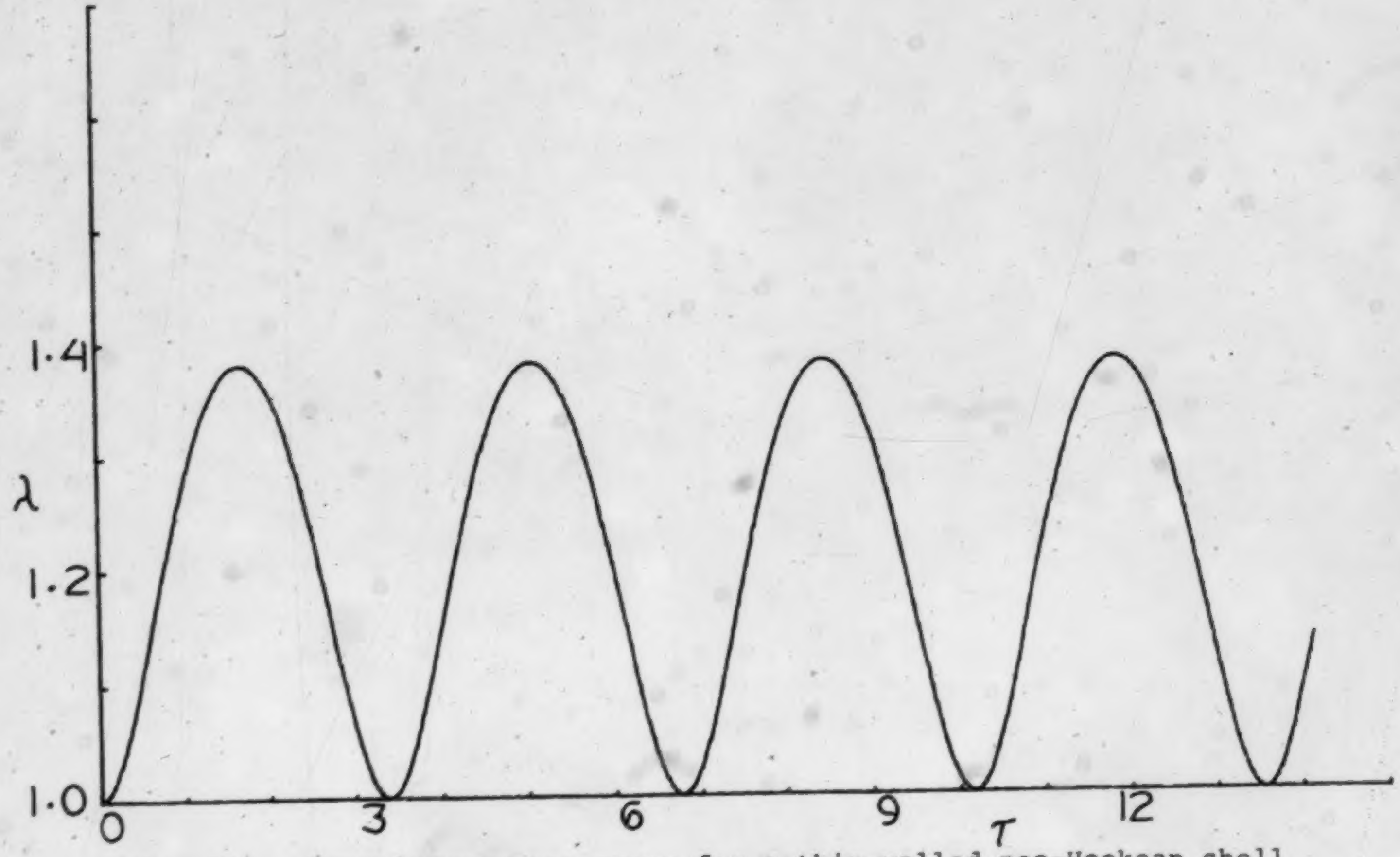

Fig. 14c. Dynamic response curve for a thin-walled neo-Hookean shell for a particular step input pressure, $Q = 0.05$.

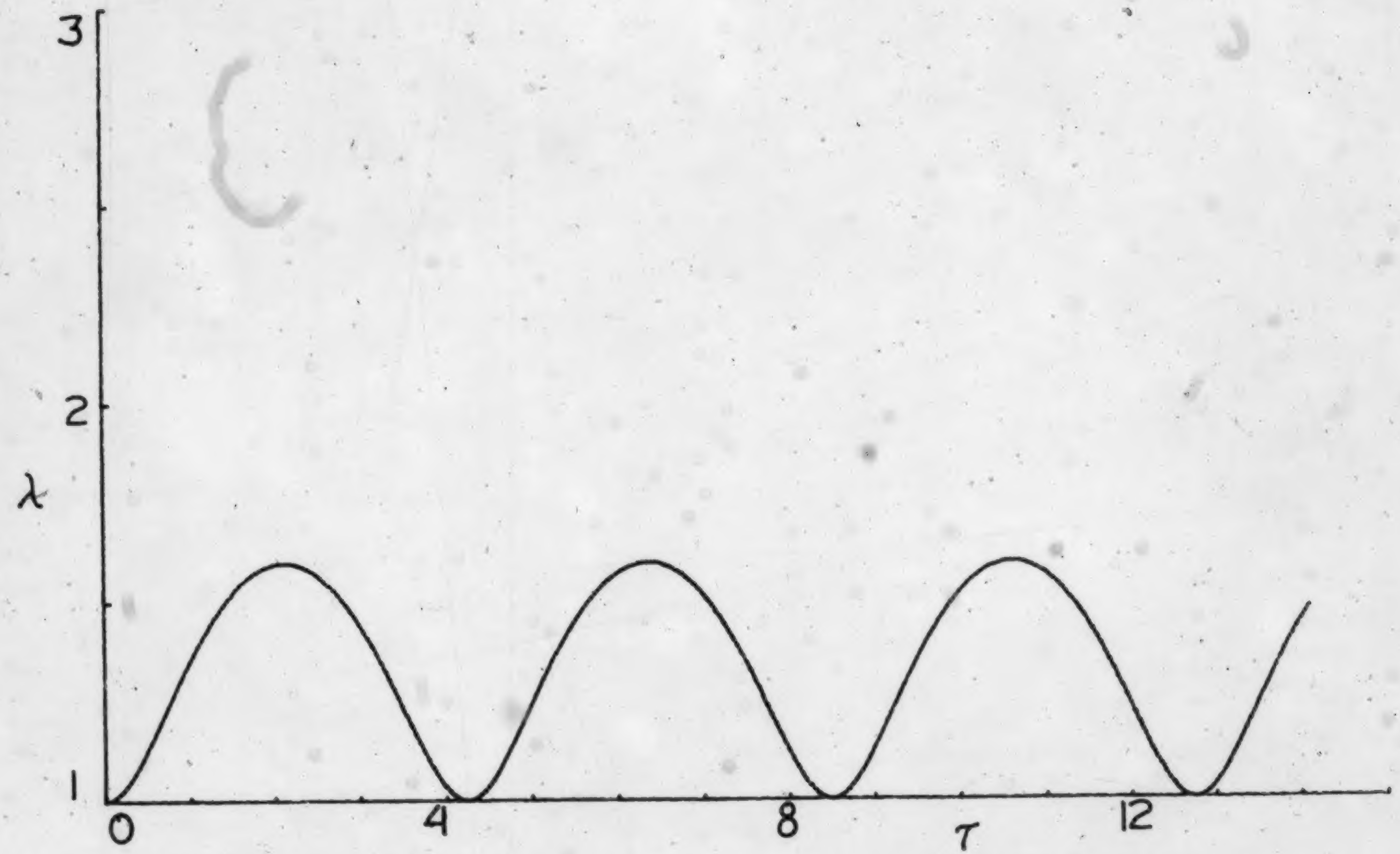

Fig. 15. Dynamic response curve for a thin incompressible shell of Mooney-Rivlin material under a step function application of pressure.

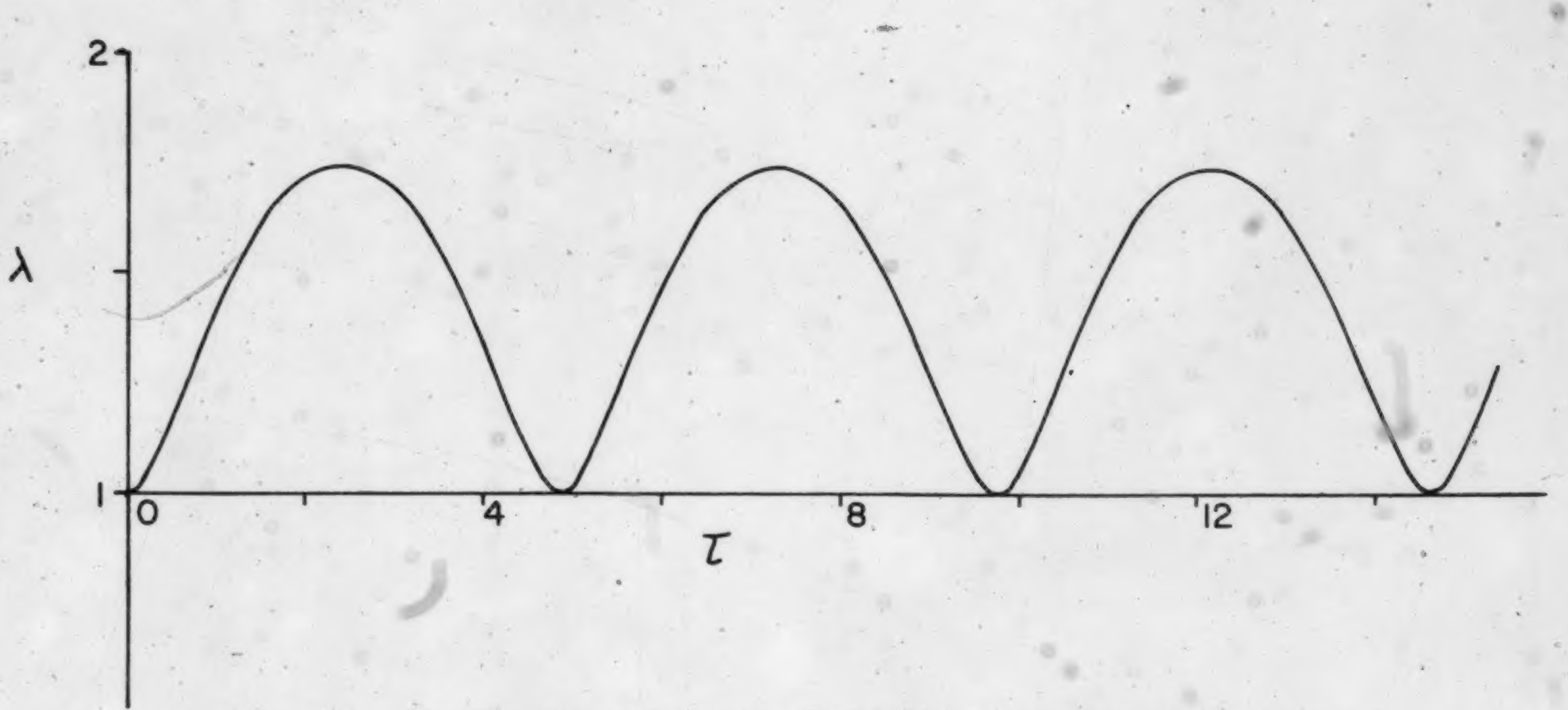

Fig. 16. Dynamic response curve for a thin incompressible shell of material with logarithmic strain energy function under a step function application of pressure, $Q = 0.08$ $c = 2$.

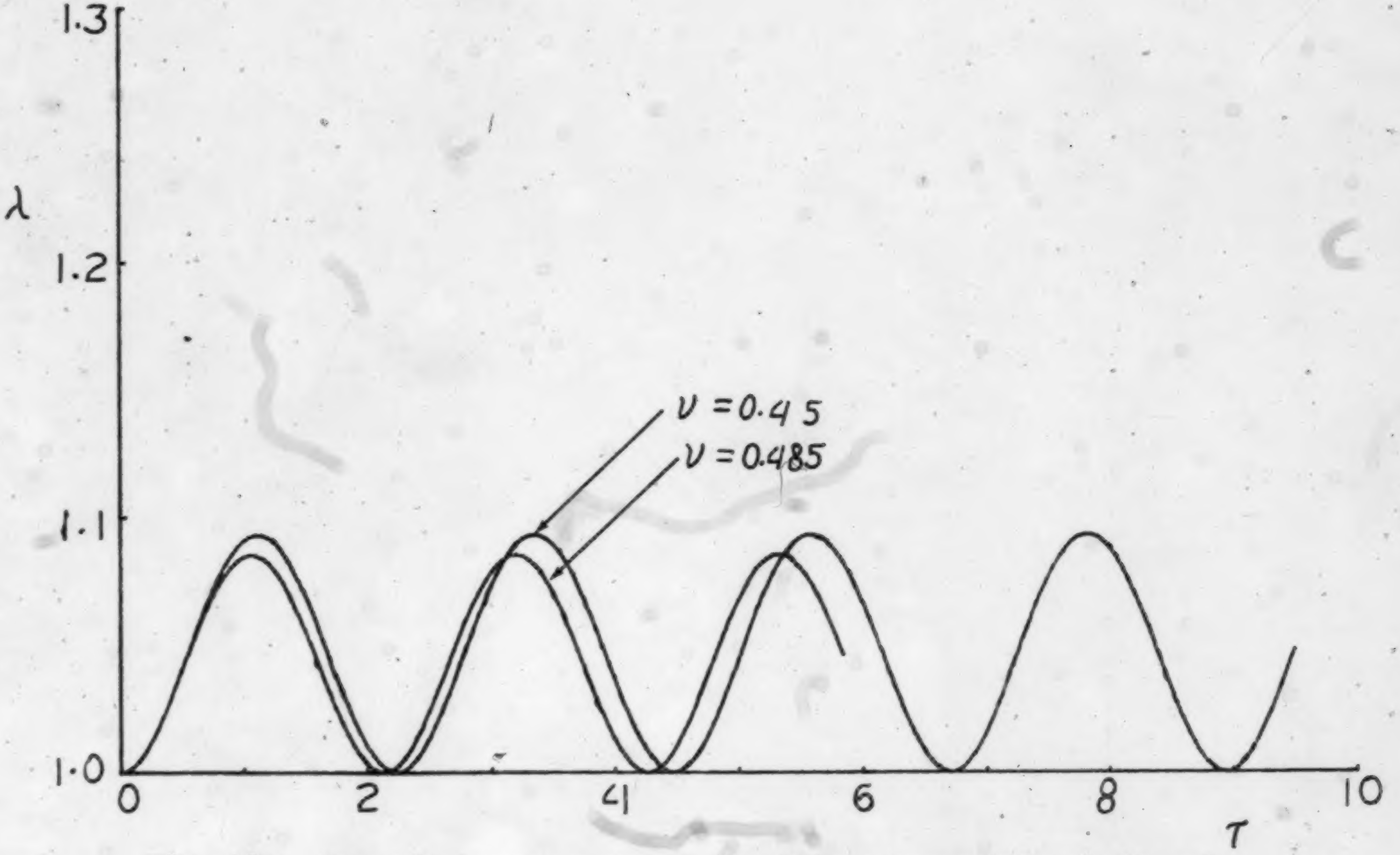

Fig. 17a. Dynamic response curves for thin compressible shells of Blatz-Ko material under a step function application of pressure, Q = 0.02.

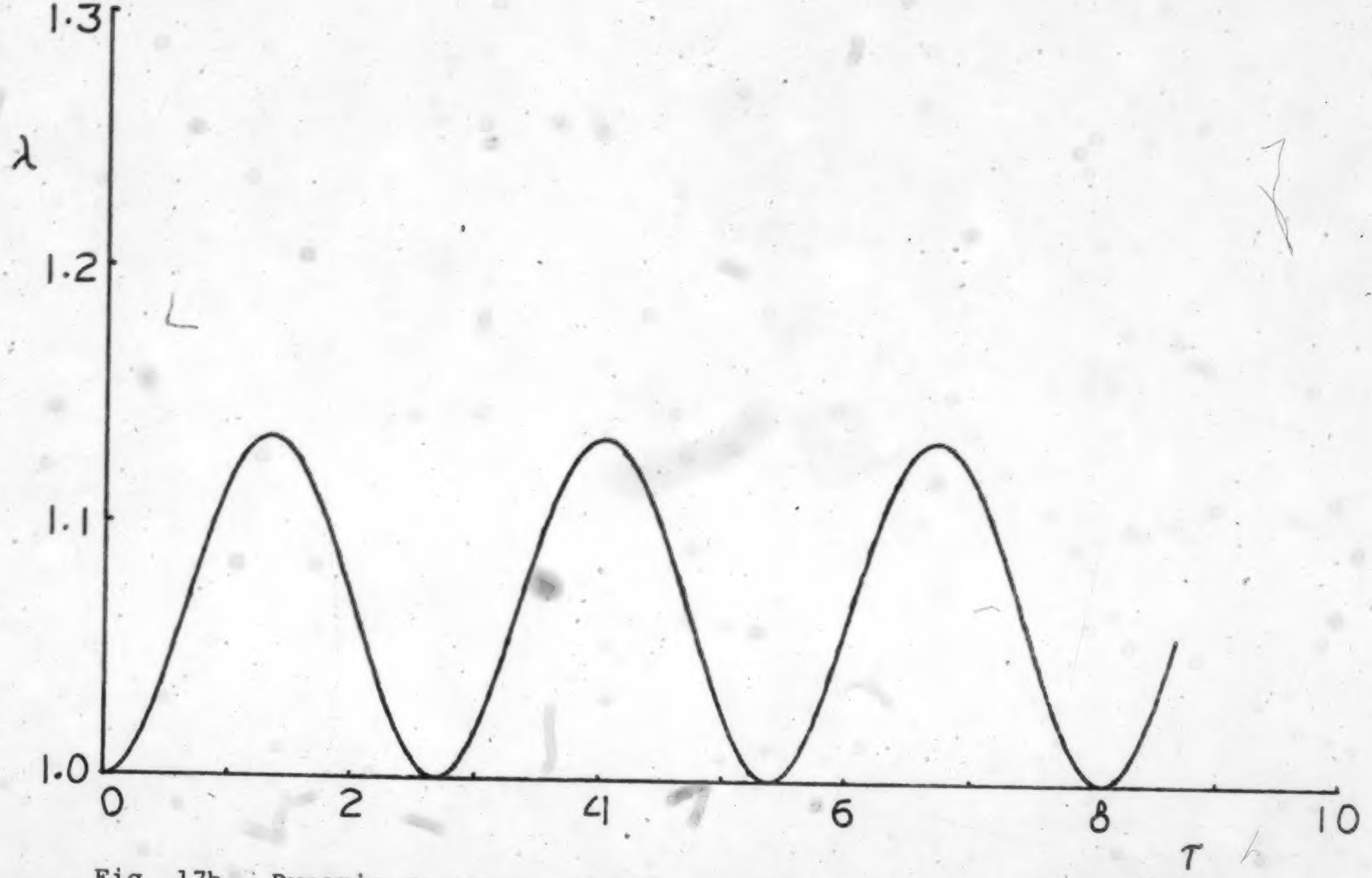

Fig. 17b. Dynamic response curve for a thin compressible shell of Blatz-Ko material: a particular case with $Q = 0.02$ and $\nu = 0.3$.

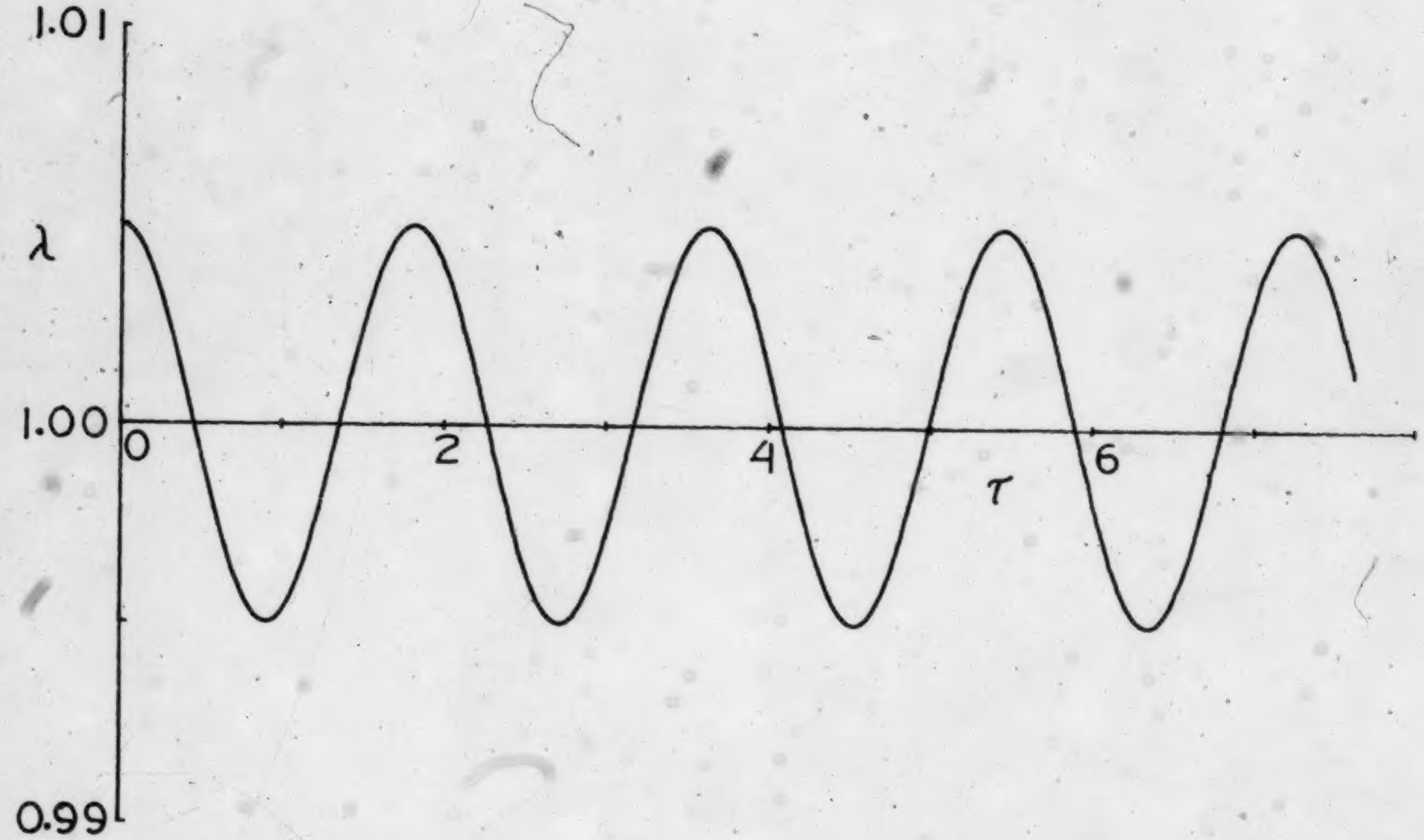

Fig. 18. Dynamic response curve for free oscillation of a neo-Hookean thin-walled shell, with small amplitude: $\lambda_0 = 1.005$.

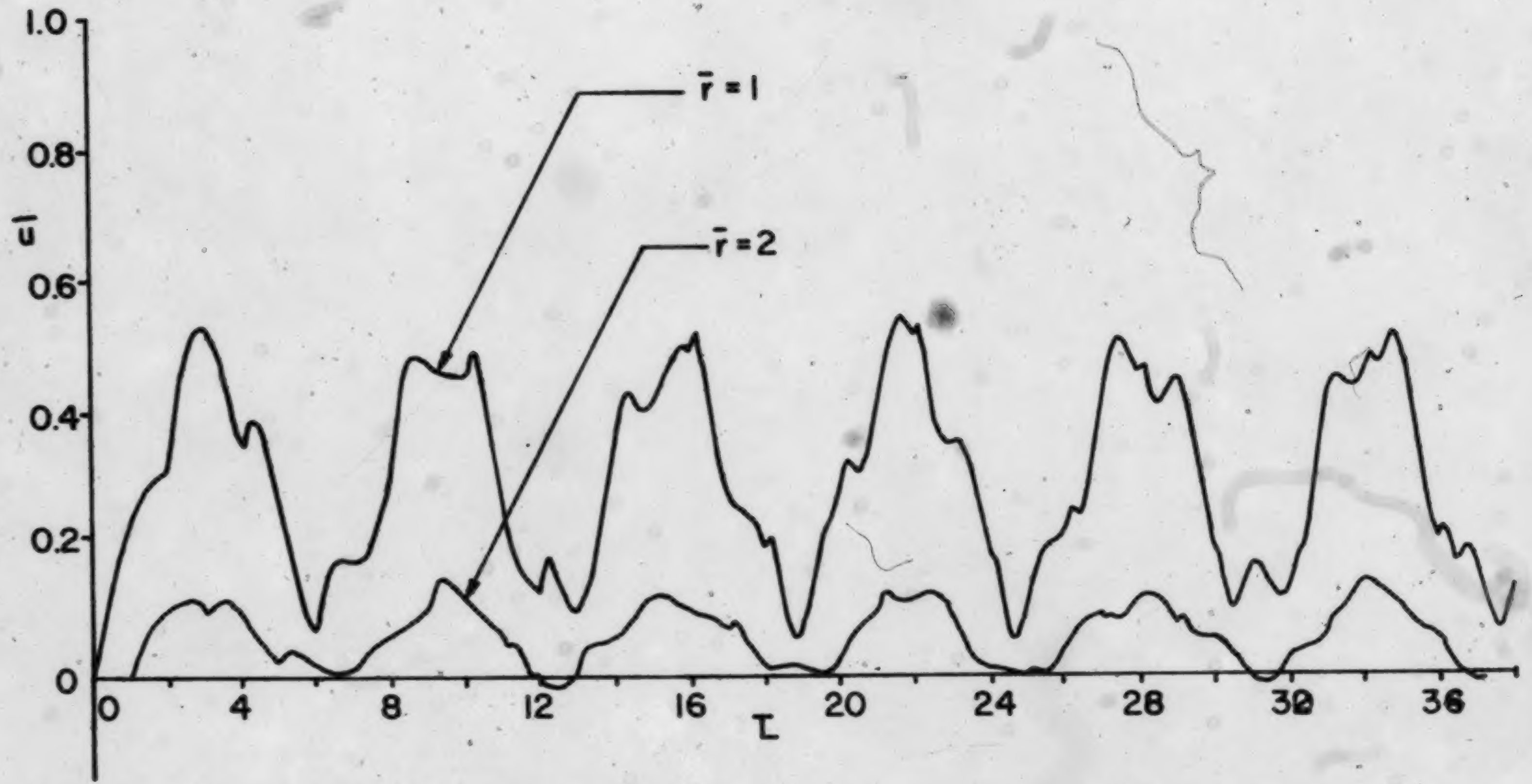

Fig. 19a. Dynamic response curve of the inner and outer surfaces of a thick compressible shell, with B/A = 2, under a step function application of pressure, Q = 1.

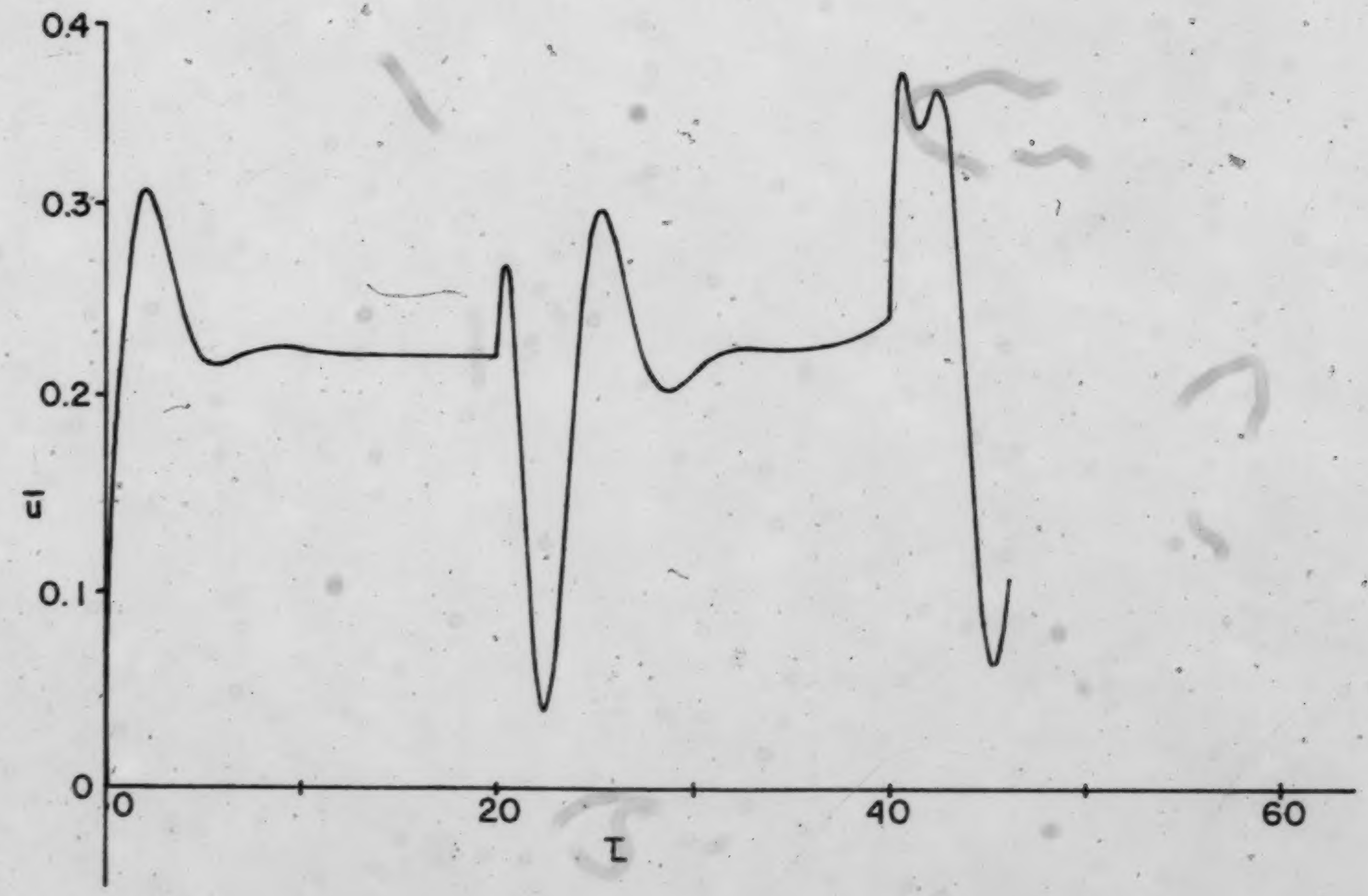

Fig. 19b. Dynamic response curve of the inner surface of a thick compressible shell with B/A = 11, under a step function application of pressure, Q = 1.

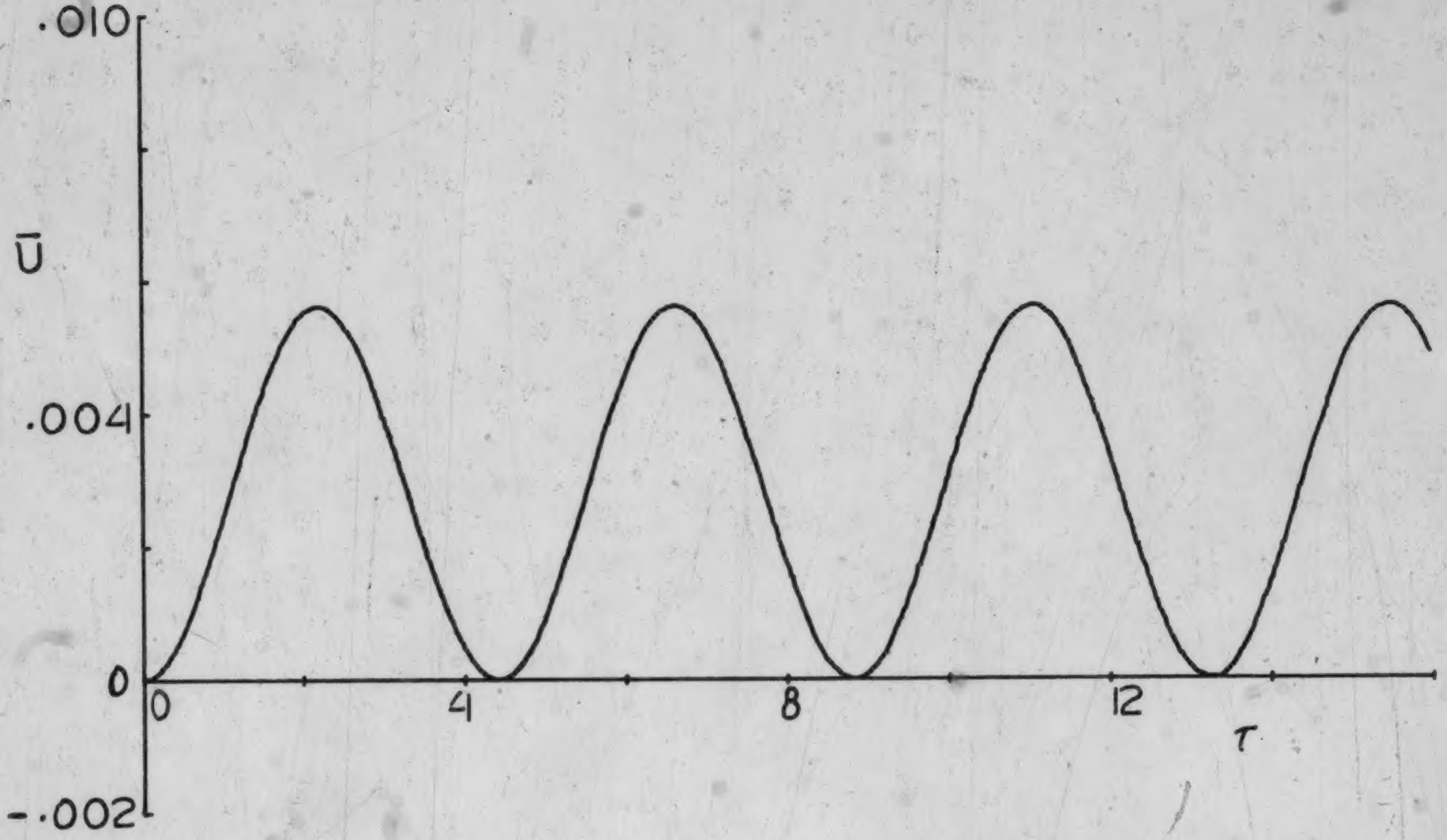

Fig. 19c. Dynamic response curve of a thin compressible shell obtained as a limiting case of Fig. 19a as B/A approaches 1.

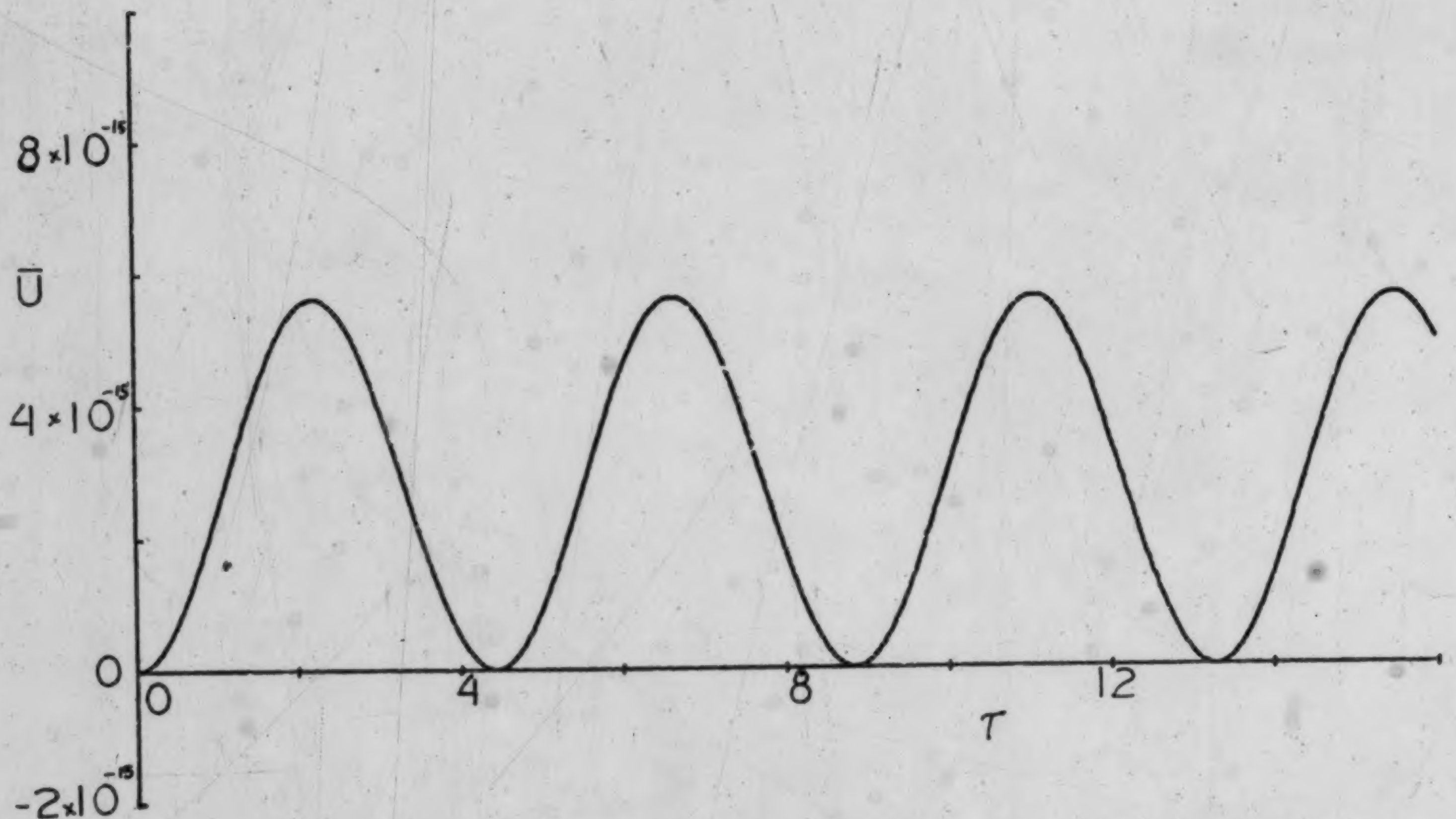

Fig. 19d. Dynamic response curve of a thin compressible shell obtained as a limiting case of Fig. 19a: case of Q approaching zero.

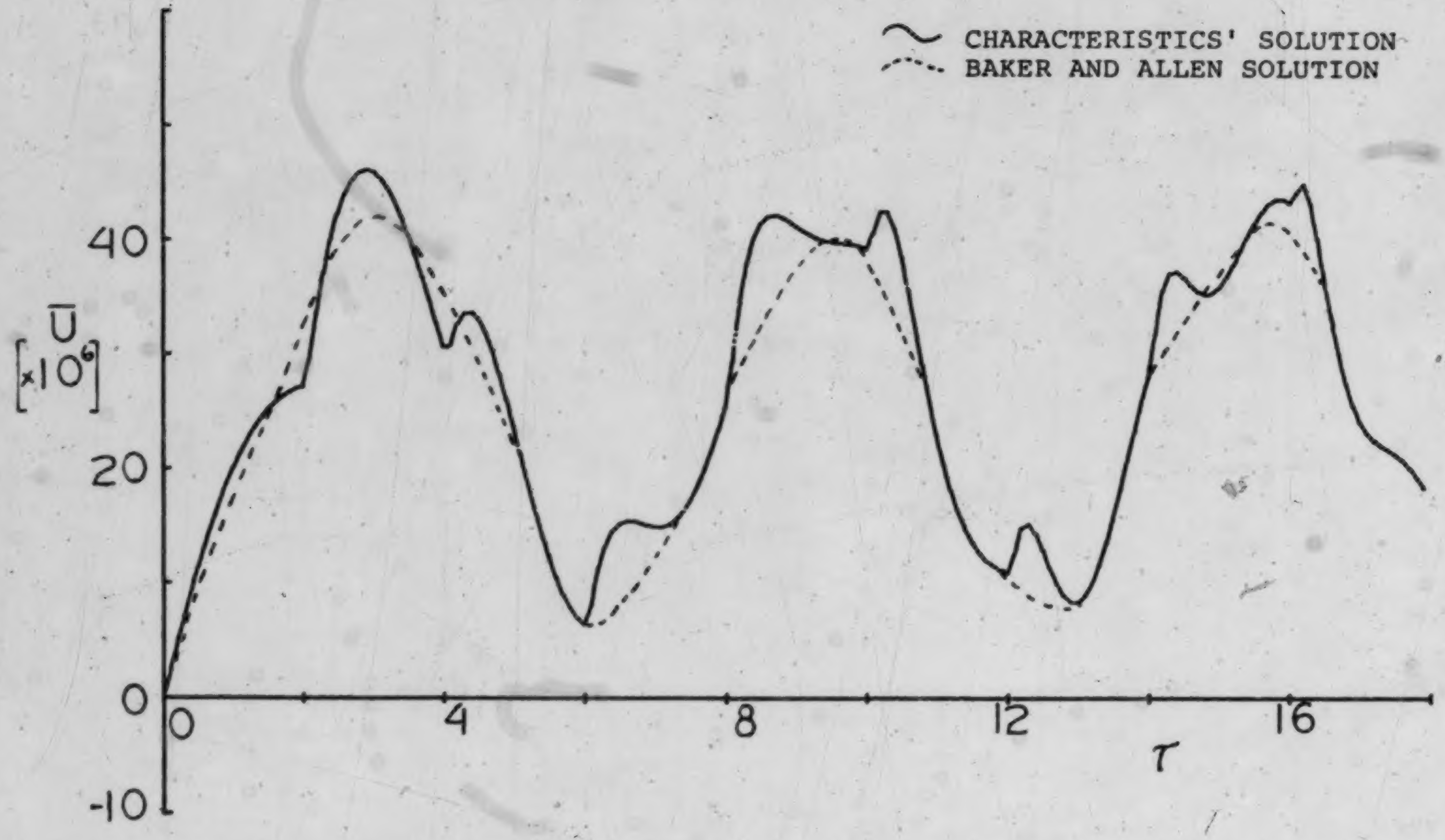

Fig. 19e. Comparison of a response curve of Fig. 19a with that obtained by other investigators.

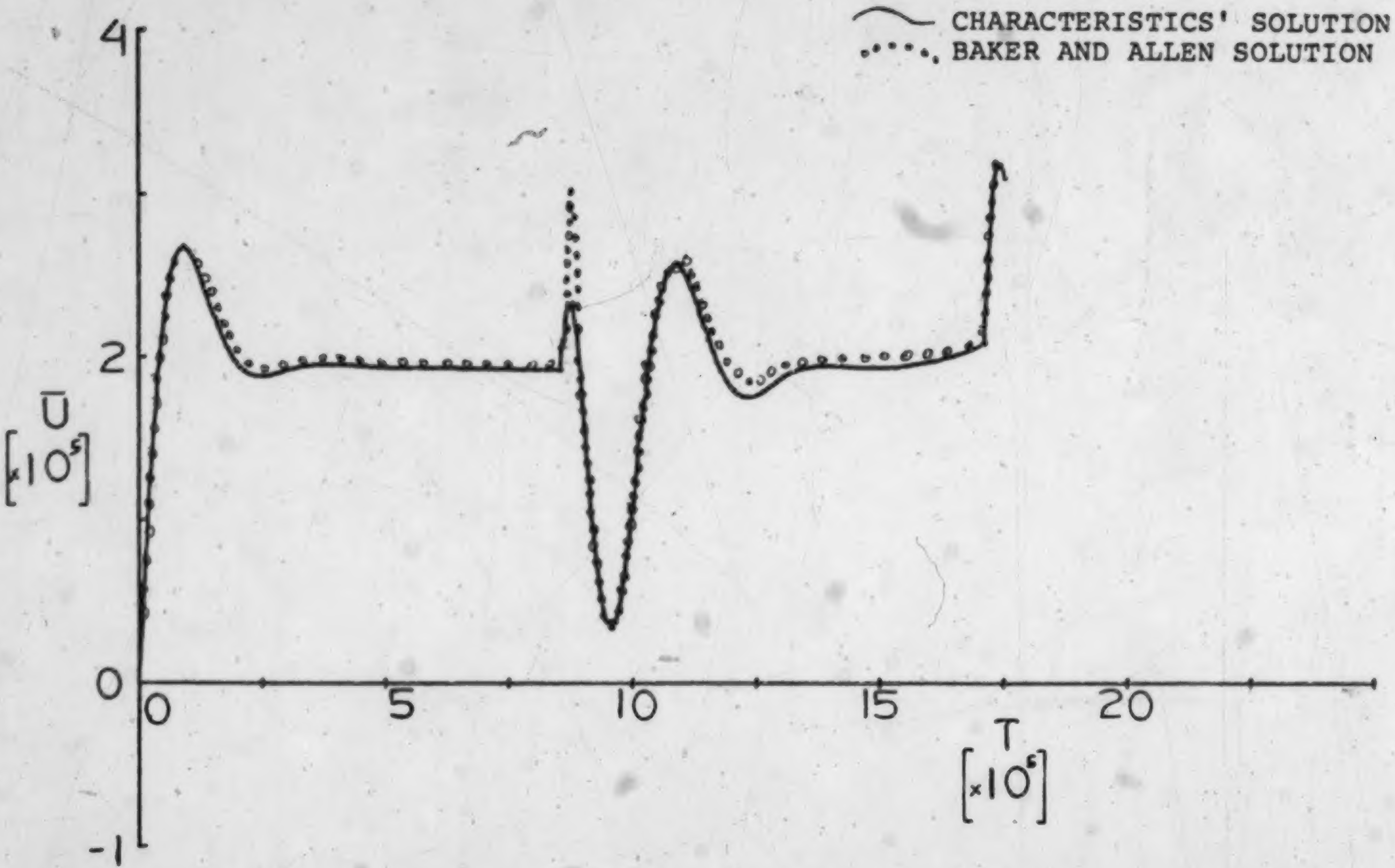

Fig. 19f. Comparison of response curve of Fig. 19b with that obtained by other investigators.

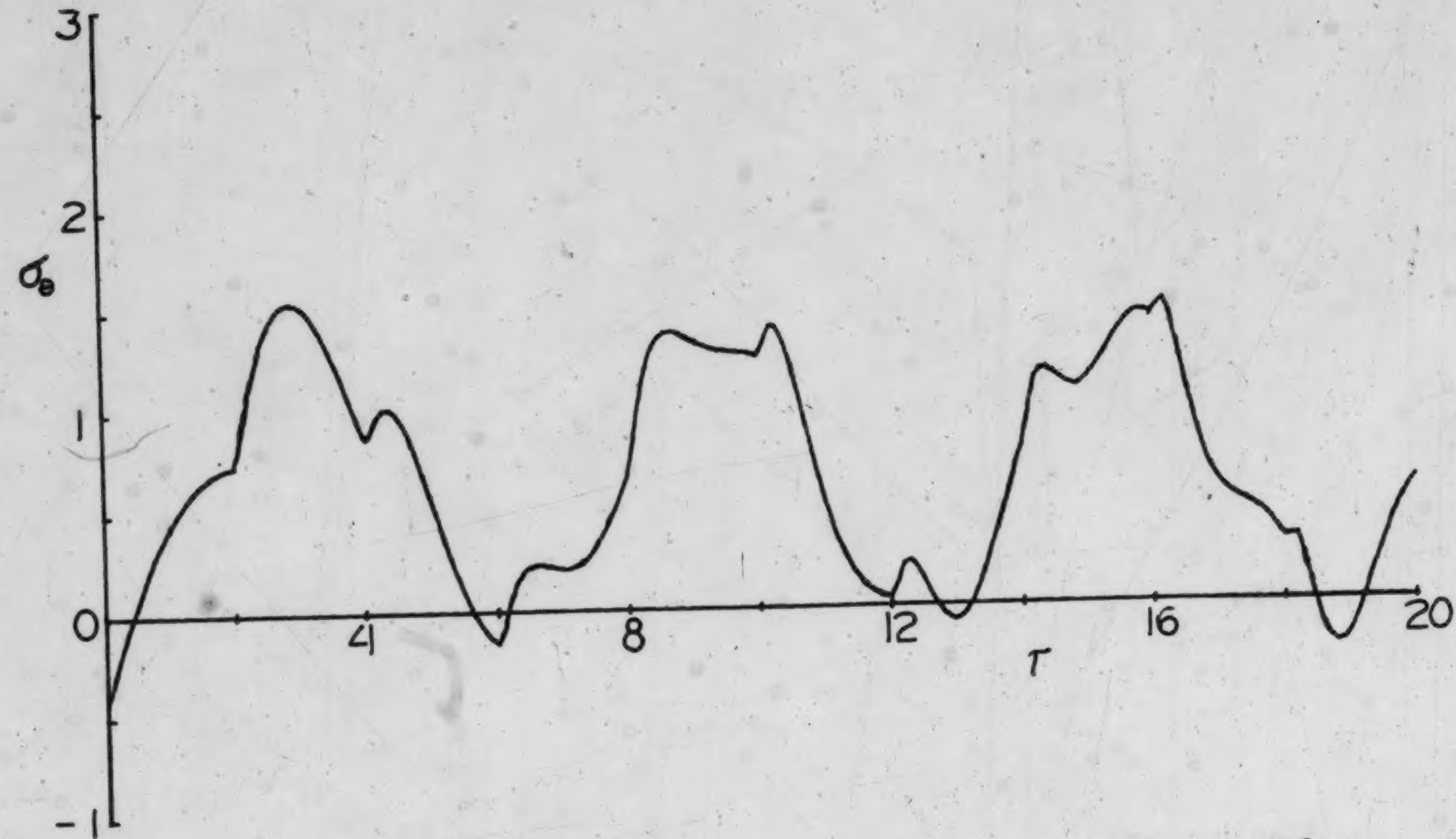

Fig. 20. Variation of tangential stress with time at the inner surface of a thick compressible shell under a step function application of pressure, $Q = 1$.

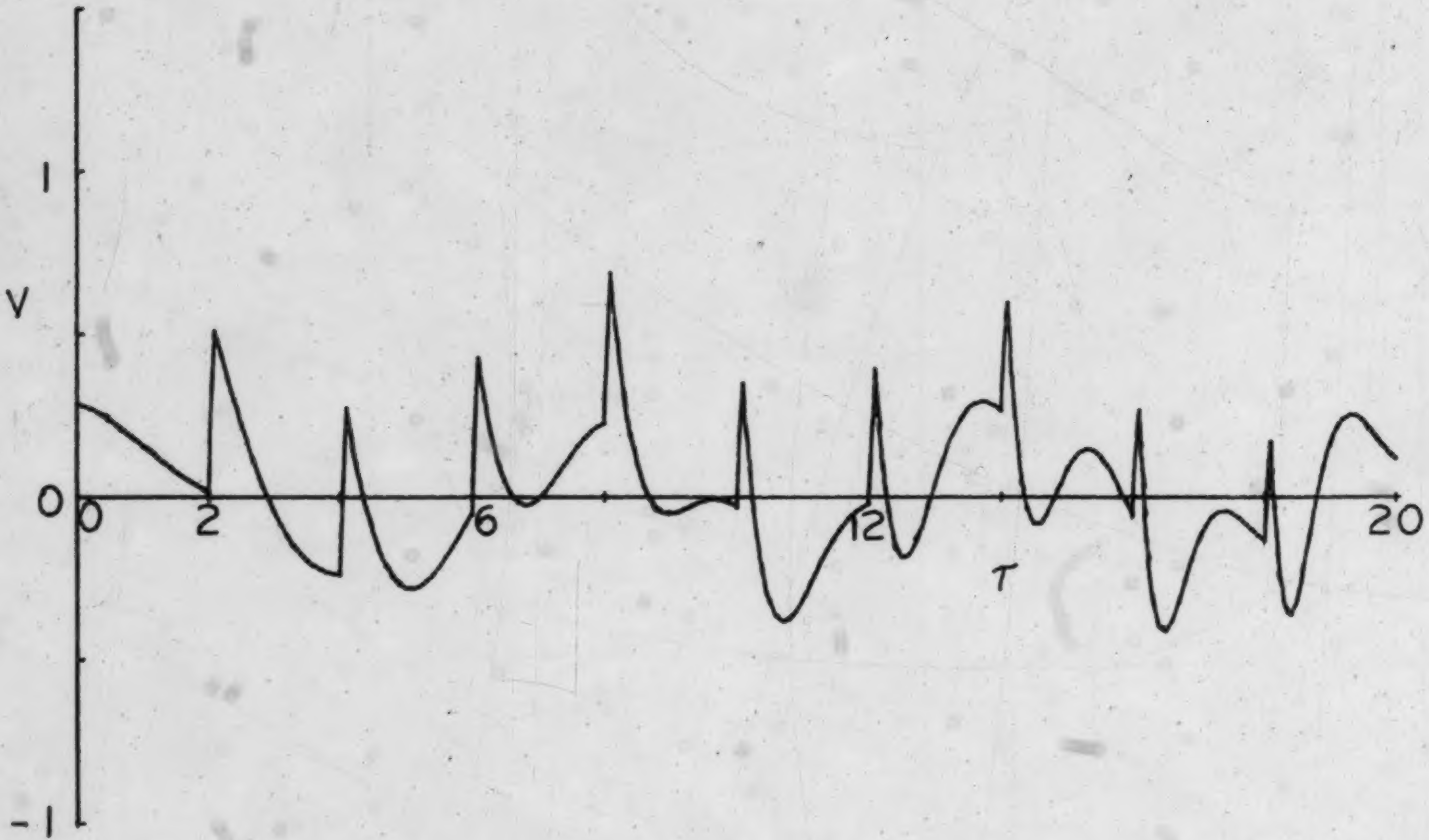

Fig. 21. Variation of particle velocity with time at the inner surface of a thick compressible shell under a step function application of pressure, Q = 1.

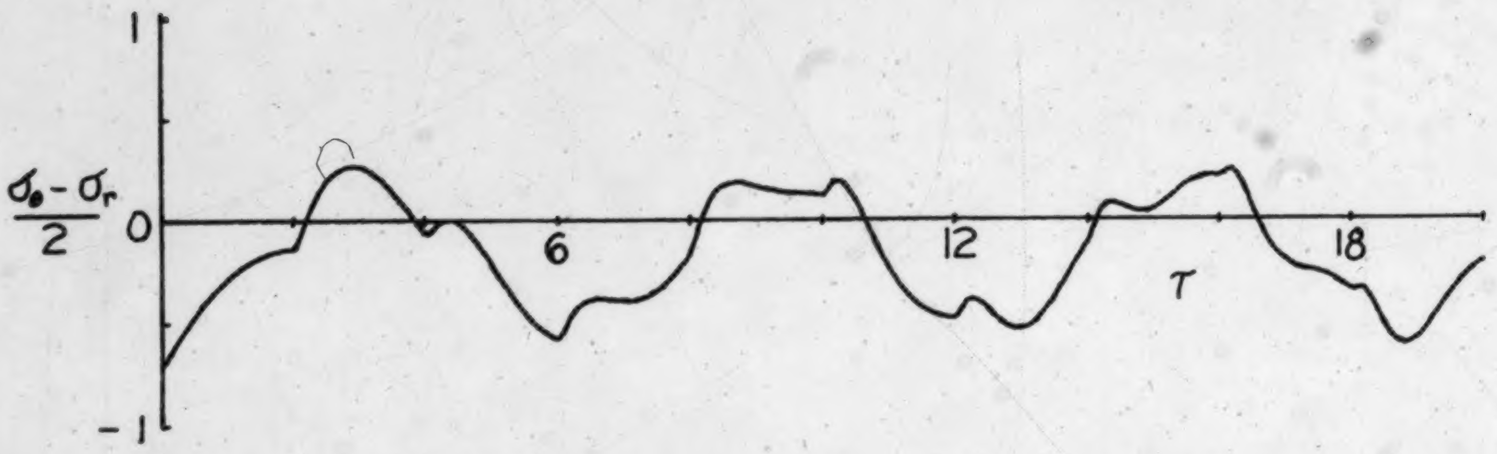

Fig. 22. Variation of shear stress with time at the inner surface of a thick compressible shell under a step input pressure, $Q = 1$.

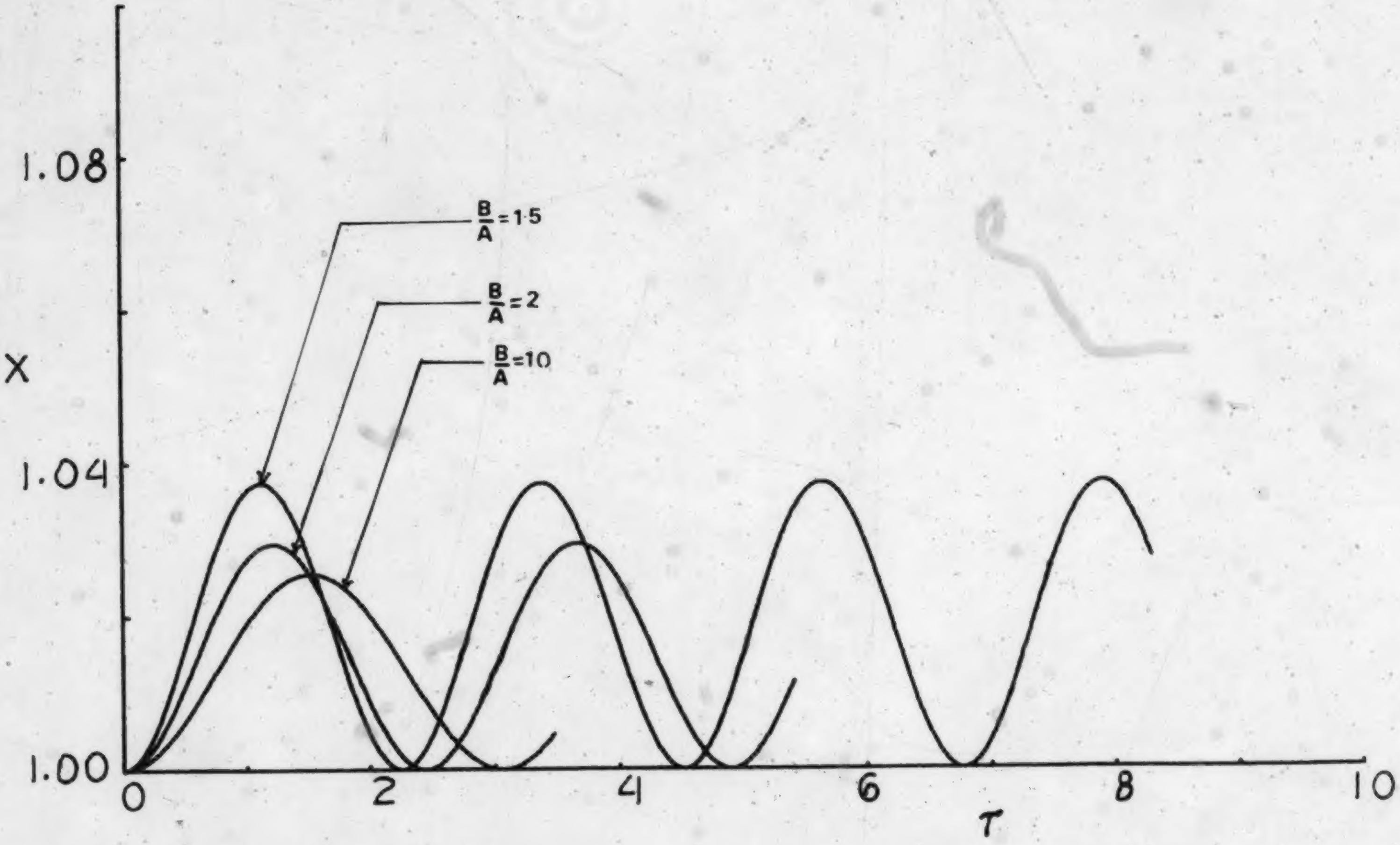

Fig. 23a. Dynamic response curve of the inner surface of thick-walled incompressible neo-Hookean shells under a given step input pressure, Q = 0.05.

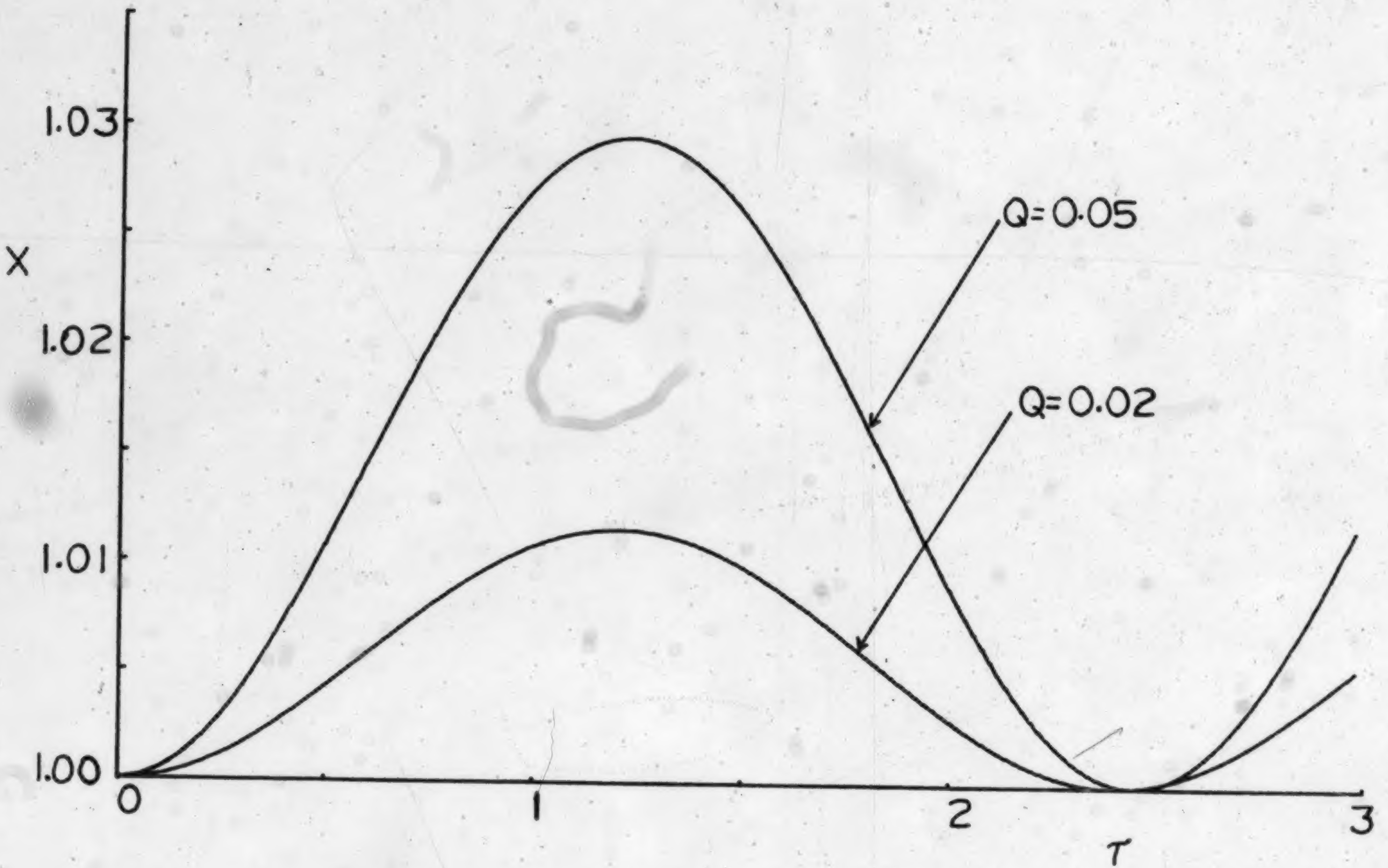

Fig. 23b. Dynamic response curve of the inner surface of a thick neo-Hookean shell, with B/A = 2, under various step input pressures.

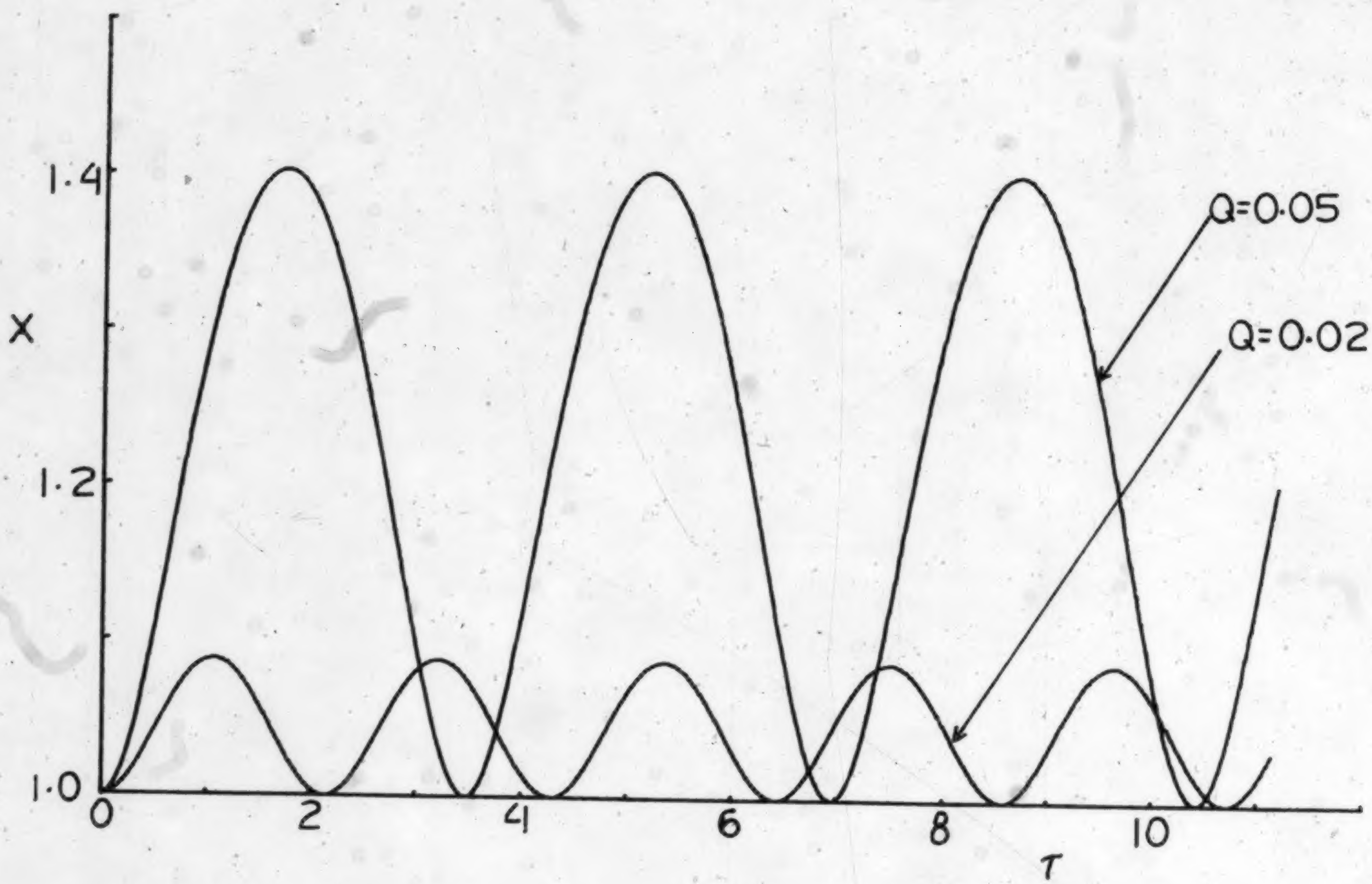

Fig. 23c. Dynamic response curve of a thin-walled neo-Hookean shell obtained as a limiting case of Fig. 23a, as B/A approaches 1.

```
  1 INPUT P,E
  2 PRINT TAB15"STATIC EQUILM OF BLATZ KO S.E.F."
  3 PRINT
  4 PRINT TAB25"NU="P
  5 PRINT
  6 PRINT "STRETCH","PRESSURE"
  8 PRINT
 15 S=-P/(1-2*P)
 20 Q0=0.0001
 25 FOR X=1 TO 3 STEP 0.05
 30 Q=Q0
 35 K=X/(2*E)
 40 A=1/(X*X)
 45 B=2*X**(6*S-4)
 50 C=X**(12*S-6)
 55 F=Q*Q/2-A*(1-K*Q)+B*((1-K*Q)**S)-C*((1-K*Q)
      **(2*S-1))
 60 F1=Q/2+A*K-B*S*K*((1-K*Q)**(S-1))+C*(2*S-1)
       *K*((1-K*Q)**(2*S-2))
 65 Q1=Q0-F/F1
 70 IF ABS(Q1-Q0) <= 1E-10 THEN 85
 75 Q0=Q1
 80 GOTO 30
 85 PRINT X,Q1
 90 Q0=Q1
 95 NEXT X
100 END
```

Program 1. Program for solving the equilibrium equation for the thin compressible shell of Blatz-Ko material

Program 2a. Program for evaluating the maximum step input pressure, Q_{max}, for periodic motion of an incompressible shell of Mooney-Rivlin material.

```
  5 INPUT C,E,H
 15 PRINT "Q(MAX) FOR DYN.STAB.OF A GIVEN S.E.F."
 20 PRINT
 25 PRINT "C="C,"E="E,"H="H
 35 PRINT
 45 G1=0
 50 X=1+H
 55 GOSUB 230
 60 G2=F
 65 IF G1*G2<0 THEN 95
 70 IF INTX=X THEN 260
 75 IF X >= 5 THEN 270
 80 G1=G2
 85 X=X+H
 90 GOTO 55
 95 X1=X-H
100 X2=X
105 R=X2
110 X=X1
115 GOSUB 230
120 F1=F
125 X=X2
130 GOSUB 230
135 F2=F
140 X3=X1-(X2-X1)*F1/(F2-F1)
145 X=X3
150 GOSUB 230
155 F3=F
160 IF ABS(X3-R) <= 1E-10 THEN 210
165 IF F1*F3<0 THEN 180
170 IF F1*F3>0 THEN 195
175 IF F1*F3=0 THEN 210
180 X2=X3
185 R=X2
190 GOTO 125
195 X1=X3
200 R=X1
205 GOTO 110
210 PRINT
215 PRINT
220 PRINT TAB5"CRITICAL STRETCH="X3,"Q(MAX)="Q
225 END
230 A=2*C*(1/X-1/(X**7))+2*(1-C)*(X-1/(X**5))
235 B=(X**2)/2+1/(4*(X**4))
240 D=(X**4)/4+1/(2*(X**2))
245 Q=E*A
250 F=A*(X**3-1)/3-2*C*B-2*(1-C)*D+3/2
255 RETURN
260 PRINT "NO OTHER ROOT OF X'/X UP TO X="X
265 GOTO 80
270 IF H<1E-06 THEN 225
275 H=H/10
280 GOTO 35
```

Program 2b. Program for evaluating the maximum step input pressure, Q_{max}, for periodic motion of an imcompressible shell of material with logarithmic strain energy function.

```
  5 INPUT C,E,H
 15 PRINT "Q(MAX) FOR DYN.STAB.OF A GIVEN S.E.F."
 20 PRINT
 25 PRINT "C="C,"E="E,"H="H
 35 PRINT
 45 G1=0
 50 X=1+H
 55 GOSUB 230
 60 G2=F
 65 IF G1*G2<0 THEN 95
 70 IF INTX=X THEN 260
 75 IF X >= 5 THEN 270
 80 G1=G2
 85 X=X+H
 90 GOTO 55
 95 X1=X-H
100 X2=X
105 R=X2
110 X=X1
115 GOSUB 230
120 F1=F
125 X=X2
130 GOSUB 230
135 F2=F
140 X3=X1-(X2-X1)*F1/(F2-F1)
145 X=X3
150 GOSUB 230
155 F3=F
160 IF ABS(X3-R) <= 1E-10 THEN 210
165 IF F1*F3<0 THEN 180
170 IF F1*F3>0 THEN 195
175 IF F1*F3=0 THEN 210
180 X2=X3
185 R=X2
190 GOTO 125
195 X1=X3
200 R=X1
205 GOTO 110
210 PRINT
215 PRINT
220 PRINT TAB5"CRITICAL STRETCH="X3,"Q(MAX)="Q
225 END
230 A=2*C*(1/X-1/(X**7))+3*(1-C)*(X**3-1/(X**3))/(2+X**6)
235 B=(X**2)/2+1/(4*(X**4))-3/4
240 D=(LOG((2+X**6)/3))/6-(LOG((3*X**6)/(2+X**6)))/12
245 Q=E*A
250 F=A*(X**3-1)/3-2*C*B-3*(1-C)*D
255 RETURN
260 PRINT "NO OTHER ROOT OF X'/X UP TO X="X
265 GOTO 80
270 IF H<1E-06 THEN 225
275 H=H/5
280 GOTO 35
```

```
 14 INPUT Q,E,P,H
 18 PRINT "Q="Q,"E="E,"NU="P,"H="H
 20 PRINT
 30 PRINT "Q(MAX) FOR BLATZ KO MATERIAL"
 35 J=1
 40 X0=1
 42 V0=0
 45 D0=1
 48 C=-1/(1-2*P)
 49 GOSUB 50
 50 X=X0
 52 GOSUB 450
 53 X0=X
 55 N=0
 65 A0=(Q*X0*X0/E)-2*(X0-D0**2/X0)
 70 A1=A0
 75 V1=V0+(A1+A0)*H/2
 80 X1=X0+(V1+V0)*H/2
 85 X=X1
 90 GOSUB 450
 95 A2=(Q*X*X/E)-2*(X-D**2/X)
100 IF ABS(A2-A1)<1E-08 THEN 115
105 A1=A2
110 GOTO 75
115 IF A1*A2<0 THEN 500
120 N=N+1
121 V0=V1
122 X0=X
123 D0=D
150 IF N*H >= 500 THEN 750
160 GOTO 55
170 RETURN
450 D=D0
455 F=Q+(2*D/(X*X))-(2*(X*X*D)**C)
460 F1=(2/(X*X))-(2*C*(X**(2*C))*(D**(C-1)))
465 D1=D0-(F/F1)
470 IF ABS(D1-D0) <= 1E-10 THEN 485
475 D0=D1
480 GOTO 450
485 D=D1
490 RETURN
500 IF J=2 THEN 600
505 J=J+1
510 GOTO 120
600 L=1
605 X0=X
610 V0=V1
615 D0=D
620 IF L=3 THEN 650
625 H=H/2
630 L=L+1
635 GOSUB 50
650 IF V0 <= 1E-08 THEN 700
655 IF V0>0 THEN 680
660 PRINT "APPROX Q(MAX)="Q
```

```
665 Q=Q+(Q/10)
670 GOTO 35
680 PRINT "APPROX Q(MAX)="Q
685 Q=Q-(Q/10)
690 GOTO 35
700 PRINT "CRITICAL STRETCH="X0,"Q(MAX)="Q
750 END
```

Program 2c. Program for evaluating the maximum step input pressure, Q_{max}, for periodic motion of a compressible shell of Blatz-Ko material

```
10 FORMAT 11X,F4.1,6X,F12.9,6X,F12.9,6X,F12.9
12 FORMAT 11X,F6.3,4X,F6.3,4X,F6.3,4X,F7.4
14 INPUT Q,E,C,H
16 PRINT
18 WRITE (15,12)"Q="Q,"E="E,"C="C,"H="H
20 PRINT
22 PRINT TAB11"DYNAMICS OF A COMPR THIN SPH SHELL"
24 PRINT
26 PRINT TAB11"METHOD 2: MODIFIED DISCRETE VARIABLE"
28 PRINT
30 PRINT TAB11"TIME"TAB24"ACCN"TAB41"STRETCH"TAB56
         "RATE OF STRETCH"
32 PRINT
34 PRINT TAB12"0.0"TAB40"1.0"TAB58"0.0"
40 X0=1
42 V0=0
54 O=1
55 N=0
65 X=X0
66 GOSUB 450
68 A0=A
70 A1=A0
75 V1=V0+(A1+A0)*H/2
80 X1=X0+(V1+V0)*H/2
85 X=X1
90 GOSUB 450
95 A2=A
100 IF ABS(A2-A1)<1E-08 THEN 120
105 A1=A2
110 GOTO 75
120 N=N+1
121 V0=V1
122 X0=X
130 T=N*H*O
135 WRITE(15,10)T,A2,X0,V0
150 IF T >= 500 THEN 180
155 O=O+1
160 GOTO 55
180 END
450 A=Q*X*X/E-2*C*(X-(1/X**5))-2*(1-C)*(X**3-(1/X**3))
460 RETURN
```

Program 3a. Discrete variable method for solving the governing equation for a thin incompressible shell of Mooney-Rivlin material

Program 3b. Discrete variable method for solving the governing equation for a thin compressible shell of Blatz-Ko material.

```
 10 FORMAT 11X,F4.1,6X,F12.9,6X,F12.9,6X,F12.9
 12 FORMAT 11X,F6.3,4X,F6.3,4X,F6.3,4X,F7.4
 14 INPUT Q,E,P,H
 16 PRINT
 18 WRITE (15,12)"Q="Q,"E="E,"NU="P,"H="H
 20 PRINT
 22 PRINT TAB11"DYNAMICS OF A COMPR THIN SPH SHELL"
 24 PRINT
 26 PRINT TAB11"METHOD 2: MODIFIED DISCRETE VARIABLE"
 28 PRINT
 30 PRINT TAB11"TIME"TAB24"ACCN"TAB41"STRETCH"TAB56
          "RATE OF STRETCH"
 32 PRINT
 34 PRINT TAB12"0.0"TAB40"1.0"TAB58"0.0"
 40 X0=1
 42 V0=0
 45 D0=1
 48 C=-1/(1-2*P)
 50 X=X0
 52 GOSUB 450
 53 X0=X
 54 O=1
 55 N=0
 65 A0=(Q*X0*X0/E)-2*(X0-D0**2/X0)
 70 A1=A0
 75 V1=V0+(A1+A0)*H/2
 80 X1=X0+(V1+V0)*H/2
 85 X=X1
 90 GOSUB 450
 95 A2=(Q*X*X/E)-2*(X-D**2/X)
100 IF ABS(A2-A1)<1E-08 THEN 120
105 A1=A2
110 GOTO 75
120 N=N+1
121 V0=V1
122 X0=X
123 D0=D
125 IF N*H=0.1 THEN 130
127 GOTO 65
130 T=N*H*O
135 WRITE (15,10)T,A2,X0,V0
150 IF T >= 10 THEN 180
155 O=O+1
160 GOTO 55
180 END
450 D=D0
455 F=Q+(2*D/(X*X))-(2*(X*X*D)**C)
460 F1=(2/(X*X))-(2*C*(X**(2*C))*(D**(C-1)))
465 D1=D0-(F/F1)
470 IF ABS(D1-D0) <= 1E-10 THEN 485
475 D0=D1
480 GOTO 450
485 D=D1
490 RETURN
```

Program 4a. Fourth order Runge-Kutta process for solving the governing equation for a thin incompressible shell of Mooney-Rivlin material.

```
 10 FORMAT 11X,F4.1,6X,F12.9,6X,F12.9,6X,F12.9
 14 INPUT Q,E,C,H
 16 PRINT
 18 PRINT "Q="Q,"E="E,"C="C,"H="H
 20 PRINT
 22 PRINT TAB11"DYNAMICS OF A COMPR THIN SPH SHELL"
 24 PRINT
 26 PRINT TAB11"METHOD 1: 4TH ORDER RUNGE KUTTA"
 28 PRINT
 29 PRINT
 30 PRINT TAB11"TIME"TAB24"ACCN"TAB41"STRETCH"TAB56
         "RATE OF STRETCH"
 32 PRINT
 34 PRINT TAB12"0.0"TAB40"1.0"TAB58"0.0"
 40 X0=1
 42 V0=0
 44 D0=1
 50 O=1
 55 N=0
 60 X=X0
 64 GOSUB 500
 66 K1=K
 70 X=X0+H*V0/2+H*K1/8
 74 GOSUB 500
 76 K2=K
 80 X=X0+H*V0+H*K2/2
 84 GOSUB 500
 86 K3=K
 95 X1=X0+H*V0+H*(K1+2*K2)/6
100 V1=V0+(K1+4*K2+K3)/6
105 A1=Q*X1*X1/E-2*C*(X1-(1/X1**5))-2*(1-C)*(X1**3-
      (1/X1**3))
110 N=N+1
115 X0=X1
120 V0=V1
130 IF N*H=0.1 THEN 140
135 GOTO 60
140 T=N*H*O
145 WRITE (15,10)T,A1,X1,V1
150 IF T >= 10 THEN 180
155 O=O+1
160 GOTO 55
180 END
500 K=H*(Q*X*X/E-2*C*(X-(1/X**5))-2*(1-C)*(X**3-
      (1/X**3)))
510 RETURN
```

```
 10 FORMAT 11X,F4.1,6X,F12.9,6X,F12.9,6X,F12.9
 12 FORMAT 11X,F6.3,4X,F6.3,4X,F6.3,4X,F7.4
 14 INPUT Q,E,P,H
 16 PRINT
 18 WRITE (15,12)"Q="Q,"E="E,"NU="P,"H="H
 20 PRINT
 22 PRINT TAB11"DYNAMICS OF A COMPR THIN SPH SHELL"
 24 PRINT
 26 PRINT TAB11"METHOD 4: 4TH ORDER RUNGE KUTTA"
 28 PRINT
 29 PRINT
 30 PRINT TAB11"TIME"TAB24"ACCN"TAB41"STRETCH"TAB56
         "RATE OF STRETCH"
 32 PRINT
 34 PRINT TAB12"0.0"TAB40"1.0"TAB58"0.0"
 40 X0=1
 42 V0=0
 44 D0=1
 48 C=-1/(1-2*P)
 50 O=1
 55 N=0
 60 X=X0
 62 GOSUB 450
 64 GOSUB 500
 66 K1=K
 70 X=X0+H*V0/2+H*K1/8
 72 GOSUB 450
 74 GOSUB 500
 76 K2=K
 80 X=X0+H*V0+H*K2/2
 82 GOSUB 450
 84 GOSUB 500
 86 K3=K
 95 X1=X0+H*V0+H*(K1+2*K2)/6
100 V1=V0+(K1+4*K2+K3)/6
105 A1=(Q*X1*X1/E)-(2*X1)+(2*D*D/X1)
110 N=N+1
115 X0=X1
120 V0=V1
125 D0=D
130 IF N*H=0.1 THEN 140
135 GOTO 60
140 T=N*H*O
145 WRITE (15,10)T,A1,X1,V1
150 IF T >= 10 THEN 180
155 O=O+1
160 GOTO 55
180 END
450 D=D0
455 F=Q+(2*D/(X*X))-(2*(X*X*D)**C)
460 F1=(2/(X*X))-(2*C*(X**(2*C))*(D**(C-1)))
465 D1=D0 F/F1
470 IF ABS(D1-D0) <= 1E-10 THEN 485
```

```
475 D0=D1
480 GOTO 450
485 D=D1
490 RETURN
500 K=H*(Q*X*X/E-2*X+2*D*D/X)
510 RETURN
```

Program 4b. Fourth order Runge-Kutta process for solving the governing equations for a thin compressible shell of Blatz-Ko material.

```
  4 INPUT Q,E,C,H
  6 T=0
  8 X0=1
 10 V0=0
 12 N=1
 14 X=X0
 16 L1=V0
 18 GOSUB 400
 20 A0=A
 22 A1=A0
 24 V1=V0+(A1+A0)*H/2
 26 X1=X0+(V1+V0)*H/2
 28 X=X1
 30 GOSUB 400
 32 A2=A
 34 IF ABS(A2-A1)<1E-08 THEN 40
 36 A1=A2
 38 GOTO 24
 40 IF N/10=INT(N/10) THEN 80
 42 IF L1*V1<0 THEN 54
 44 N=N+1
 46 V0=V1
 48 X0=X
 50 GOTO 14
 54 PRINT
 56 T=T+(N-1)*H
 58 PRINT TAB15"APPROX PERIOD OF OSCILLATION=" 2*T
 59 PRINT
 60 IF H=1E-10 THEN 74
 62 H=H/10
 64 V0=L1
 66 X0=X
 70 GOTO 12
 74 END
 80 PRINT T+N*H,V1,X
 84 GOTO 42
400 A=Q*X*X/E-2*C*(X-1/(X**5))-2*(1-C)*(X**3-1/(X**3))
410 RETURN
```

Program 5a. Program for finding the period of oscillation of a thin incompressible shell of Mooney-Rivlin material

```
  4 INPUT Q,E,C,H
  6 T=0
  8 X0=1
 10 V0=0
 12 N=1
 14 X=X0
 16 L1=V0
 18 GOSUB 400
 20 A0=A
 22 A1=A0
 24 V1=V0+(A1+A0)*H/2
 26 X1=X0+(V1+V0)*H/2
 28 X=X1
 30 GOSUB 400
 32 A2=A
 34 IF ABS(A2-A1)<1E-08 THEN 40
 36 A1=A2
 38 GOTO 24
 40 IF N/10=INT(N/10) THEN 80
 42 IF L1*V1<0 THEN 54
 44 N=N+1
 46 V0=V1
 48 X0=X
 50 GOTO 14
 54 PRINT
 56 T=T+(N-1)*H
 58 PRINT TAB15"APPROX PERIOD OF OSCILLATION="2*T
 59 PRINT
 60 IF H=1E-10 THEN 74
 62 H=H/10
 64 V0=L1
 66 X0=X
 70 GOTO 12
 74 END
 80 PRINT T+N*H,V1,X
 84 GOTO 42
400 B1=X-(1/(X**5))
405 B2=X**5-(1/X)
410 B3=2+(X**6)
420 A=Q*X*X/E-2*C*B1-3*(1-C)*B2/B3
425 RETURN
```

Program 5b. Program for finding the period of oscillation of a thin incompressible shell of material with logarithmic strain energy function

Program 5c. Program for finding the period of oscillation of a thin compressible shell of Blatz-Ko material.

```
  2 D0=1
  4 INPUT Q,E,P,H
  5 C=-1/(1-2*P)
  6 T=0
  8 X0=1
 10 V0=0
 12 N=1
 14 X=X0
 16 L1=V0
 18 GOSUB 400
 20 A0=A
 22 A1=A0
 24 V1=V0+(A1+A0)*H/2
 26 X1=X0+(V1+V0)*H/2
 28 X=X1
 30 GOSUB 400
 32 A2=A
 34 IF ABS(A2-A1)<1E-08 THEN 40
 36 A1=A2
 38 GOTO 24
 40 IF N/10=INT(N/10) THEN 80
 42 IF L1*V1<0 THEN 54
 44 N=N+1
 46 V0=V1
 48 X0=X
 50 GOTO 14
 54 PRINT
 56 T=T+(N-1)*H
 58 PRINT TAB15"APPROX PERIOD OF OSCILLATION="2*T
 59 PRINT
 60 IF H=1E-10 THEN 74
 62 H=H/10
 64 V0=L1
 66 X0=X
 70 GOTO 12
 74 END
 80 PRINT T+N*H,V1,X
 84 GOTO 42
400 GOSUB 450
405 A=Q*X*X/E-2*(X-D**2/X)
410 RETURN
450 D=D0
455 F=Q+(2*D/(X*X))-(2*(X*X*D)**C)
460 F1=(2/(X*X))-(2*C*(X**(2*C))*(D**(C-1)))
465 D1=D0-(F/F1)
470 IF ABS(D1-D0) <= 1E-10 THEN 485
475 D0=D1
480 GOTO 450
485 D=D1
490 RETURN
```

```
  2 PRINT "Q=APPLIED PRESSURE","P=POISSONS RATIO"
  3 PRINT "Z=SHELL THICKNESS","K=INTERVAL SIZE"
  4 PRINT "M=NUMBER OF VERT.GRID LINES=(Z/K)+1"
  5 PRINT "R9=PLOTTING RADIUS","T6=INITIAL TIME"
  6 PRINT "INPUT Q,P,Z,K,M  ","INPUT R9,T6"
  8 INPUT Q,P,Z,K,M
  9 INPUT R9,T6
 10 C1=2*(1-P)/(1-2*P)
 15 C2=P/(1-P)
 20 FORMAT F7.3,2X,F6.3,2X,E15.8,4X,E15.8,4X,E15.8
 25 DIM H(105),U(105),W(105),P(105),Q(105),R(105)
 30 DIM A(3,3),S(3,1),B(3,1)
 35 DIMC(2,2),D(2,1),E(2,1)
 40 DIM F(2,2),T(2,1),G(2,1)
 42 PRINT "CHARACTERISTICS METHOD(TRIANGULAR REGIONS)"
 43 PRINT
 45 PRINT "APPLIED PRESSURE="Q,"POISSON'S RATIO="P
 50 PRINT "SHELL THICKNESS="Z,"INTERVAL SIZE="K
 55 PRINT
 65 READ R0,T0
 70 DATA 1,0
 75 PRINT TAB1"TIME"TAB9"RADIUS"TAB21"S(R)"TAB42"S(T)"
          TAB57"PARTICLE VEL"
 76 GOSUB 952
 85 I=1
 87 I3=I4=1
 95 M1=M
 97 A=1
100 IF INT(I/2)=I/2 THEN 290
105 R=R0
110 FOR N=1 TO M
120 IF I#1 THEN 130
125 P(N)=Q(N)=R(N)=0
130 H(N)=P(N)-(I3*Q/R)
135 U(N)=Q(N)-(I3*C2*Q/R)
140 W(N)=R(N)+(I3*Q/(C1*R))
145 R=R+K
150 NEXT N
152 I3=-1*I3
155 GOSUB 920
175 T2=T0+((I-1)*Z)
180 R2=R0
182 I1=1
185 N=1
195 GOSUB 630
200 GOSUB 685
205 IF I1=Z/K THEN 280
210 N=2
215 T1=T4
220 R1=R4
225 GOSUB 770
230 GOSUB 410
235 IF N=M1 THEN 250
```

```
240 N=N+1
245 GOTO 215
250 T2=T4-((M1-1)*K)
255 R2=R0
260 GOSUB 920
270 I1=I1+1
275 GOTO 185
280 GOSUB 920
281 IF I=39 THEN 285
282 I=I+1
284 GOTO 95
285 PEN
286 END
290 R=R0+Z
292 FOR N=1 TO M
294 H(N)=P(N)+(I4*Q/R)
296 U(N)=Q(N)+(I4*C2*Q/R)
298 W(N)=R(N)+(I4*Q/(C1*R))
300 R=R-K
302 NEXT N
303 I4=-1*I4
304 GOSUB 920
306 T2=T0+((I-1)*Z)
308 R2=R0+Z
310 I2=1
315 N=1
325 GOSUB 1005
330 GOSUB 545
335 IF I2=Z/K THEN 280
340 N=2
345 T1=T4
350 R1=R4
355 GOSUB 1065
360 GOSUB 410
365 IF N=M1 THEN 375
370 N=N+1
372 GOTO 345
375 T2=T4-((M1-1)*K)
380 R2=R0+Z
385 GOSUB 920
395 I2=I2+1
400 GOTO 315
410 Z3=R4/K
412 Z1=R1/K
413 Z4=R3/K
415 A(1,1)=1+Z3
420 A(1,2)=-1
425 A(1,3)=C1*(-C2-Z3)
430 A(2,1)=Z3-1
435 A(2,2)=1
440 A(2,3)=C1*(Z3-C2)
445 A(3,1)=-P
450 A(3,2)=1-P
```

```
455 A(3,3)=-2*(1+P)/Z3
460 IF INT(I/2)=I/2 THEN 480
465 B(1,1)=X1*(Z1-1)+Y1+V1*C1*(C2-Z1)
470 B(2,1)=X3*(1+Z4)-Y3+V3*C1*(Z4+C2)
475 GOTO 490
480 B(1,1)=X3*(Z4-1)+Y3+V3*C1*(C2-Z4)
485 B(2,1)=X1*(1+Z1)-Y1+V1*C1*(Z1+C2)
490 B(3,1)=-X2*P+Y2*(1-P)+V2*2*(1+P)/Z3
495 MAT A=INV(A)
500 MAT S=A*B
505 X4=S(1,1)
510 Y4=S(2,1)
515 V4=S(3,1)
525 H(N)=X4
530 U(N)=Y4
535 W(N)=V4
540 RETURN
545 X4=0
548 Z3=R3/K
550 Z4=R4/K
555 F(1,1)=-1
560 F(1,2)=C1*(-C2-Z4)
565 F(2,1)=1-P
570 F(2,2)=-2*(1+P)/Z4
575 G(1,1)=X4*(-1-Z4)+X3*(Z3-1)+Y3+V3*C1*(C2-Z3)
580 G(2,1)=X4*P-X2*P+Y2*(1-P)+V2*2*(1+P)/Z4
585 MAT F=INV(F)
590 MAT T=F*G
595 Y4=T(1,1)
600 V4=T(2,1)
612 H(N)=X4
615 U(N)=Y4
620 W(N)=V4
625 RETURN
630 X2=H(1)
635 Y2=U(1)
640 V2=W(1)
645 X3=H(2)
650 Y3=U(2)
655 V3=W(2)
660 T3=T2+K
665 R3=R2+K
670 T4=T2+2*K
675 R4=R2
680 RETURN
685 X4=-Q
688 Z3=R3/K
690 Z2=R4/K
695 C(1,1)=1
700 C(1,2)=C1*(Z2-C2)
705 C(2,1)=1-P
710 C(2,2)=-2*(1+P)/Z2
715 E(1,1)=X4*(1-Z2)+X3*(1+Z3)-Y3+V3*(Z3+C2)*C1
```

```
720 E(2,1)=X4*P-X2*P+Y2*(1-P)+V2*2*(1+P)/Z2
725 MAT C=INV(C)
730 MAT D=C*E
735 Y4=D(1,1)
740 V4=D(2,1)
745 GOSUB 962
750 H(N)=X4
755 U(N)=Y4
760 W(N)=V4
765 RETURN
770 J=N-1
775 L=N+1
780 X1=H(J)
785 Y1=U(J)
790 V1=W(J)
795 X2=H(N)
800 Y2=U(N)
805 V2=W(N)
810 X3=H(L)
815 Y3=U(L)
820 V3=W(L)
825 T2=T1-K
830 R2=R1+K
835 T3=T1
840 R3=R1+2*K
845 T4=T1+K
850 R4=R2
855 RETURN
920 N=M1
922 P(A)=H(N)
924 Q(A)=U(N)
926 R(A)=W(N)
928 A=A+1
930 M1=M1-1
940 RETURN
952 SCALE 0,40,-0.2,0.7
954 XAXIS 0,2
956 YAXIS 0,0.1
958 F0=0
960 PLOT T6,F0
961 RETURN
962 F1=R4*(Y4*(1-P)-P*X4)/(2*(1+P))
970 WRITE (15,20)T4,R4,F1,Y4,V4
972 PLOT T4,F1
980 RETURN
1005 T3=T2+K
1010 R3=R2-K
1015 T4=T2+(2*K)
1020 R4=R2
1025 L=N+1
1030 X2=H(N)
1035 Y2=U(N)
1040 V2=W(N)
```

```
1045 X3=H(L)
1050 Y3=U(L)
1055 V3=W(L)
1060 RETURN
1065 J=N-1
1070 L=N+1
1075 X1=H(J)
1080 Y1=U(J)
1085 V1=W(J)
1090 X2=H(N)
1095 Y2=U(N)
1100 V2=W(N)
1105 X3=H(L)
1110 Y3=U(L)
1115 V3=W(L)
1120 T2=T1-K
1125 R2=R1-K
1130 T3=T1
1135 R3=R1-(2*K)
1140 T4=T1+K
1145 R4=R1-K
1150 RETURN
```

Program 6. Method of characterists for solving the governing equations for the thick compressible shell

```
  5 PRINT "NEO-HOOKEAN SPHERE STEP FUNCTION APPLICATION
          OF PRESSURE"
 10 DISP "Q,N";
 20 INPUT Q,N1
 30 DISP "INT STEP SIZE ?";
 40 INPUT T
 50 PRINT "Q="Q,"N="N1,"INT STEP SIZE="T
 60 SCALE 0,5,1,1.1
 70 XAXIS 1,0.5
 80 YAXIS 0,0.025
 90 N=0
100 G=N1**3-1
110 X=1
120 V=0
130 PLOT N*T,X
135 IF N*T/0.1#INT(N*T/0.1) THEN 150
140 PRINT "T="N*T,"X="X,"V="V
150 D=(1+G*X**(-3))**(-1/3)
160 E=((G+X**3)/(1+G))**(-1/3)
170 F=G*X**(-3)
180 A=-(V*V*(3-(F*D**4)/(1-D))-(4/X+X**(-4)-4*E-E**4+2*Q)
      /(1-D))/(2*X)
190 A2=A
200 W=V+(A2+A)*T/2
210 Y=X+(W+V)*T/2
220 D=(1+G*Y**(-3))**(-1/3)
230 E=((G+Y**3)/(1+G))**(-1/3)
240 F=G*Y**(-3)
250 A1=-(W*W*(3-(F*D**4)/(1-D))-(4/Y+Y**(-4)-4*E-E**4+2*Q)
       /(1-D))/(2*Y)
260 IF ABS(A1-A2)<1E-08 THEN 290
270 A2=A1
280 GOTO 200
290 N=N+1
310 X=Y
320 V=W
330 IF N*T=5 THEN 350
340 GOTO 130
350 PEN
360 END
```

Program 7. Program for solving the governing equation for the thick-walled incompressible neo-Hookean shell

REFERENCES

1. LOVE, A.E.H., "A treatise on the Mathematical Theory Elasticity". Fourth Edition. Dover Publications 1944.

2. BAKER, W.E. and ALLEN, F.J., "The Response of Elastic Spherical Shells to Spherically Symmetric Internal Blast Loading". Proc. 3rd U.S. Nat. Congr. Appl. Mech. (1958) pp 79-87.

3. TRANTER, C.J., "The Application of the Laplace Transformation to a Problem on Elastic Vibrations". Phil. Mag. Vol. 33, 1942, p 614.

4. CINELLI, G., "Dynamic Vibrations and Stresses in Elastic Cylinders and Spheres". J. Appl. Mech. Vol 33, 1966, pp 825-830.

5. MEHTA, P.K. and DAVIDS, N., "A Direct Numerical Analysis Method for Cylindrical and Spherical Elastic Waves". A.I.A.A. Journal, Vol 4, no 1, pp 112-117.

6. SMITH, P.D., "On Some Numerical Schemes for the Solution of Wave Propagation Problems". Intern. J. for Num. Methods in Engineering, Vol 8, no 1, 1974, pp 91-102.

7. CHOU, S.C. and GREIF, R., "Numerical Solution of Stress Waves in Layered Media". A.I.A.A. Journal, Vol 6, no 6, June 1968, pp 1067-1074.

8. CHOU, P.C. and KOENIG, H.A., "A Unified Approach to Cylindrical and Spherical Elastic Waves by Method of Characteristics". J. Appl. Mech. Vol 33, March 1966, pp 159-167.

9. LEONARD, R.W. and BUDIANSKY, B., "On Travelling Waves in Beams". N.A.C.A. TN2874, 1953.

10. ERINGEN, C.A. and ŞUHUBI, E.S., "Elastodynamis. Volume 1. Finite Motions". Academic Press 1974.

11. ZHONG-HENG, G. and SOLECKI, R., "Free and Forced Finite Amplitude Oscillation of an Elastic Thick-walled Sphere of Incompressible Material." Arch. Mech. Stos. 15. (1963), pp 427-433.

12. HADDOW, J.B. and FAULKNER, M.G., "Finite Expansion of a Thick Compressible Spherical Elastic Shell". Intern. J. Mech. Sci., Vol 16, 1974, pp 63-73.

13. WANG, C.C., "On the Radial Oscillations of a Spherical Thin Shell in the Finite Elasticity Theory". Quart. Appl. Math., Vol 23, (1965), pp 270-274.

14. GREENSPAN, D., "Numerical Approximation of Periodic Solutions of van der Pol's Equation". J. Math. Analy. and Applications, Vol 39, (1972), pp 574-579.

15. ADKINS, J.E., "Large Elastic Deformations". Progress in Solid Mechanics, Vol II, Chp. 1.

16. BLATZ, P.J. and KO, W.L., "Application of Finite Elastic Theory to the Deformation of Rubbery Materials". Trans. Soc. Rheo., 6, 223, (1962).

17. ROSE, J.L., CHOU, S.C., and CHOU, P.C., "Vibration Analysis of Thick-walled Spheres and Cylinders". A.I.A.A. Journal, Vol 53, no 3, 1973, pp 771-776.

APPENDIX A

NUMERICAL METHODS AND ERROR ANALYSES

A.1 Numerical Scheme for the Method of Discrete Variables

For a time interval $\Delta t > 0$, let $t_k = k\,\Delta t$, $k = 0,1, \cdots$ be the time after the kth interval, and let a particle in motion be at position λ_k at time t_k. Then, we can define the particle velocity $\lambda_k' = \lambda'(t_k)$, $k = 1,2, \ldots$ and the particle acceleration $\lambda_k'' = \lambda''(t_k)$, $k = 1,2, \ldots$ at time t_k by the equations

$$\frac{\lambda_k' + \lambda_{k-1}'}{2} = \frac{\lambda_k - \lambda_{k-1}}{\Delta t}\ , \quad k = 1,2, \ldots \tag{A.1}$$

and

$$\frac{\lambda_k'' + \lambda_{k-1}''}{2} = \frac{\lambda_k' - \lambda_{k-1}'}{\Delta t}\ , \quad k = 1,2, \ldots \tag{A.2}$$

respectively.

If the particle acceleration, λ_k'', is a function

$$\lambda_k'' = \lambda_k''(\lambda_{k-1})\ , \tag{A.3}$$

then, an improved version of discrete mechanics can be described by the following algorithm, which is written in BASIC computer language in Program 3a.

(i) Set $k = 1$.

(ii) Read λ_{k-1} and λ'_{k-1}

(iii) Find λ''_{k-1} from equation (A.3) .

(iv) Set $\lambda''_k = \lambda''_{k-1}$.

(v) Find an approximate λ'_k using equation (A.2), and from this, an approximate λ_k, using equation (A.1).

(vi) Substitute the approximate λ_k in equation (A.3) to find an approximate λ''_k , denoted by λ'' .

(vii) Transfer λ'' into λ''_k .

(viii) Repeat steps (v) to (vii) until λ''_k is found within a specified error tolerance, e.

(ix) Substitute the final λ''_k into equation (A.2) to find the final λ'_k , and this in equation (A.1) to find the final λ_k .

(x) Transfer λ_k into λ_{k-1} and λ'_k into λ'_{k-1} to proceed to the next time interval, t_{k+1} .

(xi) Repeat steps (iii) to (x) for the interval, t_{k+1} .

The flow chart for this algorithm is shown in Fig. 5.

A.2 Error Analysis of the Discrete Variable Method

Equations (A.1) and (A.2) are basically the trapezoid rule of integration for which the error, E, is given by

$$E \approx - \frac{h^3}{12} f''(\eta) \tag{A.4}$$

where $h = \Delta t$ is the constant time interval which would be specified, and η is such that $0 < \eta < h$.

Then, for the particle velocity, v_k, the error E_1 is

$$E_1 \approx - \frac{h^3}{12} \dot{a}(\eta) \tag{A.5}$$

which by forward finite difference formula of differentiation becomes

$$E_1 \approx - \frac{h^3}{12} \frac{(a_k - a_{k-1})}{h} = - \frac{h^2}{12} (a_k - a_{k-1}) \tag{A.6}$$

where $(a_k - a_{k-1})$ is the maximum difference, over the whole time range, between the particle accelerations at consecutive times t_{k-h} and t_k.

Similarily, the error E_2 in evaluating the particle displacement x_k, is

$$E_2 \approx - \frac{h^3}{12} \frac{(v_k - v_{k-1})}{h} = - \frac{h^2}{12} (v_k - v_{k-1}) \tag{A.7}$$

where $(v_k - v_{k-1})$ is defined in a similar way to $(a_k - a_{k-1})$.

The values of $(a_k - a_{k-1})$ and $(v_k - v_{k-1})$ can be found in specific cases. For example, if we take $h = 0.01$, then, for a thin neo-Hookean shell with $\varepsilon = \frac{T}{R} = 0.05$, under an internal step input pressure $Q = 0.05$, $(a_k - a_{k-1}) = 0.021$ and $(v_k - v_{k-1}) = 0.4849$. Hence, from equations (A.6) and (A.7), $E_1 = -0.175 \times 10^{-6}$ and $E_2 = -0.4041 \times 10^{-6}$. The specified error tolerance, E', on the acceleration $a(t_k)$ is -0.01×10^{-6}. Consequently, the total error, E_T, in the computed particle displacement $x(t_k)$, is

$$E_T = E_1 + E_2 + E' = -0.5891 \times 10^{-6}$$

or

$$|E_T| \approx 0.6 \times 10^{-6} .$$

In general, since E_1 and E_2 are $O(h^3)$, and E' can be chosen within $O(h^3)$, then E_T is also $O(h^3)$.

A.3 The Fourth Order Runge-Kutta Process

Let the acceleration λ'', be a function

$$\lambda'' = \lambda''(\lambda) \tag{A.8}$$

of the stretch λ, then the fourth order Runge-Kutta process uses the following iterative formulae to solve the differential equation (A.8).

$$\lambda_{n+1} = \lambda_n + h\lambda_n' + \frac{1}{6} h^2 \, (K_1 + K_2 + K_3) \tag{A.9}$$

$$\lambda_{n+1}' = \lambda_n' + \frac{1}{6}h \, (K_1 + 2K_2 + 2K_3 + K_4) \tag{A.10}$$

where

$$K_1 = \lambda''(\lambda_n)$$

$$K_2 = \lambda''(\lambda_n + \frac{h}{2}\lambda_n')$$

$$K_3 = \lambda''(\lambda_n + \frac{h}{2}\lambda_n' + \frac{h^2}{4} K_1)$$

$$K_4 = \lambda''(\lambda_n + h\lambda_n' + \frac{h^2}{2} K_2) \tag{A.11}$$

and $h = \Delta t$ is the constant time interval between positions represented by displacements λ_n and λ_{n+1}, and λ_n, λ_n' are respectively the displacement and velocity at time t_n. A program using this method to integrate the differential equation governing the motion of a thin incompressible shell is shown in Program 4a.

The error, E, in an r^{th} order Runge-Kutta method is given by

$$E \quad \frac{\lambda^{(2)} - \lambda^{(1)}}{2^{r} - 1} \tag{A.12}$$

where $\lambda^{(1)}$ and $\lambda^{(2)}$ are the values of λ at time t_n using step sizes h and $\frac{h}{2}$ respectively in stepping forward from t_{n-1}. Values for these can be found in specific cases. For example, in the forced vibration of the thin neo-Hookean shell for which $\varepsilon = 0.05$, under an internal step input pressure $Q = 0.055$, $\lambda^{(1)} = 1.561290868$ and $\lambda^{(2)} = 1.561289352$. Since $r = 4$, we find $E = 0.1011 \times 10^{-6}$.

In general, E is $O(h^3)$ as is the case with the discrete variable method.

A.4 Error Analysis of the Method of Characteristics

As discussed in Section C.1 of Appendix C, the trapezoid rule is used to integrate the characteristic equations. Consequently, the error, e, in the numerical computation is that incurred in the use of the trapezoid rule.

Thus e is $O(h^3)$, where $h = \Delta\bar{r} = \Delta\tau$.

A.5 Algorithm for Integrating Governing Equations for the Thin Compressible Shell

The second order non-linear ordinary differential equations governing the motion of the compressible thin shell are equations (3.30) and (3.31) written as follows.

$$q = -2\left[\frac{\delta}{\lambda^2} - (\lambda^2\delta)^{2s-1}\right] \qquad (A.13)$$

$$\lambda'' = q\,\frac{\lambda^2}{\varepsilon} - 2\,(\lambda - \frac{\delta^2}{\lambda}) \qquad (A.14)$$

To develop an algorithm for the numerical solution of these equations, let $t_k = k\Delta t$, $k = 0,1,2..$ represent the time after k equal intervals of Δt. Also, for $\Delta t > 0$, let $\lambda_k = \lambda(t_k)$, $\lambda'_k = \lambda'(t_k)$, $\lambda''_k = \lambda''(t_k)$ and $\delta_k = \delta(t_k)$, $k = 1,2,3$ ... Further let λ''_k be a function

$$\lambda''_k = \lambda''_k(\lambda_{k-1}, \delta_{k-1}) \qquad (A.15)$$

of $\lambda(t_{k-1})$ and $\delta(t_{k-1})$.

Then under a known internal step input pressure q, there corresponds a δ_k for each λ_k at any time t_k. This δ_k is found by solving the transcendental equation (A.13). The values of δ_k and λ_k are then used to integrate equation (A.14) by some suitable stepwise procedure, for example the fourth order Runge-Kutta process or the method of discrete variables.

Equation (A.13) is best solved by the Newton-Raphson method. This, along with the discrete mechanics procedure described in Section (A.1) is the basis of the following algorithm.

(i) Set k = 1

(ii) Read $\lambda_{k-1} = 1$, $\lambda'_{k-1} = 0$, and $\delta_{k-1} = 1$, where δ_{k-1} is the initial guessed value for the Newton-Raphson operation.

(iii) Find the correct δ_{k-1} from (A.13) to within a specified error tolerance by the Newton-Raphson method.

(iv) Use λ_{k-1} and δ_{k-1} to find λ''_{k-1} from equation (A.15)

(v) Set $\lambda''_{k-1} = \lambda''_k$.

(vi) Find an approximate λ'_k using equation (A.2) and from this, find an approximate λ_k using equation (A.1).

(vii) Substitute the approximate λ_k in equation (A.13) to find an approximate δ_k, then, from (A.3), find approximate λ''_k, and denote this by λ''.

(viii) Transfer λ'' into λ''_k .

(ix) Repeat steps (vi) to (viii) until λ_k'' is found within a specified error tolerance.

(x) Substitute the final λ_k'' into equation (A.2) to find the final λ_k', and this in (A.1) to find the final λ_k.

(xi) Transfer λ_k into λ_{k-1}, λ_k' into λ_{k-1}', and δ_k into δ_{k-1} to proceed to the next time interval t_{k+1}.

(xii) Repeat steps (iii) to (xi) for the interval, t_{k+1}.

The flow chart for this algorithm is shown in Fig. 6.

APPENDIX B

CONDITIONS FOR A PERIODIC MOTION

B.1 Periodicity of Motion

B.1.1 The necessary condition

A necessary condition for a periodic motion under a step function application of pressure, Q, is that an equilibrium state, $\lambda(e)$, must exist for this pressure. The conditions for the existence of this equilibrium stretch is examined here for a thin shell for which $\lambda(e)$ refers to the mean equilibrium stretch. In what follows, we refer to the Mooney-Rivlin material as material I, the material with the logarithmic strain energy function of equation (2.7) as material II, and the Blatz-Ko material as material III.

To investigate the existence of an equilibrium stretch for a given step input pressure, we examine the static curves, sketched in Figure 1, for the materials I, II, and III.

For material I, there are three distinct types of static curves marked as (i), (ii) and (iii) in Figure 1a. Curve (i) is the static curve for the neo-Hookean solid, (for which $c = 1$), curve (ii) has one maximum followed by a minimum point; this shape is obtained for all values of c for which

$$c_{crit} < c < 1 \tag{B.1}$$

where c_{crit} is the value of c at which the maximum and minimum points merge into an inflexion point denoting a transition from curve (ii) to curve (iii). Curve (iii) shows Q increasing monotonically with λ; this curve is obtained for values of c for which

$$0 < c < c_{crit} \tag{B.2}$$

For the cases for which, $0 < c \leqslant c_{crit}$, there exists an equilibrium stretch for any value of the step input pressure Q, consequently, the motion resulting from any step input application of pressure is periodic. When, however, $c_{crit} < c \leqslant 1$, there could be more than one equilibrium stretch for a given applied pressure Q. Consequently, as discussed in Section (B.3), there exists a maximum value, Q_{max}, of the applied pressure Q, beyond which a periodic motion is not possible.

For materials II and III, the static curves are similar to the one for the neo-Hookean material and so, as in the latter case, there is a maximum value, Q_{max}, of the applied step input pressure Q, beyond which a periodic motion is not possible. The value of Q_{max} is calculable as discussed in Section (B.3).

B. B.1.2 The sufficient condition

The sufficient condition for a periodic motion is that the expression obtained for λ'^2, as in equations (3.23) and (3.35), which can be represented as a function, $\lambda'^2 = p(\lambda)$, of λ, must be positive. Then and only then will the resulting motion be periodic, with two velocities, which are continuous functions of λ thus

$$\lambda' = \pm \sqrt{p(\lambda)} \quad . \tag{B.3}$$

This condition imposes some restrictions on the form of the strain energy function W, as shown by ZHONG-HENG and SOLECKI [11] for an incompressible material.

Thus we have the following sufficient conditions to ensure a periodic motion of the incompressible shell

$$W_0(\lambda) \sim M\lambda^m \text{ as } \lambda \to \infty \tag{B.4}$$

and

$$W_0(\lambda) \sim N\lambda^{-n} \text{ as } \lambda \to 0 \tag{B.5}$$

where M,N,m,n are positive constants such that $m > 1$ and $n \geqslant 1$,

and where

$$W_0(\lambda) = \frac{2}{\rho A^2} W(I_1, I_2) \tag{B.6}$$

B.2 The Critical Value, c_{crit}, of c, for the Mooney-Rivlin Material

The equation for the static inflation of the incompressible thin-walled shell of Mooney-Rivlin material, from equation (3.20), is

$$\frac{Q\lambda^2}{\varepsilon} = 2c(\lambda - \frac{1}{\lambda^5}) + 2(1 - c)(\lambda^3 - \frac{1}{\lambda^3})$$

$$\frac{Q}{\varepsilon} = 2c(\frac{1}{\lambda} - \frac{1}{\lambda^7}) + 2(1 - c)(\lambda - \frac{1}{\lambda^5}) \tag{B.7}$$

The turning points of the Q/λ curve, shown in Fig. 7, occur at values of λ for which

$$\frac{dQ}{d\lambda} = 0 ,$$

that is, at the roots of the equation

$$\frac{dQ}{d\lambda} = 2c(-\frac{1}{\lambda^2} + \frac{7}{\lambda^8}) + 2(1 - c)(1 + \frac{5}{\lambda^6}) = 0 \tag{B.8}$$

Putting

$$\gamma = \frac{1-c}{c}$$

and

$$x = \lambda^2$$

equation (B.8) becomes:

$$\gamma x^4 - x^3 + 5\gamma x + 7 = 0 \tag{B.9}$$

By Descarte's rule of signs, this equation cannot have more than two real positive roots, so that there are at most two positive values of λ for which Q has a stationary value.

Furthermore, from (B.8), it follows that if c and $(1-c)$ are both positive, that is, if we have

$$0 < c \leqslant 1 \tag{B.10}$$

then

$$\frac{dQ}{d\lambda} > 0 \quad \text{for} \quad \lambda = 1 \quad \text{and for} \quad \lambda \gg 1$$

this implies that there exists some values of $\lambda > 1$ for which

$$\frac{dQ}{d\lambda} < 0$$

that is, for which from equation (B.9), we have

$$f(x) = \frac{x^3-7}{x^4 + 5x} > \gamma \tag{B.11}$$

This is possible if and only if γ is less than the maximum value which $f(x)$ can attain.

Solving the equation

$$\frac{df(x)}{dx} = 0$$

we find that the maximum value of $f(x)$ occurs when $x = 3.3883$, that is, when $\lambda = 1.8407$. Consequently, the critical value, c_{crit}, of c is 0.8234.

B.3 The Maximum Step Input Pressure, Q_{max}, for a Periodic Motion.

Since for a periodic motion, the phase trajectory closes, the maximum value, Q_{max}, of the applied pressure Q, for a periodic motion is the value of Q for which the trajectory just fails to close as depicted in Fig. 2(b). This limiting case occurs when an equilibrium stretch, $\lambda(e)_2$, coincides with a root, λ_d, of the energy equation

$$\lambda' = \lambda'(\lambda) .$$

Thus for the Mooney-Rivlin material, by setting

$$\left.\begin{aligned} &\lambda'' = 0 \\ \text{and} \quad &\lambda' = 0 \end{aligned}\right\} \quad \text{(B.12)}$$

in equations (3.20) and (3.23) respectively, we have at $Q = Q_{max}$, the pair of simultaneous equations;

$$0 = \frac{Q\lambda^2}{\varepsilon} - 2c(\lambda - \frac{1}{\lambda^5}) - 2(1-c)(\lambda^3 - \frac{1}{\lambda^3})$$

(B.13)

$$0 = \frac{Q}{3\varepsilon}(\lambda^3-1) - 2c(\frac{\lambda^2}{2} + \frac{1}{4\lambda^4}) - 2(1-c)(\frac{\lambda^4}{4} + \frac{1}{2\lambda^2}) + \frac{3}{2}$$

(B.14)

By eliminating Q between (B.13) and (B.14) we get a polynomial in λ, the lowest positive root, λ_d, of which, when substituted in (B.13) gives

$$Q_{max} = 2\varepsilon\left[c(\frac{1}{\lambda_d} - \frac{1}{\lambda_d^7}) + (1-c)(\lambda_d - \frac{1}{\lambda_d^5})\right]$$

(B.15)

The values computed for Q_{max} for different cases of each of materials I, II and III are shown on the respective phase plane diagrams.

The period of oscillation, T, is finite if Q is less than Q_{max} and is given by

$$T = \oint_c \frac{d\lambda}{\lambda'} \qquad \text{(B.16)}$$

The numerical method for evaluating this integral is described in Program 5a.

APPENDIX C

NOTES ON THE METHOD OF CHARACTERISTICS

C.1 Integration of the Characteristic Equations

Using the notations for the thick compressible shell, let the functions

$$\bar{\sigma}_r = \bar{\sigma}_r(\bar{r},\tau) \ , \quad \bar{\sigma}_\theta = \bar{\sigma}_\theta(\bar{r},\tau) \text{ and } \bar{v} = \bar{v}(\bar{r},\tau) \tag{C.1}$$

vary linearly in the small intervals between grid points. Then, referring to Fig. 8, the integral of the differential $d\bar{\sigma}_r$ for example, along I^+ is given by

$$\int_1^4 d\bar{\sigma}_r = \left(\bar{\sigma}_r\right)_4 - \left(\bar{\sigma}_r\right)_1 \tag{C.2}$$

and similar relations obtain for integrals along I^- and II characteristics.

Furthermore, by assuming the functions of equation (C.1) to be linear along the characteristics the trapezoid rule of integration becomes suitable for integration, from one grid point to the next, along these lines. For example, along the I^+, the following integration formula holds

$$\int_1^4 \left(\frac{\bar{\sigma}_r}{\bar{r}}\right) d\bar{r} = \frac{1}{2}\left[\left(\frac{\bar{\sigma}_r}{\bar{r}}\right)_4 + \left(\frac{\bar{\sigma}_r}{\bar{r}}\right)_1\right] \Delta\bar{r} \tag{C.3}$$

For convenience of integration, we set

$$\Delta\bar{r} = \Delta\tau \ . \tag{C.4}$$

Using equations (C.2) and (C.3) in (4.24) and (4.25), and dropping the bars on the dimensionless quantities, we get the integrated forms of the characteristic equations in non-dimensional form as follows.

Along I^+,

$$(\sigma_{r_4} - \sigma_{r_1}) - \alpha(v_4 - v_1) = -\left[\left(\frac{\sigma_r}{r}\right)_4 + \left(\frac{\sigma_r}{r}\right)_1\right]\Delta r$$
$$+ \left[\left(\frac{\sigma_\theta}{r}\right)_4 + \left(\frac{\sigma_\theta}{r}\right)_1\right]\Delta r + \beta\left[\left(\frac{v}{r}\right)_4 + \left(\frac{v}{r}\right)_1\right]\Delta r \ , \tag{C.5}$$

along I^-,

$$(\sigma_{r_3} - \sigma_{r_4}) + \alpha(v_3 - v_4) = -\left[\left(\frac{\sigma_r}{r}\right)_3 + \left(\frac{\sigma_r}{r}\right)_4\right]\Delta r$$
$$+ \left[\left(\frac{\sigma_\theta}{r}\right)_3 + \left(\frac{\sigma_\theta}{r}\right)_4\right]\Delta r - \beta\left[\left(\frac{v}{r}\right)_3 + \left(\frac{v}{r}\right)_4\right]\Delta r \ , \tag{C.6}$$

along II,

$$\nu(\sigma_{r_4} - \sigma_{r_2}) - (1 - \nu)(\sigma_{\theta_4} - \sigma_{\theta_2})$$

$$= -(1 + \nu)\left[\left(\frac{v}{r}\right)_4 + \left(\frac{v}{r}\right)_2\right](2\Delta\tau) \ , \tag{C.7}$$

where

$$\alpha = \frac{2(1-\nu)}{1-2\nu} \ , \qquad \beta = \frac{2\nu}{1-2\nu} \tag{C.8}$$

and ν is Poisson's ratio for infinitesimal strain from the undeformed state.

To evaluate the stresses σ_r and σ_θ and the velocity v at each grid point of the characteristic network of Fig. 4, we proceed as follows. In the undisturbed region ABC, σ_r, σ_θ and v are all zero. Consequently, the values of these quantities at grid points on line AC are obtained directly from the discontinuity relations of equations (4.26) - (4.28). With these initial values, a step-by-step solution is started by solving equations (C.6) and (C.7) simultaneously for the half-mesh in the lower corner of the triangular region ACD. This gives σ_θ and v at the third point of the triangular mesh and since σ_r is already prescribed at this point, we can now solve equations (C.5) - (C.7) simultaneously for the full interior mesh next to this first half-mesh. This gives values of σ_r, σ_θ and v at the fourth point of the grid, from which we can evaluate the next mesh in a similar way. This process is repeated until all the grid points in the triangular region ACD have been treated.

CD is a path of wavefront propagation, therefore, the strong discontinuities in σ_r, σ_θ and v given by equations (4.26) - (4.28) must be added to the values previously calculated for these quantities along this line in order to proceed to the next triangular region CDE. CD is now the initial line and the foregoing stepwise process is repeated, this time starting with the first outer half-mesh in the lower corner of CDE.

Jumps are again added for points along DE before going into the next triangular region which then becomes evaluable. In this way we can cover as many triangular regions as we desire.

C.2 Boundary Conditions and the Constants K and K'

The discontinuity relations across an I^+ wavefront are

$$[\sigma_r] = \frac{K}{r}$$

$$[\sigma_\theta] = \frac{\nu}{1-\nu}\frac{K}{r}$$

$$[v] = -\frac{1}{\rho c}\frac{K}{r} \qquad (C.9)$$

and across an I^- wavefront, these are

$$[\sigma_r] = \frac{K'}{r}$$

$$[\sigma_\theta] = \frac{\nu}{1-\nu}\frac{K'}{r}$$

$$[v] = +\frac{1}{\rho c}\frac{K'}{r} \qquad (C.10)$$

where the notations for the thick compressible shell have been used and K, K' are constants to be determined from the boundary conditions.

These boundary conditions are

$$\sigma_r = -q \quad \text{at} \quad r = A \ (\text{or } \bar{r} = 1) \ ,$$

and

$$\sigma_r = 0 \quad \text{at} \quad r = B \ (\text{or } \bar{r} = \frac{B}{A}). \qquad (C.11)$$

For the first I^+ wave propagation line AC, of Fig. 5, we have, from the first of equations (C.9) and the first boundary condition in (C.11), the equation

$$\sigma_{r+} - \sigma_{r-} = -q = \frac{K}{A} \qquad (C.12)$$

where σ_{r+}, σ_{r-} are the values of σ_r ahead of and behind the wavefront respectively. Equation (C.12), therefore, gives

$$K = -qA \qquad (C.13)$$

and the discontinuity relations along AC become

$$[\sigma_r] = -\frac{qA}{r}$$

$$[\sigma_\theta] = \frac{\nu}{1-\nu}\left(-\frac{qA}{r}\right)$$

$$[v] = -\frac{1}{\rho c}\left(-\frac{qA}{r}\right) \qquad (C.14)$$

At the endpoint C of line AC, the first of equations (C.14) gives

$$\sigma_r = -\frac{qA}{B}$$

and in order to satisfy the second boundary condition in equation (C.11), we should have, from the first of equation (C.10),

$$+\frac{qA}{B} = \frac{K'}{B}.$$

This implies that, for the first I^- wave propagation line CD,

$$K' = qA \tag{C.15}$$

and the discontinuity relations along this line become

$$[\sigma_r] = \frac{qA}{r}$$

$$[\sigma_\theta] = \frac{\nu}{1-\nu}\left(\frac{qA}{r}\right)$$

$$[v] = +\frac{1}{\rho c}\left(\frac{qA}{r}\right) . \tag{C.16}$$

Again, the first of equations (C.16) gives, for the endpoint D of CD, the discontinuity in σ_r as

$$[\sigma_r] = q .$$

Consequently, to satisfy the first boundary condition in equation (C.11), we must have, for the value of K along the second I^+ propagation line DE, the expression

$$K = qA . \tag{C.17}$$

Similarily, for the line EF,

$$K' = -qA \tag{C.18}$$

It follows, therefore, that for succeeding I^+ propagation lines, the values of K are given by

$$K = -qA, +qA, -qA, +qA, \ldots \qquad (C.19)$$

with alternating signs, and for the I^- propagation lines.

$$K' = +qA, -qA, +qA, -qA, \ldots \qquad (C.20)$$

also with signs alternating.

APPENDIX D

PROOFS OF THEOREMS

D.1 Proof of the Theorem Relating Surface Tractions To the Average Hydrostatic Stress

The theorem leads to the equation

$$\int_S \underset{\sim}{T} \cdot \underset{\sim}{r}\, dS - \int_V \rho \ddot{\underset{\sim}{r}} \cdot \underset{\sim}{r}\, dV = 3V\sigma \qquad \text{(D.1)}$$

where $\underset{\sim}{T}$ is the surface traction, $\underset{\sim}{r}$ the position vector, V the volume, S the surface and σ the average hydrostatic stress.

Denote the left hand side of equation (D.1) by L, so that

$$L = \int_S \underset{\sim}{T} \cdot \underset{\sim}{r}\, dS - \int_V \rho \ddot{\underset{\sim}{r}} \cdot \underset{\sim}{r}\, dV\ , \qquad \text{(D.2)}$$

and put $\underset{\sim}{f} = \rho \ddot{\underset{\sim}{r}}$. Then, in tensor notation, equation (D.2) becomes

$$L = \int_S \sigma_{ij}\, n_j\, r_i\, dS - \int_V f_i\, r_i\, dV\ .$$

Applying the divergence theorem, this equation becomes

$$L = \int_V \left[\frac{\partial}{\partial r_j} (\sigma_{ij}\, r_i) - f_i\, r_i \right] dV$$

$$= \int \left[\left(\frac{\partial\sigma_{ij}}{\partial r_j} - f_i\right) r_i + \sigma_{ii}\right] dV \; .$$

(D.3)

By Cauchy's first law of motion, when there are no body forces present, we have

$$\frac{\partial\sigma_{ij}}{\partial r_j} - f_i = 0 \; .$$

It follows, therefore, from this and equation (D.3) that

$$L = \int_V \sigma_{ii} \, dV = 3V\sigma$$

or

$$\int_S \underset{\sim}{T} \cdot \underset{\sim}{r} \, dS - \int_V \rho \ddot{\underset{\sim}{r}} \cdot \underset{\sim}{r} \, dV = 3V\sigma$$

as stated above.

D.2 The Characteristic Curves

Let the characteristic curve in the (r-t) plane be defined by the parametric equations

$$r = r(s) \quad \text{and} \quad t = t(s) \; . \qquad \text{(D.4)}$$

Then the dependent variables σ_r, σ_θ and v have the following total differentials

$$\frac{\partial \sigma_r}{\partial r}\frac{dr}{ds} + \frac{\partial \sigma_r}{\partial t}\frac{dt}{ds} = \frac{d}{ds}\sigma_r$$

$$\frac{\partial \sigma_\theta}{\partial r}\frac{dr}{ds} + \frac{\partial \sigma_\theta}{\partial t}\frac{dt}{ds} = \frac{d}{ds}\sigma_\theta$$

$$\frac{\partial v}{\partial r}\frac{dr}{ds} + \frac{\partial v}{\partial t}\frac{dt}{ds} = \frac{d}{ds}v \qquad (D.5)$$

The partial derivatives of σ_r, σ_θ and v become indeterminate when the determinant of the coefficients of the left hand sides of the six equations (4.18) - (4.20) and (D.5) is zero. This condition is expressed by the equation

$$\det \begin{bmatrix} 1 & 0 & 0 & 0 & 0 & -\rho \\ 0 & 0 & 0 & 1 & -\bar{E}\nu & 0 \\ 0 & 1 & 0 & 0 & -\bar{E}(1-\nu) & 0 \\ \frac{dr}{ds} & \frac{dt}{ds} & 0 & 0 & 0 & 0 \\ 0 & 0 & \frac{dr}{ds} & \frac{dt}{ds} & 0 & 0 \\ 0 & 0 & 0 & 0 & \frac{dr}{ds} & \frac{dt}{ds} \end{bmatrix} = 0$$

which implies that

$$\left(\frac{dr}{dt}\right)^2 = \frac{\bar{E}(1-\nu)}{\rho} \text{ and } dr = 0$$

that is

$$\frac{dr}{dt} = \pm c \quad \text{and } dr = 0$$

where c is the velocity of propagation of dilatational spherical waves.